UNIVERSITA' DEGLI STUDI DI TORINO

Doctoral School in Life and Health Sciences

PhD Program in Complex System for Life Sciences

XXXIII Cycle

Control of Endothelial cells phenotypic switch by ncRNAs

Author: Sushant Parab

Tutor: Prof. Federico Bussolino
Coordinator: Prof. Michele De Bortoli

A thesis submitted in fulfilment of the requirements
for the degree of Doctor of Philosophy

May 2021

ACKNOWLEDGEMENTS

Writing a scientific thesis is a hard work and it would be impossible without the support from various people. I would like to begin by expressing my gratitude towards the scholarship awarded by University of Torino for the completion of my Doctorate thesis. I am grateful for this opportunity and would hereby like to thank all of them – academics, administrative staff and PhD cohorts in the department of Complex System of Life sciences and Candiolo Cancer Institute IRCC.

First and foremost, I would like to express my deep and sincere gratitude to my supervisor, Professor Federico Bussolino for his guidance, insightful comments, motivational advice and continuous support throughout the entire process of my PhD. His close supervision helped me complete this journey successfully. I will always be thankful to him, for giving me the freedom and exposure to get involved into multiple projects which eventually improved my craft.

I would also like to take this opportunity to thank Alessio Noghero, Davide Còra and Stefania Rosano, who have been like co-tutors for me. The thesis would not have been written successfully without there continuous supervision and guidance. There suggestions and comments have helped me improve a lot not just professionally but also personally.

My special appreciation towards all my lab mates and friends; Edoardo, Emanuele, Valentina, Elena, Gabriella, Camila, Anna, Roxana, Alejandra, Chiara, Serena who made it easier for me to get absorbed in the lab and get adjusted to the new surroundings.

Last, but not the least, I am extremely grateful to my parents, Mr. Dilip Parab and Mrs. Dipali Parab for their constant support and love. It was with their blessings that I came to Turin, and their faith which always acted as an extra motivation for me.

Abstract:

Angiogenesis is a multi-step, tightly regulated process that plays a crucial role in development, as well as in pathological conditions such as tumor growth. During sprouting angiogenesis (SA), endothelial cells (EC) are activated by VEGF-A, a potent angiogenic growth factor, which triggers the transition from quiescent to active EC. However, the gene expression events which sustain this phenotypic switch have not been elucidated so far. Previous studies have already elucidated the importance of miRNAs, in the regulation of angiogenesis. But research on lncRNAs in angiogenesis is still in its infancy. We hypothesize that lncRNAs participate, together with miRNAs, to the regulatory network that sustains SA ultimately contributing to EC phenotype specification. To study the activation of quiescent ECs induced by an angiogenic stimulus, and the impact that lncRNAs and miRNAs may exert on this process, we exploited, by using a global transcriptomic approach, a three-dimensional model that recapitulates SA in vitro. This allowed the annotation of non-coding RNAs whose expression is modulated during sprouting. The use of miRNA target prediction tools, together with co-expression analysis between miRNAs, lncRNAs and protein-coding genes, identified biological pathways whose activity is modulated during SA, and the genes that are more subjected to post-transcriptional control. The information obtained was used to generate a non-coding RNA regulatory network that sustains EC phenotypic transition during SA.

Abbreviations:

SA	Sprouting Angiogenesis
IA	Intussusceptive Angiogenesis
ECs	Endothelial Cells
PCGs	Protein-coding genes
miRNAs	microRNAs
3D	Three Dimensional
HUVEC	Human Umbilical Vein Endothelial Cells
SPHV	Spheroids stimulated with VEGF-A
SPHC	Control spheroids
ceRNA	Competitive Endogenous RNA
MMLI	mRNA-miRNA-lncRNA interaction
GSEA	Gene Set Enrichment Analysis
MTIs	miRNA – target interactions
GO	Gene Ontology
TS	TargetSCAN
DEA	Differential Expression Analysis

Table of Contents

Chapter 1

Chapter 2

Chapter 3

Chapter 4

1. Introduction:

1.1 Angiogenesis:

Angiogenesis is a process of development of new blood vessels from preexisting vasculature. It is a complex multifaceted process that occurs throughout life: it is essential during embryonic development, tissue repair and regeneration, formation of granulation tissue during wound healing or menstrual cycle (Schmidt et al., 2010). The angiogenic process needs to be elegantly balanced during the growth and development, this balance depends on positive and negative angiogenic modulators within the vascular microenvironment (Ribatti et al., 2013). Excessive or insufficient angiogenesis contributes to various pathological conditions such as cancer (Carmeliet et al., 2005).

Generally, angiogenesis refers to two different mechanisms of vasoformation: sprouting angiogenesis (SA) and intussusceptive angiogenesis (IA). Both the types of angiogenesis occur in utero and adults virtually in all tissues and organs (presented in the following figure). IA was discovered by Burri about two decades ago (Burri et al.,1990; Caduff et al.,1986). It is also called splitting angiogenesis because the vessel wall extends into the lumen causing a single vessel to split in two. This type of angiogenesis is thought to be efficient and fast compared with sprouting angiogenesis because, initially, it only requires reorganization of existing endothelial cells (ECs) and does not rely on immediate endothelial migration or proliferation. For these reasons intussusceptive angiogenesis plays a prominent role in vascular development in embryos where growth is fast and resources are limited (Kurz et al., 2003; Djonov et al.,2003). On the other hand, SA having been discovered 200 years ago, is fundamental process characterized by sprouts of endothelial cells which usually grow towards

an angiogenic stimulus. SA can therefore add new blood vessels and can initiate the transition of tumors from a benign state to a malignant one, as first proposed in 1971 by Judah Folkman. This PhD thesis will mainly focus on sprouting angiogenesis regulation.

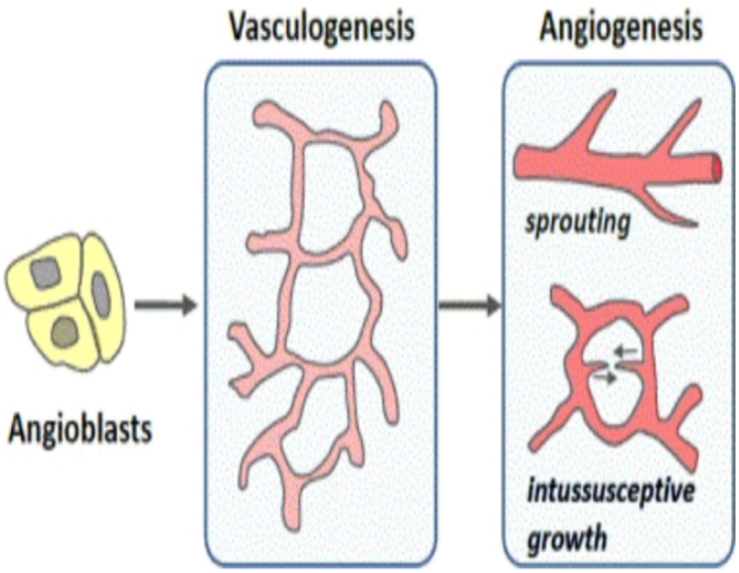

Basic types of primary vascular growth (Adair et al., 2010).

1.2 Sprouting Angiogenesis

Sprouting angiogenesis (SA) having been discovered nearly 200 years ago. It is a well characterized process; the intensive research about this process is due to the fact that it is closely linked to tumor development (Auspeunk et al., 1977). As implied by its name, SA is characterized by sprouts composed of ECs generated from preexisting vessel as consequence of pro-angiogenic stimulation. Among others biological process, angiogenesis relies on the proliferation and migration of ECs. Ausprunk and Folkman demonstrated that blood vessel sprouting initially can progress without cell division and relies on cell migration, while, in later phases, proliferation is required to sustain new vessel growth. The angiogenic growth provides an excellent example for the tight coordination of cell proliferation, differentiation, migration, matrix adhesion and cell–cell signaling processes during tissue morphogenesis. The basic steps of sprouting angiogenesis include: 1) enzymatic degradation of capillary basement membrane; 2) weakening of inter-endothelial contacts; 3) directed ECs migration into the connective tissue; 4) elongation of sprouts by ECs proliferation to form solid cords; 5) lumen formation; 6) anastomosis to form functionally capillary loops; 8) stabilization with synthesis of the new basement membrane and recruitment of pericytes (Figure 1) (Adams et. al., 2007). In healthy adults, under physiological conditions where there is a balance of pro- and anti- angiogenic factors, ECs remain quiescent as ‘phalanx’ cells for years (Potente et al., 2011). However, in conditions of injury, inflammation, cancer, or other pathologies, when pro-angiogenic factors dominate, ECs quickly switch to angiogenic phenotypes and can very rapidly start to migrate and later to proliferate to form new vessels. Sprouting angiogenesis is induced by hypoxic conditions; most types of parenchymal cells (myocytes, hepatocytes, astrocytes,

etc.) respond to a hypoxic environment by secreting a key proangiogenic growth factor, the vascular endothelial growth factor (VEGF-A) (Guy et al., 2015). VEGF-A signaling pathway has been established as the master regulator of angiogenesis. The functions of this pathway will be exhaustively described in the chapter 4. Initiation of sprouting requires the specification of ECs into two subtypes with different morphologies and functional properties. Tip cells are migratory and polarized; these cells adopts a highly branched shape while moving. Tip cells express high levels of VEGF receptor-2 (VEGFR-2) and for this reasons are the favored cells to respond at VEGF stimulation. Tip phenotype is also characterized by high levels of Dll-4 and low levels of Notch signaling activity (Gerhardt et al., 2003; Claxton et al., 2004; Lu et al., 2004; Siekmann et al., 2007; Suchting et al., 2007). Tip cells migration depends on a gradient of VEGF; in fact they extend numerous filopodia, that serve to guide the new vessels in the direction of the angiogenic stimulus (Bentley et al., 2009). Stalk cells are the proliferating cells during sprout extension and form the nascent vascular lumen cell. Stalk cells proliferation is regulated by VEGF concentration Thurston et al., 2008). Their phenotype is characterized by high levels of Notch and low levels of VEGFR2. The phenotypic specialization of ECs as tip or stalk cells is very transient and reversible, depending on the balance between pro-angiogenic factors, such as VEGF, and suppressors of endothelial cell proliferation, such as delta-like ligand 4 (Dll4)- Notch activity (Eilken et al., 2010, Eilken et al., 2011; Geudens et al., 2011). Tip and stalk cell differentiation is tightly regulated by a feedback system involving VEGF and Notch pathway. In brief, VEGF induces endothelial tip cell mobilization and expression of delta-like ligand 4 (DLL4). DLL4-mediated activation of Notch signaling in neighboring cells suppresses the expression of VEGFR2 and, thereby, promotes the stalk cell phenotype (Wacker et al., 2011). Endothelial cells dynamically switch phenotypes during angiogenesis, depending

on their fitness as the tip cell (Jakobsson et al., 2010). By ensuring that the most suitable endothelial cells are in the tip and stalk positions, the DLL4– Notch feedback system promotes efficient sprouting and mediates vascular growth patterns. After the ECs specification, new sprouts continue to growth, until they meet other sprouts or capillaries and anastomose.

The next step required to obtain a functional blood vessel is the formation of a vascular lumen and the establishment of blood flow. Though the molecular pathways controlling lumen morphogenesis are currently under intense investigation, it is clear that lumen formation involves the transition through a number of discrete phases and several complex molecular mechanisms that include endothelial cell shape and polarity change and junctional rearrangement. The first phase to initiate lumen formation is the correct acquisition of apico-basal polarity and spatial redistribution of EC–EC junctions (Shane et al., 2011; Zovein et al., 2010).

The last event in the angiogenic process is the stabilization of the newly formed vessel and the maintenance of the existing vasculature. Several cellular and non-cellular components in the blood vessels, including ECs, pericytes, smooth muscle cells, fibroblasts, glial cells, inflammatory cells, and the extracellular matrix, coordinately regulate the maintenance of vessel integrity at varying degrees in different vascular beds (Xu et al., 2011; Patel-Hett et al., 2011). In particular, EC wrapping by surrounding pericytes is a basic event in blood vessel stabilization and maturation. It has been hypothesized that concomitant with sprouting, ECs direct the differentiation of mural cell precursors from the adjacent tissue by secretion of soluble factors (Stratman et al., 2012; Beck et al., 1997).

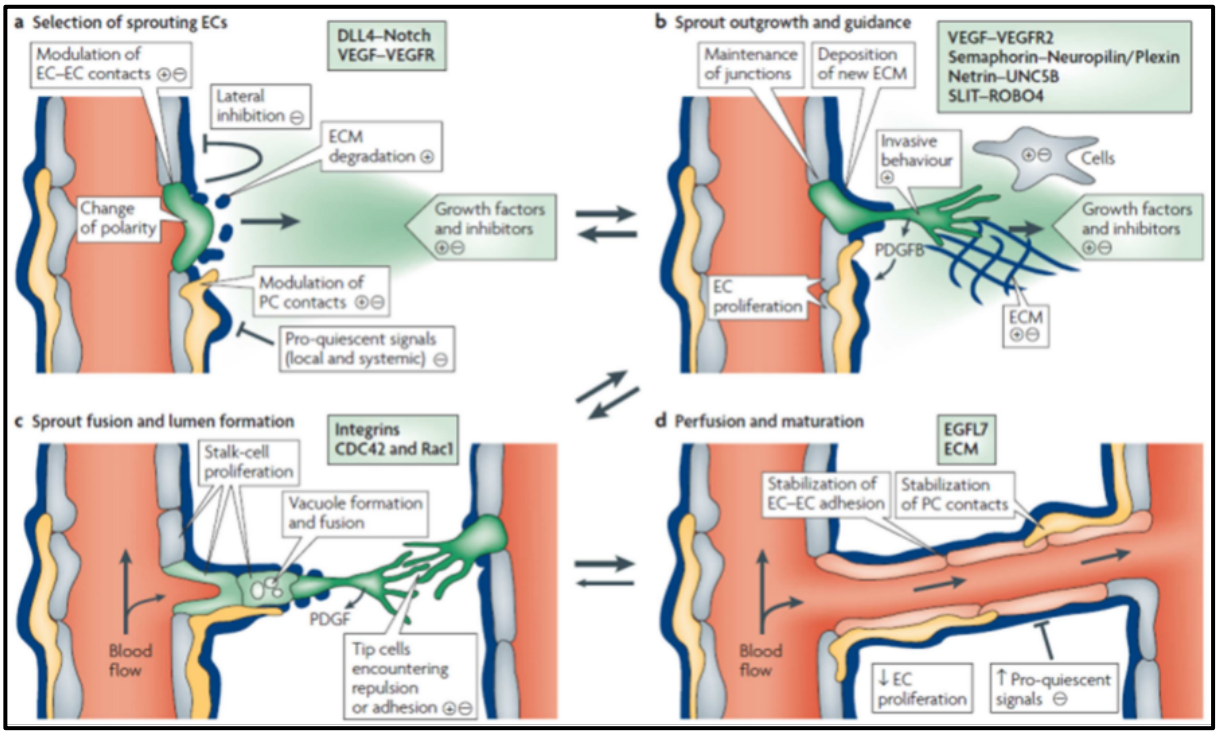

Figure 1. a | Sprouting is controlled by the balance between pro-angiogenic signals (+), such as VEGF, and factors that promote quiescence (-), such as tight pericyte (PC; yellow) contact, certain extracellular matrix (ECM) molecules or VEGF inhibitors. Under pro-angigenic stimulation, someECs can sprout (green), whereas others fail to respond (grey). Sprouting requires the induction of motile and invasive activity, the flipping of apical–basal polarity, the modulation of cell–cell contacts and local matrix degradation. b | The growing EC sprout is guided by VEGF gradients.. Release of platelet-derived growth factor B (PDGFB) by the tip cells promotes the recruitment of PCs to new sprouts. EC–EC junctions need to be maintained after lumen formation. c | Adhesive or repulsive interactions that occur when tip cells encounter each other regulate the fusion of adjacent sprouts and vessels. Lumen formation in stalk ECs involves the fusion of vacuoles and other mechanisms d | Fusion processes at the EC–EC interfaces establish a continuous lumen.. DLL4, delta-like-4 ligand; EGFL7, epidermal growth factor ligand-7; ROBO4, roundabout homologue-4(from Adams et al., 2007).

1.3 VEGF/VEGFR2: the master regulator of sprouting angiogenesis

Vascular endothelial growth factors (VEGFs) are crucial regulators of vascular development during embryogenesis as well as of angiogenesis in the embryo and in the adult life. VEGF is also recognized as the major factor inducing tumor angiogenesis (Ferrara et al., 2003). VEGF family consists of five distinct secreted proteins: VEGF-A, VEGF-B, VEGF-C, VEGF-D, and Placental Growth Factor (PlGF). In terms of endothelial biology and tumor angiogenesis, VEGF-A is considered the most physiologically relevant form. The human VEGF-A gene is expressed in at least 5 different isoforms that derive from alternative splicing variants. The more common isoforms are termed VEGF-A121, VEGF-A145 VEGF A165, VEGF-A189, VEGF-A206, based on the number of amino acids (Tischer et al., 1991).

Three different tyrosine kinase receptor (RTK) are able to bind the VEGFs protein. VEGFR1 (also called Flt1 in the mouse) is expressed in vascular endothelial cells at relatively high levels throughout development and in the adult. It is activated in response to binding of VEGFA, VEGFB and PlGF. The affinity of VEGFR-1 for VEGF is ten-fold higher than VEGFR-2 but its tyrosine kinase activity is ten-fold weaker compared to VEGFR-2 (Koch et al., 2011). VEGFR2 (also known as KDR in the human and Flk1 in the mouse) is the receptor that binds VEGFA but also VEGFC and VEGFD. A soluble form of this receptor (sVEGFR2) is expressed by alternative splicing in various tissues such as the skin, heart, spleen, kidney and ovary, and in plasma, where it acts as decoy by preventing the binding of the ligand to other receptor (McColl et al., 2003). VEGFR3 (also denoted Flt4), is activated by the binding of VEGFC and VEGFD. In the endothelium, VEGFR3 is expressed in venous endothelial cells in the cardinal vein, which subsequently gives rise to VEGFR3-expressing lymphatics during a

later stage of embryogenesis. VEGFR3 is also expressed in non- endothelial cells such as osteoblasts, neuronal progenitors and macrophages.

VEGFR2 SIGNALING PATHWAY

Binding of VEGF to VEGFR-2 promotes receptor dimerization, allowing auto-phosphorylation of intracellular tyrosine residues. Auto-phosphorylation occurs in trans: one kinase of the dimer catalyzes the phosphorylation of tyrosine residues in the other, and vice versa. Among the 19 tyrosine residues present in the intracellular domain of VEGFR-2, five are the major phosphorylation sites: Y951, Y1054, Y1059, Y1175, and Y1214. The Y1054 and Y1059 are critical for receptor catalytic activity (Kendall et al., 1999). Y951 serves as a binding site for T-cell specific adaptor (TSAD) also known as VEGFR-2 associated protein (VRAP) (Matsumoto et al., 2005; Wu et al., 2000). The Y1175 and Y1214 are located in the carboxy-terminal domain. The phosphorylation of Y1175 is well recognized as a critical mediator of VEGFR-2 signaling. This residue creates a binding site for PLCγ (Chem, 2000), p85 subunit of PI3K (Dayanir et al., 2001), the adaptor proteins SHB (Holmqvist et al., 2004) and SCK (Warner et al., 2000). Phosphorylated Y1214 has been described to bind the adaptor protein NCK (Lamalice et al., 2006).

VEGFR-2 activation initiates several intricate signaling pathways which lead to different endothelial responses: cell survival, proliferation, migration, invasion into the surrounding tissue, vascular permeability and vascular inflammation (Takahashi et al., 1999). These responses involve the activation of different effectors, such as phosphoinositide 3 kinase (PI3K), phospholipase Cγ (PLCγ), SRC, focal adhesion kinase (FAK), Rho family of GTPases.

1.4 MicroRNAs: biogenesis and functions

MicroRNAs (miRNAs) are a class of small (17–25 nucleotide) endogenous single-stranded noncoding RNAs that control gene expression by promoting degradation or repressing translation of target mRNAs. miRNAs have emerged as key post-transcriptional regulators of gene expression in several biologic processes and in different organism such as animals, plants, and unicellular eukaryotes (Boyer et al., 2006; Bartel et al., 2004; Molnar et al., 2007).

miRNAs are highly evolutionary conserved; in human it is predicted that miRNA account for 1- 5% of genome and regulate at least 30% of protein-coding genes (Rajewsky, 2006; Liu et al., 2007; Berezikov et al., 2005; Stanczyk et al., 2008). Based on their genomic location, miRNAs can be classified in four groups: intronic miRNAs in noncoding transcription units; exonic miRNAs in noncoding transcription units; intronic miRNAs in protein-coding transcript units or exonic miRNAs in protein-coding transcripts. About one-third of miRNA genes are located in the introns of protein-coding genes (Rodriguez et al., 2004; Smalheiser et al., 2005). However, in humans approximately 50% of known miRNAs are found in clusters and are transcribed as polycistronic primary transcripts (1Lagos-Quintana et al., 2001; Lau et al., 2001). In this group of miRNAs, the same genomic cluster encodes for a family of several identical, or closely related, mature miRNAs. Therefore, it is expected that a certain degree of redundancy would exist among miRNAs; the simultaneous expression of similar miRNAs possibly leads to a synergistic effect in the regulation of some target genes (Abbott et al., 2005, Miska et al., 2007). There are usually two or three genes per cluster and the largest cluster, at 13q31, is composed of seven (C alin et al., 2004; He et al., 2005).

microRNAs are transcribed by RNA polymerases II and III; the biogenesis of miRNAs represents a series of sequential processes that generate the mature miRNAs form. Two cleavage processes are required for miRNAs maturation, one in the nucleus and one subsequent in the cytoplasm, performed by two distinct *ribonuclease III endonucleases* that are Drosha and Dicer (Yoontae et al., 2004).

Primary miRNAs (pri-miRNAs) are initially transcribed from the intergenic or intragenic regions. In the nucleus these pri-miRNAs are excised by Drosha to produce a specific stem– loop or hairpin precursor. The resulting stem– loop precursor, also called pre-miRNA, seems to be a signature motif for all dsRNAs that are involved in the small-RNA pathways. Exportin-5 recognizes this signature motif and exports pre-miRNAs to the cytoplasm through nuclear pores on a GTP– GDP gradient. In the cytoplasm, pre-miRNAs are additionally processed by Dicer into 21-14 nucleotide long duplex miRNAs. The strand designated to be the mature sequence is then loaded onto Argonaute proteins, forming the miRNA induced silencing complex (RISC). There is still a great deal of uncertainty regarding the exact composition of the miRNA complex. The core component of the mRNP complex is the Argonaute protein and in mammals one of the four Argonaute proteins (AGO1-4) is recruited into the complex. AGO2 is the only Argonaute with “slicer” activity and is responsible for the cleavage of the mRNA target midway into the complementary region. Other proteins are also essential for this silencing complex to work, such as the RNA-binding protein fragile-X-mental-retardation protein (FMRP), the p-body marker GW182, and the decapping activator RCK/p54, which likely dictate how the silencing of the mRNA target will occur (Izabella et al., 2010). The miRNA-RISC complex can control target gene expression basically with two mechanisms of post-

transcriptional silencing, depending on the degree of complementarity between the miRNA and the target: translation inhibition or mRNA destabilization and degradation (Leigh-Ann et al., 2010).

In case of perfect or near-perfect complementarity to the miRNA, target mRNAs can be cleaved (sliced) and degraded (Hutvagner et al., 2002, Martinez et al., 2004). For silencing process, RISC must contain the AGO2 protein that is capable of endonucleolytic cleavage. (Liu et al., 2004; Meister et al., 2004; Okamura et al., 2004). In most cases of miRNAs base-pair imperfect complementarity with their targets genes, they promote translational repression rather than cleavage and degradation. In this mode of repression, target mRNAs are not actively degraded but can be destabilized owing to de-adenylation and subsequent decapping (Behm-Ansmant et al., 2006; Giraldez et al., 2006; Jaclson et al., 2007; Wu et al., 2006).

The mechanism of translational repression by miRNAs remains unclear. There is evidence that miRNAs block translation initiation, whereas other studies suggest a block in elongation (Humphreys et al., 2005; Nottrott et al., 2006; Petersen et al., 2006).

1.5 Long non-coding RNAs characterization

Long noncoding RNAs (lncRNAs) are regulatory RNA molecules longer than 200 nucleotides with poor protein coding potential. They are usually considered collectively as a heterogeneous class of RNAs; most of them are generated by RNA polymerase II, the same transcriptional machinery for other mRNAs, as evidenced by RNA polymerase II occupancy and histone modifications associated with transcription initiation and elongation (Guttman et al., 2009). These lncRNAs have a 5' terminal methyl guanosine cap and are often spliced and polyadenylated. However, there are also alternative pathways that contribute to the generation of known lncRNAs: a still poorly characterized contingent of non-polyadenylated lncRNAs is likely expressed from RNA polymerase III promoters (Kapranov et al., 2007; Dieci et al., 2007), while several lncRNAs are excised during splicing and small nucleolar RNA production (Mercer et al., 2013). lncRNAs share the same basic structural features with mRNAs that undergo protein translation (Cabili et al., 2011). The lack of an extended open reading frame (ORF) is the unique theoretical discerning tool to discriminate a lncRNA from a protein coding transcript (Dinger et al., 2008). However, although the ability to encode a protein does not necessarily preclude a transcript from having a regulatory function (bi-functional RNA), demonstration of function may be ultimately required for annotation as a lncRNA.

LncRNAs genes have been found to be located in both eukaryotic and prokaryotic genomes (Niazi et al., 2012). However, unlike protein-coding genes which are usually conserved across the species, most lncRNAs are poorly conserved (Wang et al., 2004). The firsts cDNA libraries obtained with a large-scale sequencing approach have revealed an unexpected abundance of lncRNAs

(Carninci et al., 2005). Currently it is still difficult to gauge an exact number of human lncRNAs. GENCODE consortium within the ENCODE project has interpreted an extensive collection of human lncRNAs. Based on this project, lncRNA genes are the biggest class of lncRNA genes that have been annotated in humans so far (Kornienko et al., 2013).This collection includes 9277 manually annotated lncRNA gene loci, producing 14,880 lncRNA transcripts (Derrien et al., 2011, Pauli et al., 2012). Furthermore, whereas the number of known human protein coding genes has remained stable over recent years, the annotation of lncRNAs within databases is a very dynamic process because of actively increasing knowledge in this field. Increasing experimental evidences and a number of detailed RNA sequencing studies have revealed that lncRNA are preferentially expressed in a tissue-specific manner. This peculiar expression makes difficult to robustly detect and to achieve comprehensive annotations of lncRNA, and requires specific sequencing projects for different developmental stages and tissue types (Cabili et al 2011; Mercer et al., 2009).

lncRNAs are expressed generally in lower amounts compared to their protein-coding counterparts. According to their proximity to protein-coding genes in the genome, lncRNAs had been categorized into five different biotypes (Ponting et al., 2009; Kapranov et al., 2007):

- Sense - The lncRNA sequence overlaps with the sense strand of a protein coding gene.
- Antisense - The lncRNA sequence overlaps with the antisense strand of a protein coding gene.
- Bidirectional - The lncRNA sequence is located on the opposite strand from a protein coding gene whose transcription is initiated

less than 1000 base pairs away.

- Intronic - The lncRNA sequence is derived entirely from within an intron of another transcript. This may be either a true independent transcript or a product of pre-mRNA processing
- Intergenic - The lncRNA sequence is not located near any other protein coding loci.

1.6 The theory of Complex networks

To completely understand the complexity of a biological system it is necessary to examine the structure of cells and organisms, and their underlying molecular dynamics, at a global level, rather than isolated parts. The recent theory of complex networks constitutes a particularly promising possibility to characterize and model the intricate structures that govern the biological process. By means of a holistic approach, where the 'omics data find wide use, network theory aims to describe complex interactions and the effects of those interactions on a global scale, linking hundreds of different biological molecules simultaneously.

The early history of complex network theories can be traced back at graph theory, founded by Leonhard Euler in 1736 and then developed, among others, by Barabási and Albert in recent times (1999). However only very recently the research on complex networks has been applied to fundamental areas such as economics, linguistics, medicine, social sciences technology, transport and biology. Complex networks research has progressed steadily in the last 10 years to become one of the most promising and dynamic scientific areas (Boccaletti et al., 2006; Costa et al., 2017; Newman, 2003). One of the reasons for the impressive popularization of complex networks research consist in its intrinsic potential to represent virtually any system composed of discrete elements. Fortunately, most natural and biological systems are indeed discrete and can be represented as networks. For instance, in a protein-protein interaction network each protein is represented as a node, while the possible interactions between proteins are expressed as edges between respective nodes.

Many natural networks are well approximated by *scale-free network* models. Compared to a random network, the scale-free network has a very different kind of connectivity because the degree distribution is defined by a power law distribution and not by a Poisson distribution that is normally associated with a random network. The main difference between a random and a scale-free network comes in the tail of the degree distribution. In a power law distribution, most nodes have relatively few links but a few nodes (called hubs) have a high number of links. In a random network most nodes have comparable degrees and hence hubs are forbidden. Hubs are not only tolerated, but are expected in scale-free networks. The contribution of the hubs to the overall connectivity is very high. The connectivity contribution of the nodes with fewer links is much lower. To summarize, in a simplified way, the features that differentiate scale-free networks from random networks are:

In scale-free networks hub nodes contribute heavily to connectivity. In a random network, each node contributes approximately the same to the overall connectivity of the network.

More nodes a scale-free network has, the larger are its hubs. Indeed, the size of the hubs grow polynomially with network size, hence they can grow quite large in scale-free networks. In contrast, in a random network the size of the largest node grows logarithmically or slower with N, implying that hubs will be tiny even in a very large random network.

In a scale-free networks, any two arbitrarily chosen nodes, even in a very large network, can be connected via few other intermediary nodes.

The scale-free name captures the lack of an internal scale, a consequence of the fact that nodes with widely different degrees coexist in the same network. This feature distinguishes scale-free networks from lattices, or from random networks, whose degrees vary in a narrow range.

Scale-free networks are "self-similar". Any part of the network is statistically similar to the whole network. Self-similarity is the key feature of fractals.
A scale-free network is "robust". It can still operate with a random removal of a few nodes.

Why the naturally occurring complex systems tend to self-organize themselves into scale-free networks is not clear at present, but the power law connectivity distribution appears to emerge as one of the important phenomena of patterns in nature. To understand the properties of real networks, it is often sufficient to remember that in scale-free networks a few highly connected hubs coexist with a large number of small nodes and the presence of these hubs play an important role in the system’s behavior (Albert - Laszlo).

AIM OF THE STUDY

SA is a broadly studied process, the knowledge about the molecular basis that sustain SA is progressively increased. Currently, several molecules and different signaling pathways are described to be essential in the regulation of this process. Available data are largely based on an approach designed to study the role of single molecules, however, the coordination of the different cellular activities implicated in SA requires the combined action of multiple players, controlled through multiple layers of regulation including both transcriptional and miRNA-mediated post-transcriptional activity. Several miRNAs have been already associated with SA, but the work on lncRNAs is still in its infancy. Nonetheless, the extent to which miRNAs activity globally affects all the biological pathways during SA has not been explored so far. Furthermore, the increase of knowledge about the molecular mechanisms involved in SA has not been accompanied by an improvement in the efficacy of anti-angiogenic therapies; current anti-angiogenic therapies are still largely based on the inhibition of VEGF activity. There is therefore an urgent clinical need to better understand the complexity of vascular formation, and to identify new molecules useful for targeting tumor angiogenesis.

To develop new therapeutic strategies, the molecular complexity that sustain angiogenesis should be addressed by comprehensive studies, by taking into consideration the multiple layers of transcriptional and post-transcriptional activities controlled by coding and non-coding RNA. For this purpose, the interdisciplinary work was devoted to: I) generate a systematic annotation of the coding and non-coding transcriptome in endothelial cells in a 3D model of SA; II) describe, at the transcriptional level, the biological processes implicated

in SA dynamics, based on a multi-gene systems view rather than a single-gene/molecule approach approach; III) generate an integrated and systematic description of the microRNA-mediated regulatory processes that sustain SA in order to identify new biologically relevant key molecules to be exploited for clinical applications. Finally, since lncRNAs biology represents a highly innovative and unexplored area of research, we were also interested in IV) to characterize the role of some unknown lncRNAs in the regulation of SA.

2. A regulatory miRNA network controls endothelial cell phenotypic switch during sprouting angiogenesis.

MicroRNAs (miRNAs) are a class of small non-coding RNAs that extensively modulate gene expression at the post-transcriptional level by targeting the mRNAs of protein-coding genes (PCGs), directing their repression through mRNA degradation or (to a lesser extent) inhibition of protein translation (Guo et al., 2010).

A role for miRNAs in ECs biology and vascular development has been established in vitro and in vivo by inhibition of two endonucleases that are required for mature miRNAs generation, namely Dicer and Drosha (Ha and Kim, 2014). The consequent reduction in the level of miRNAs resulted in alteration of several key properties of ECs, including their sprouting ability (Kuehbacher et al., 2007), and impaired postnatal angiogenesis (Suárez et al., 2008). The activity of specific miRNAs in connection with the VEGF signaling pathway components has been studied more extensively (Dang et al., 2013). Several studies have demonstrated that miR-15a and miR-16, among other miRNAs, repress VEGF expression (Chamorro-Jorganes et al., 2011; Yin et al., 2012), whereas miR-126 promotes VEGF signaling by targeting the downstream effector PIK3R2 (Fish et al., 2008). Furthermore, miR-27b and miR-221 are required for tip cell specification (Biyashev et al., 2012; Nicoli et al., 2012).

As described before, various events are involved in angiogenesis, including ECs division, degradation of the basal membrane and the surrounding extracellular matrix, ECs migration and the formation of neo vessels (Berthod F., 2013; Duscha et. al., 2013; Santulli et al., 2014). miRNAs can affect all these functions.

Numerous studies investigated the mechanistic role of miRNAs in the regulation of angiogenesis. The following table summarizes miRNAs with known pro-or anti-angiogenic effect.

Pro-angiogenic miRs	**Target gene**	**Ref.**
miR-9	*SOCS5*	Zhuang et al. (2012)
miR-10a	*MAP3K7; HOXA1; bTRC*	Fang et al. (2010)
miR-21	*STAT3*	Liu et al. (2015)
miR-23/27	*SEMA6A; SPROUTY2*	Zhou et al. (2011a)
miR-107	*DICER1*	Li et al. (2015)
miR-126	*PI3KR2; SPRED1;VCAM1; SDF1*	Nicoli et al. (2010)
miR-130	*HOXA5, GAX*	Li et al. (2015)
miR-132/212	*RASA1, SPRED2*	Lei et al. (2015)
miR-210	*EFNA3*	Wang et al. (2013)
miR-217	*SIRT1- FOXO/eNOS*	Menghini et al. (2009)
miR-424	*HIF-1α*	Kim et al. (2013)
miR891a-5p	*NF-κB*	Yao et al. (2015)
Anti-angiogenic miRs		
miR-17	*JAK-1*	Katz et al. (2014)
miR-21	*RhoB;PPARγ*	Zhou et al. (2011b)
miR-24	*GATA-2; PAK4*	Zhou et al. (2014)
miR-92a	*SIRT1; ITGA5; KLF4* and *MKK4*	Ohyagi-Hara et al. (2013)
miR-200	*Ets-1; IL-8; CXCL1*	Chan et al. (2011)
miR-221/222	*STA5a; c-KIT; eNOS*	Nicoli et al. (2012)
miR-492	*eNOS*	Patella et al. (2013)
14q32 miR cluster (329, 487b, 494, 495)	Multiple neovascularization genes	Welten et al. (2014)
miR-497	*VEGFR2*	Tu et al. (2015)
miR-505	*FGF18*	Yang et al. (2014)
miR-506	*SPHK1*	Lu et al. (2015)

Results

2.1 Global transcriptomic profile of Endothelial cells in a 3D model of Sprouting Angiogenesis

The expansion of a vascular network through the SA process requires in its different phases an orchestrated control of several cellular functions, including the activation of quiescent ECs, cell protrusion, basal lamina and extracellular matrix degradation, cell migration and proliferation, deposition of new basement membrane and activation of several metabolic pathways (Carmeliet and Jain, 2011). The coordination of these activities is precisely controlled by multiple signal pathways regulated at transcriptional level. During SA, ECs dynamically switch from a tip phenotype, which guides the network expansion, to a stalk cell state that is characterized by active proliferation. Nevertheless, the gene expression regulatory events that sustain the initial transition from quiescent to activated ECs in response to an angiogenic stimulus have not yet been fully elucidated. We hypothesized that such phenotypic transition would require profound transcriptomic alterations that are brought about through the coordination of multiple regulation layers, including microRNA-mediated post-transcriptional regulation. To fully capture the phenotypic changes occurring in ECs during SA in its complexity, we exploited a three-dimensional (3D) model that mimics the initial phase of SA in vitro (Heiss et al., 2015; Nowak-Sliwinska et al., 2018). In this model, human umbilical vein cells (HUVECs) are induced to form three-dimensional aggregates, or spheroids, to mimic the endothelial quiescent state (Weidemann et al., 2013). Spheroids are then embedded in a 3D collagen matrix and exposed to Vascular Endothelial Growth Factor-A (VEGF-A) to trigger the angiogenic sprouting (Figure 2A). For RNA-Seq experiments, after 18 hours from stimulus collagen matrix was digested, cells were collected and

total RNA from quiescent (SPHC) or stimulated spheroids (SPHV) was extracted and then processed for long- and small- RNAseq. The information obtained was used to generate a co-expression network encompassing the post-transcriptionally regulated interactions between modulated miRNAs and their predicted protein-coding gene targets.

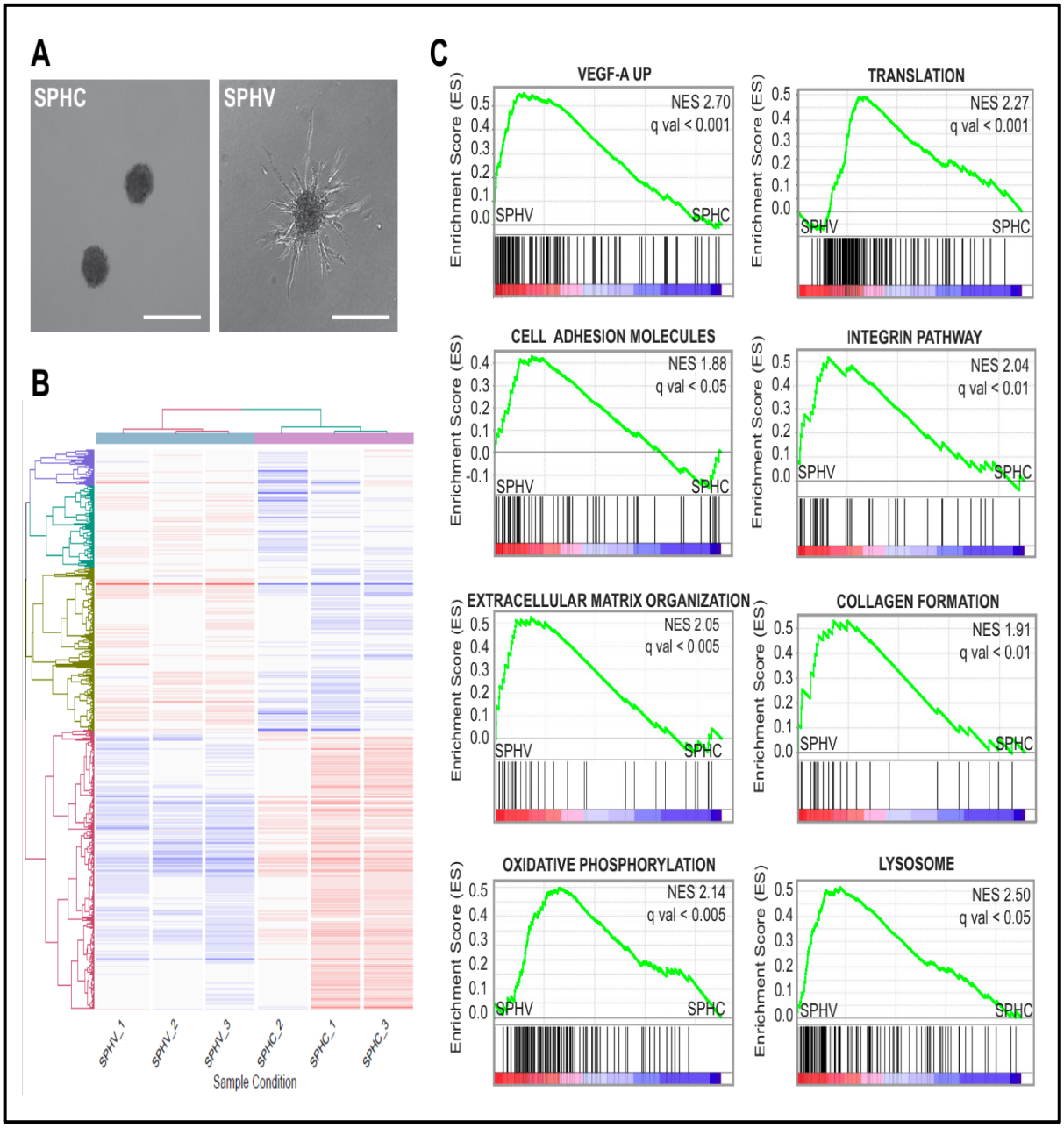

Figure 2. Analysis of PCGs in the 3D model of sprouting angiogenesis.

(A) VEGF-A induces the tip phenotype of endothelial cells in a 3D model of sprouting angiogenesis. (B) Heatmap of differentially expressed PCGs in SA. Red and blue color of the gene (rows) indicates the upregulation or downregulation respectively. (C) Positively enriched gene sets identified by the GSEA study in the gene sets collection of the canonical pathways, with an FDR < 0.05.

2.2 Transcriptomic analysis of protein coding gene and identification of significant biological pathways

Transcriptomic analysis of mRNA data allowed us to detect the expression of 11,059 protein-coding genes (PCGs) in ECs with TPM > 1 (in every sample). Differential expression analysis identified 3517 genes (log2FC > 0.5, pval < 0.05) with altered expression in the comparison between spheroids exposed to VEGF-A (SPHV) and control spheroids (SPHC), thus revealing dramatic changes in the global transcriptomic profile of PCGs during sprouting (Figure 2B). To identify key regulatory pathways involved in the angiogenic process, the gene expression profiles from the two experimental conditions were further investigated by Gene Set Enrichment Analysis (GSEA) (Subramanian et al., 2005). This analysis revealed a positive enrichment for genes up-regulated by VEGF-A stimulation, as expected, and for several biological pathways and classes of molecules such as 'Translation', 'Cell adhesion molecules', 'Integrin pathway', 'Extracellular matrix organization' and 'Collagen formation'. This highlights that the migration has a prevalent role in the ongoing process (Figure 2C). GSEA also revealed a strong positive enrichment in gene related to 'Oxidative phosphorylation' and 'Lysosome' in spheroids stimulated compared to control spheroids. This was an interesting and surprising observation, since the previous studies that focused on the role of metabolism in angiogenesis demonstrated that the EC energetic balance relies predominately on glycolysis for ATP production rather than on oxidative phosphorylation.

VEGF-A plays a fundamental role in angiogenesis and endothelial cell biology. Activation of the VEGF/VEGF-receptor pathway initiates signaling cascades that promote, among others EC proliferation. Unexpectedly, in our 3D model GSEA

showed a strong negative association with the cell cycle signature (Figure 3A), suggesting an impairment of cell cycle progression after VEGF-A stimulation. By looking at the expression data of genes directly involved in the cell cycle control, we found that 50 out of 113 genes were downregulated in SPHV compared to SPHC (Figure 3B). The finding that VEGF-A did not activate the proliferation of ECs was also confirmed by the negative ES of gene sets that are representative of pyrimidine metabolism (Figure 3C) and purine metabolism (Figure 3D).

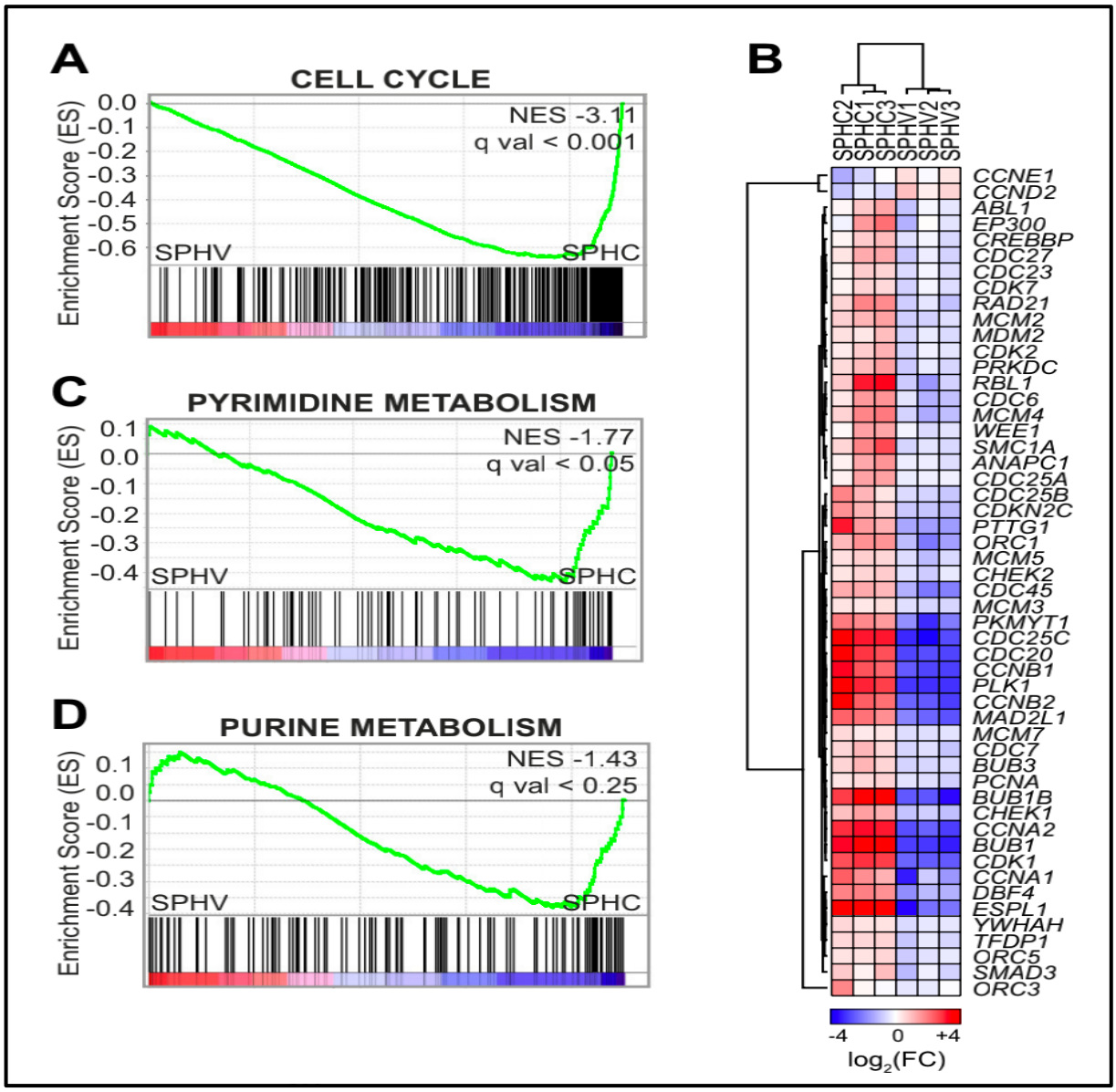

Figure 3. The initial phase of sprouting process does not rely on cell proliferation.

(A) GSEA plot showing negative association with the 'cell cycle' gene set in SPHV compared to SPHC. (B) Heatmap representing differentially expressed genes involved in the 'cell cycle' KEGG pathway. Color bar indicates the log2(fold change). (C, D) GSEA plots showing negative association with 'pyrimidine metabolism' and 'purine metabolism' gene sets in SPHV vs SPHC.

2.3 Transcriptomic analysis of microRNAs in sprouting angiogenesis

microRNAs (miRNAs) are a class of small non-coding RNAs that function as negative regulators of gene expression in sequence-specific manner. In ECs, many miRNAs are expressed, and several of them demonstrated that they could regulate different aspects of vascular physiology and angiogenesis. Currently, many specific miRNAs are known to annotate the pro- and anti- angiogenic effects (Santulli et al., 2012), but a comprehensive annotation of miRNAs expressed by ECs is still missing, and current knowledge is not sufficient to dissect the complexity of the miRNA-mediated gene regulatory network that globally affect the process of SA.

Analysis of the small-RNAs sequencing data allowed the annotation of 643 mature miRNAs expressed by ECs across the two experimental conditions, at fixed cutoff (RPM > 1). By comparing miRNA expression profiles between SPHV and SPHC, we found 128 differentially expressed miRNAs, 59 of which were upregulated and 69 down regulated (Figure 4). Some differentially expressed miRNAs, such as miR-210, miR-24-3p, miR-329 and miR-324 have been already associated to specific functions in ECs and angiogenesis (Chamorro-Jorganes et al., 2016; Fasanaro et al., 2008; Kasza et al., 2013; Welten et al., 2014). However, for the majority of them their interaction with the coding genes and role in specific biological process in ECs still remains unknown.

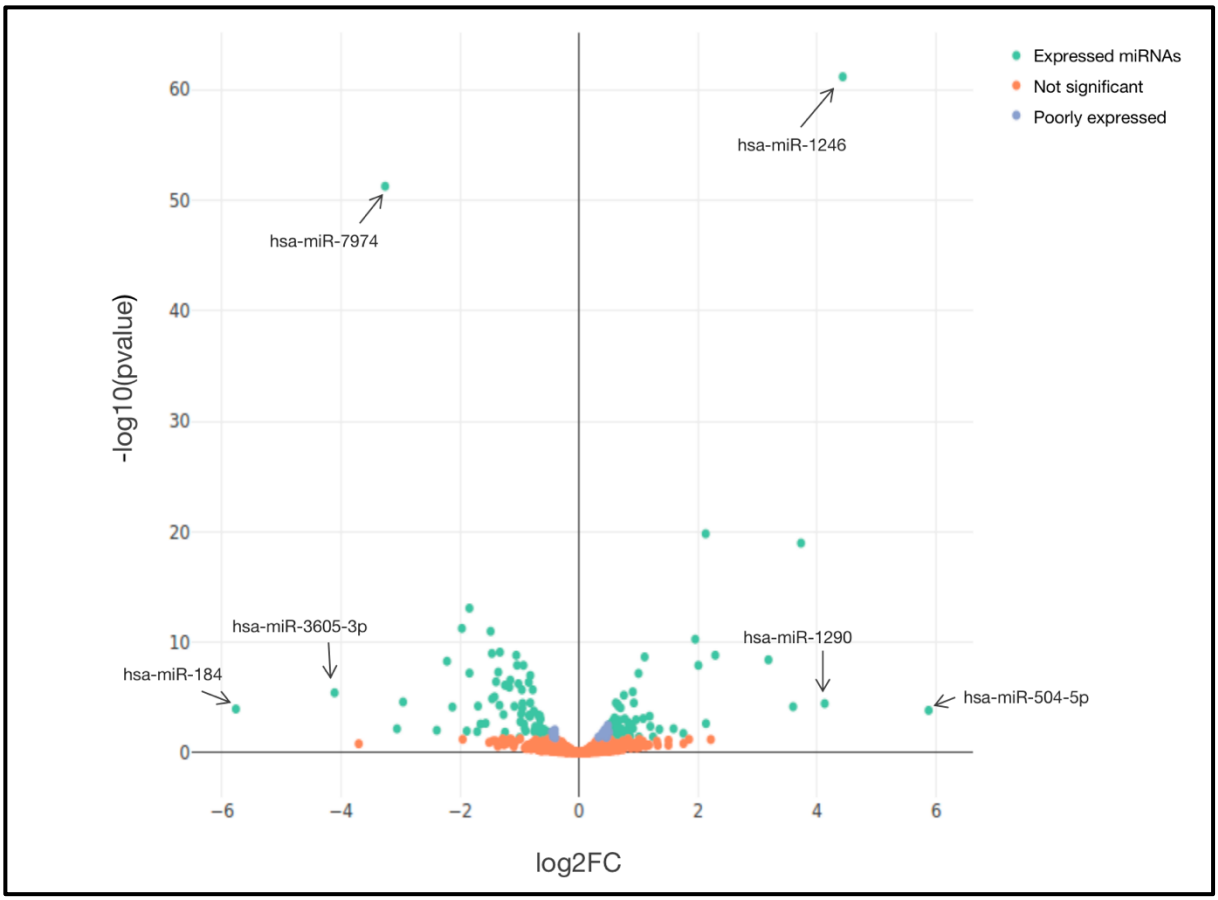

Figure 4. Analysis of miRNAs in sprouting angiogenesis.

Volcano plot showing 128 differentially expressed miRNAs in SPHV versus SPHC, 59 of which were upregulated and 69 down regulated.

2.4 A miRNA – dependent post – transcriptional regulatory network

To access the impact of miRNAs on ECs during SA, we applied a bioinformatics pipeline based on the co-expression analysis of miRNAs and PCGs, miRNA target prediction, association of miRNAs with biological pathways, followed by network analysis (Figure 5A).

We first analyzed the Pearson correlation between miRNA & PCGs, then plotted a distribution of the correlator (Figure 5B). We then isolated the subset of pairs that contained the evolutionary conserved miRNA-target interactions (MTIs), based on TargetSCAN prediction (Agarwal et al., 2015). The distribution of the correlator showed a significant negative enrichment for the conserved interactions subset as compared to the entire dataset (Figure 5B, blue line). This is an indicative of the repressive activity exerted by the miRNAs on their targets, i.e., when a miRNA is upregulated its corresponding PCG target in downregulated and vice-versa. Considering that target-site conservation is believed to be an indication of functional repression (Friedman et al., 2009), the integration of the SA gene expression dataset with the miRNA - target prediction results provide information on the global activity of miRNAs taking place during the early sprouting phase.

GSEA-based correlation analysis between miRNA and groups of PCGs represented as gene sets, was also used to support our findings (Figure 5C). This analysis identified five clusters of gene sets representing distinct biological functions that are modulated during SA, together with their associated miRNAs. Gene ontology-based enrichment analysis performed on the genes contained in each cluster showed the following classes: 1) extracellular matrix remodeling

and cell migration, 2) protein translation and metabolic processes, 3) intracellular signaling pathways, 4) RNA and protein processing and 5) cell cycle, DNA repair and MAPK cascade (Figure 5D). Clusters 1 and 2 contained gene that are mostly upregulated in SPHV compared to SPHC, whereas clusters 3, 4 and 5 contained genes that are mostly downregulated. To generate the global post-transcriptional regulatory network that sustains SA, the results from the above analyses were integrated. The resulting miRNA-centered co-expression network is composed of 149 miRNAs and 717 protein-coding genes connected by 1713 edges (Figure 6A). The degree analysis (Figure 6B) shows that the network connectivity follows a power-law distribution, indicating that this network is compatible with the scale-free hypothesis (Barabàsi and Pòsfai, 2016).

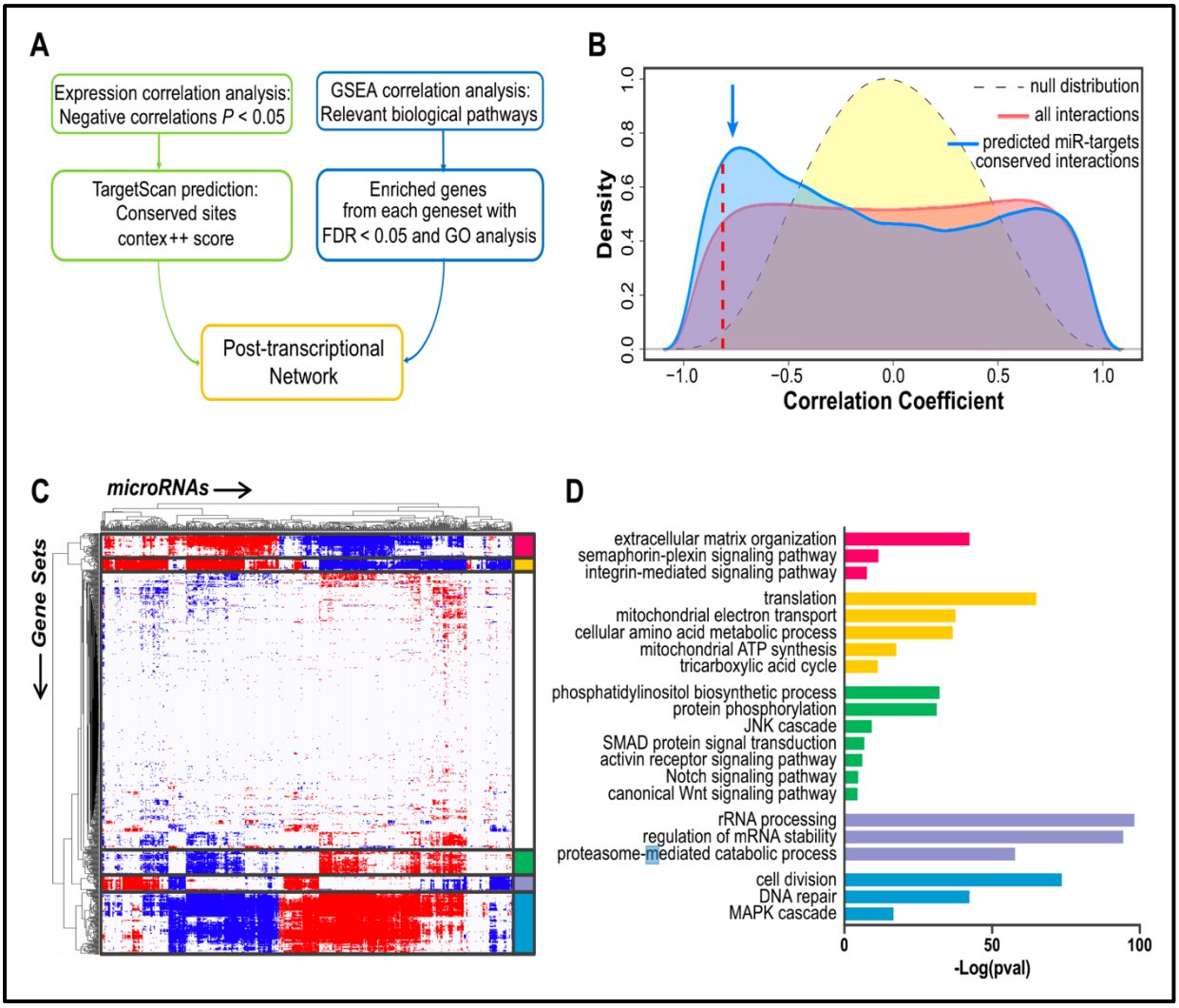

Figure 5. Construction of miRNA-dependent post-transcriptional regulatory network. (A) Computational approach used to generate the post-transcriptional regulatory network. (B) Distribution of the correlator (Pearson coefficient) of the pairwise analysis of all miRNAs and PCGs expressed in SPHC and SPHV. Red curve represents all MTIs, and the blue curve represents the conserved MTIs predicted by TargetSCAN. The blue arrow points to negative enrichment, red dashed line indicates the statistical significance threshold ($P < 0.05$). (C) GSEA coexpression analysis between miRNA profiles (columnns) and functional gene sets (rows). Significant associations (FDR < 0.05) are shown in red (positive) or blue (negative). White, not significant. Biologically relevant clusters are highlighted with different colors. (D) For each cluster in (C), gene contributing to enrichment in the correlated gene sets were analyzed by functional annotation. Graph law -Log (*P* value) of representative gene ontology terms.

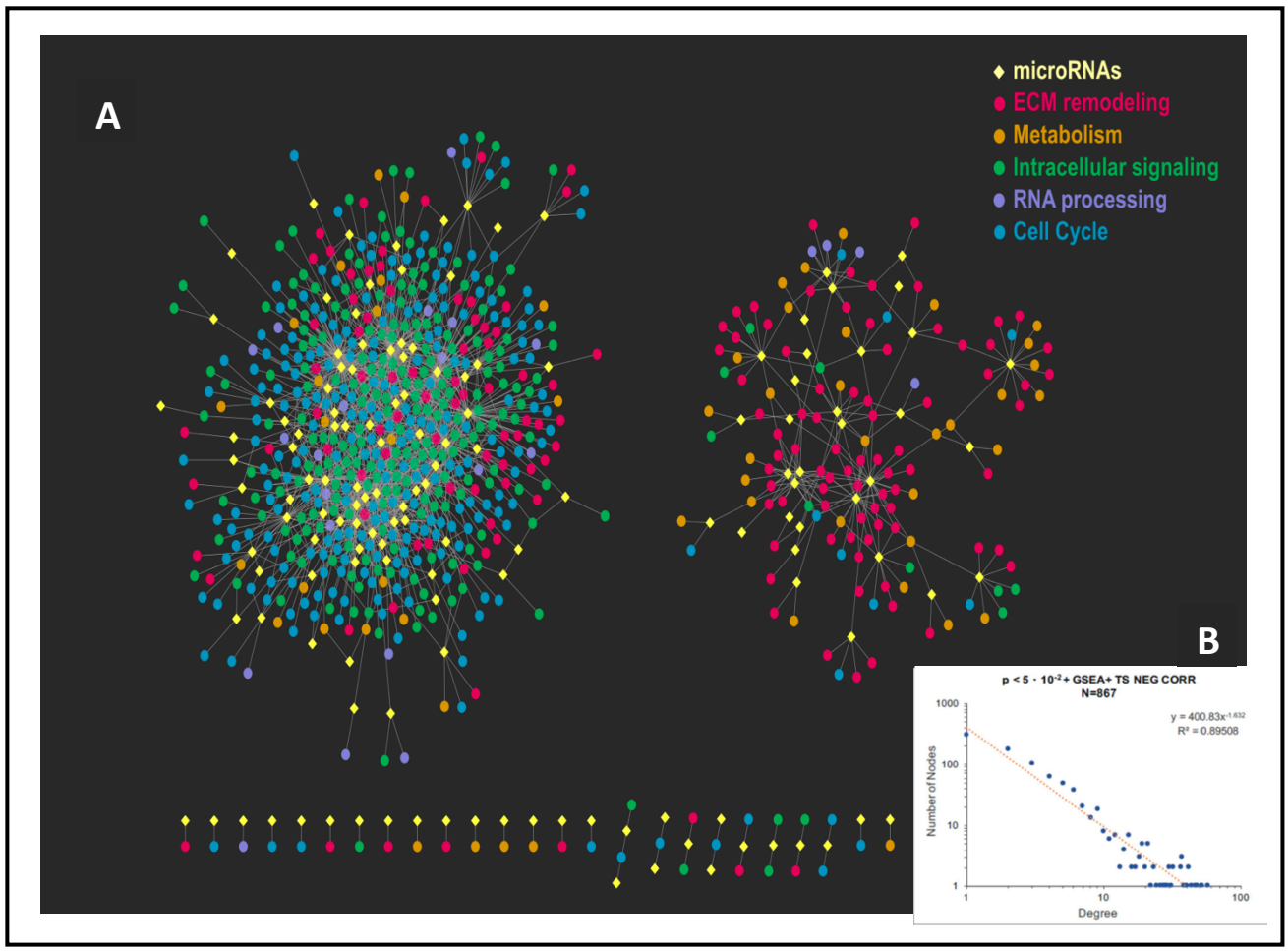

Figure 6. Graphical representation of the post-transcriptional network.

(A) The network consists of two major components; the left component includes upregulated miRNAs with downregulated target genes, while the component on the right represents downregulated miRNAs with their respective upregulated target genes. Yellow diamonds represent miRNAs and circles represent their target genes. (B) The degree analysis show that the network connectivity follows a power-law distribution.

2.5 Hub miRNA selection and network validation.

In order, to validate the information derived from the network analysis, we decided to select some representative miRNAs.

To validate the network, we selected miR-424–5p and miR-29a-3p, which are well-known miRNAs involved in angiogenesis regulation, and showed a high number of interactions with coding genes (Figure 7A, 7B). miR-424–5p was upregulated and targeted 98 genes, which were mainly related to intracellular signaling, including the MAPK pathway and cell cycle control. miR-29a-3p was downregulated and controlled the post-transcriptional regulation of 25 genes, mostly related to extracellular matrix remodeling. These MTIs are also reported in the publicly available databases miRTarBase (Chou et al., 2018), TarBase (Karagkouni et al., 2018) and StarBase (Li et al., 2014), which store miRNA–mRNA interactions supported by experimental evidence. For miR-424–5p, 97 out of 98 interactions were present in these databases (24 of them in all three databases, and 73 in one or two); for miR-29a-3p, 23 out of 25 interactions were present in the databases (7 of them in all three databases, 16 in one or two).

To assess the role of miR-424–5p and miR-29a-3p in the sprouting process, we altered their expression in ECs by using miRNA mimics or inhibitors and performed the sprouting assay (Figure 7C). Quantification of sprout areas (Figure 7D) indicated that both upregulation by miRNA mimics and downregulation by miRNA inhibitors of miR-424–5p and miR-29a-3p impaired the ability of ECs to sprout, suggesting that the equilibrium of the network architecture requires that the expression of these two hub miRNAs is maintained at controlled levels.

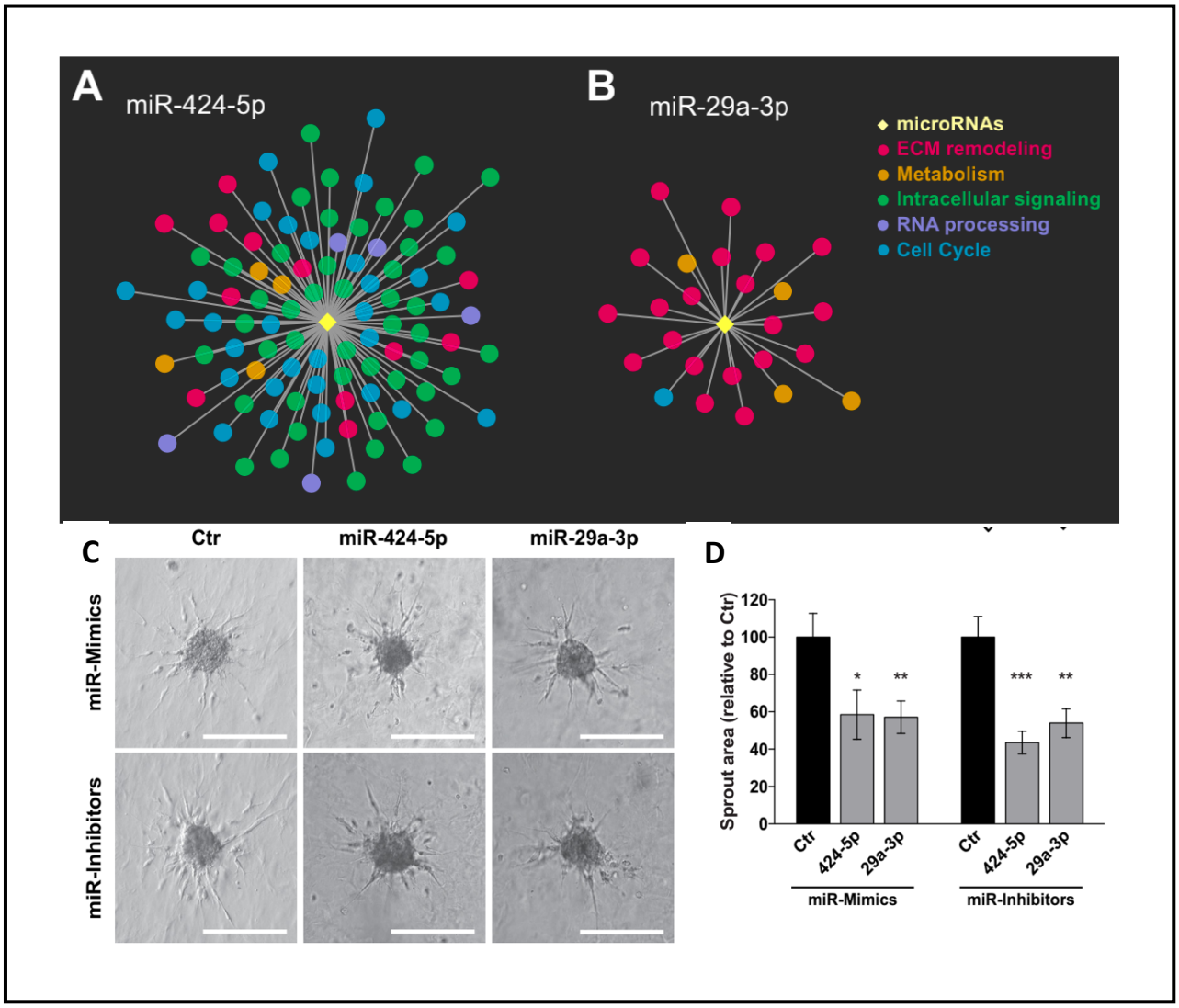

Figure 7. Hub miRNA selection and validation.

(A) Graphical representation of miR-424-5p and (B) miR-29a-3p sub-networks. (C) Sprouting assay performed with ECs transfected with miR-424-5p and miR-29a-3p mimics and inhibitors. (D) Quantification of sprout area for the cells shown in panel (C).

2.6 Discussion

In this chapter, information about the expression of miRNAs was used to generate a global post-transcriptional regulatory network based on co-expression between miRNAs and their predicted protein coding target genes. Using this unbiased approach, we were able to emphasize a role of miRNAs in repressing genes that regulate cell proliferation and other signaling pathways downstream of VEGF. Such pathways include the MAPKs signaling cascade, which is mainly involved in transducing the VEGF-A mitogenic signal. Meanwhile, miRNAs also promoted the expression of genes that are involved in extracellular matrix remodeling.

On the other hand, the coherent form of miRNA-target circuits is thought to mediate a post-transcriptional reinforcement of transcriptional regulation and is associated with negative correlation schemes of gene expression (Cora' et al., 2017). Our experimental setup intrinsically highlights and selects such negative correlations.

For the network validation, we focused on two hub miRNAs: miR-424–5p and miR-29a-3p, which belong to the network component containing up- and downregulated miRNAs, respectively. In our three-dimensional model, integration of expression data with target prediction allowed the identification of context-specific targets. In fact, miR-424–5p showed preferential targeting activity towards genes that are associated with cell-cycle progression and intercellular signaling, whereas miR-29a-3p activity was more specific to genes involved in extracellular matrix remodeling.

3. An unknown lncRNA acts as a sponge in regulating Notch signaling pathway during SA.

A peculiar "miRNA sponges" behavior was observed for some lncRNAs that function as competing endogenous RNAs (ceRNAs) for a specific miRNA. lncRNA that act as a sponge bind and sequesters a specific miRNA and the final result is the up-regulation of the miR-target mRNAs (Salmena et al., 2011; Karreth et al., 2011; Tay et al., 2011; Peng et al., 2015; Chen et al., 2015; Franco-Zorrilla et al., 2007). This activity was first described in Arabidopsis thaliana and later in mammals (Poliseno et al., 2010). In mammals, it was shown to be important in many cellular processes, and in human development; for instance, linc-ROR ceRNA function is essential for ESC pluripotency and self- renewal (Wang et al., 2013). The same is true for the muscle-specific lincMD1, which is activated in myoblasts differentiation and controls muscle development. By sequestering miR-133 and miR-135 it regulates the expression of MAML1 and MEF2C mRNAs (Cesana et al., 2011). Several experimental evidences demonstrated that ceRNA function is also implicated in malignancy and it is particular relevant during tumorigenesis (Salmena et al., 2011; Tay et al., 2014).

For example, the non-coding PTENP1 pseudogene has been described to regulate the levels of the tumor suppressor gene PTEN by competing for shared miRNAs, and it has been shown to possess tumor suppressive activity, since it is selectively lost in human cancers (Poliseno et al., 2010). Moreover, the lncRNA HULC has been identified as one of the most significantly up-regulated transcripts in hepatocellular carcinoma (HCC). Its over-expression can reduce miR-372 expression and activity in the liver cancer cell line Hep3B. The inhibition of miR-372 by HULC results in the up-regulation of its target PRKACB, thus

inducing CREB-phosphorylation and enhancing CREB-dependent HULC up-regulation in liver cancer (Wang et al., 2010).

Results

3.1 Notch signaling in sprouting angiogenesis and MAML3.

Notch signaling is one of the evolutionarily conserved pathways that regulates cell-fate determination during development. The Notch receptors, when activated by their ligands expressed on adjacent cells, mediates juxtacrine cellular signaling (Bray et al., 2006). Two Notch receptors, such as Notch-1 and Notch-4 and three Notch ligands, JAG-1, DII-1, and DII-4 are expressed in ECs (Kume et al., 2009). Notch receptors are single-pass transmembrane proteins composed of functional extracellular (NECD), transmembrane (TM), and intracellular (NICD) domains. Upon ligand binding, the NECD is cleaved away (S2 cleavage) from the TM-NICD domain by TACE (TNF-α ADAM metalloprotease converting enzyme). The NECD remains bound to the ligand and this complex undergoes endocytosis/recycling within the signal-sending cell in a myb-dependent ubiquitination. In the signal-receiving cell, γ-secretase releases the NICD from the TM (S3 cleavage), which allows for nuclear translocation where it forms a complex with CSL (CBF1/Su(H)/Lag-1) and Mastermind-like proteins (MAML1/MAML2/MAML3) to activate transcription of the canonical Notch target genes that include Myc, p21, and the HES-family members. Furthermore, MAML3 is an important target gene in our biological context, being an essential coactivator of the Notch pathway. We began by validating MAML3 expression from RNA-Seq data in our SA model.

3.2 miR-486-5p target MAML3 modulating its expression and impact in the process of sprouting angiogenesis.

Most of the miRNAs and their targets are conserved across species (Misook Ha et al., 2008. Ambros V., 2004), which means that conservation plays an important role in predicting miRNA targets. Taking this into account, we predicted miRNA target interactions (MTI's) on coding genes by TartgetSCAN (TS). The PCG of our interest - MAML3 was found to be targeted by two different miRNAs - hsa-miR-486-5p and hsa-miR-485-3p. Among these two miRNAs the first one had a higher context.score (> 90) as compared to the latter.

To further confirm whether there was a regulation of miR-486-5p on MAML3, we first analyzed the MAML3 expression in in our SA model. We found an increasing expression of MAML3 in SPHV compared to SPHC (Figure 8A); therefore, there was a negative correlation between miR-486-5p and MAML3 expression. To test if miR-486-5p can repress MAML3 through direct 3'-UTR interactions, the WT or mutated 3'-UTR of MAML3 was cloned into *pmirGLO vector* and dual luciferase reporter assays were performed in ECs cells. Co-transfection of miR-486-5p mimics and MAML3_WT repressed luciferase activity significantly, while it failed to repress the luciferase activity in cells transfected with MAML3_MUT (Figure 8B).

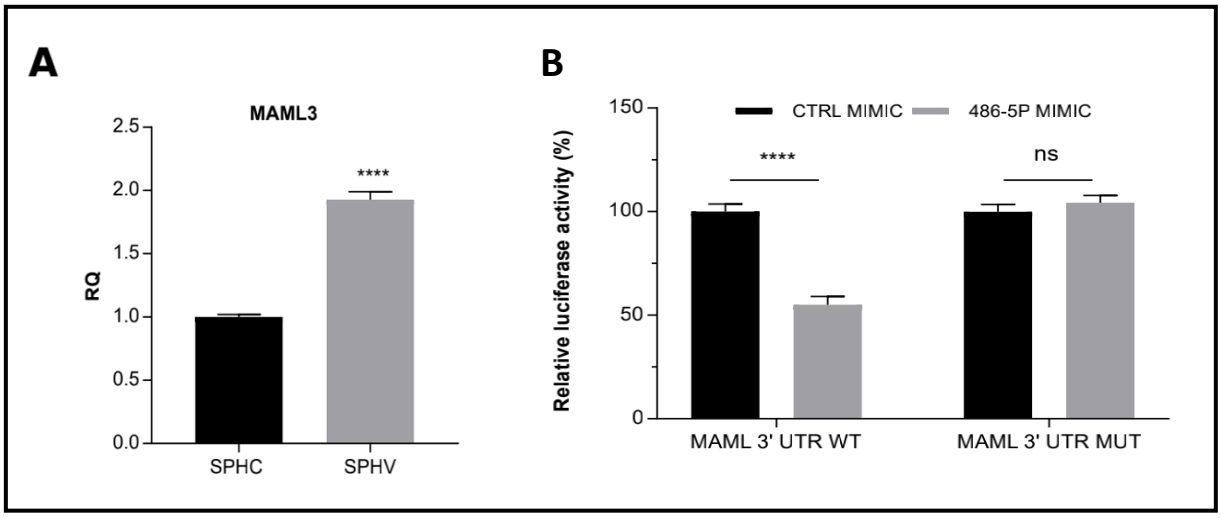

Figure 8. MAML3 expression is regulated by miR-486-5p.

(A) Validation of MAML3 in the spheroids model by real-time PCR.

(B) Luciferase reporter assay in HUVECs co-transfected with miR-486-5p mimic together with wild-type MAML 3'UTR or the mutant form in which miR-486-5p binding site has been disrupted.

3.3 LINC02802 acts as a competitive endogenous RNA for miR-486-5p

Next, we started investigating lncRNAs (transcriptomic analysis of lncRNAs explained in Chapter 4) in our sprouting model (Figure 9A) which are targeted by miR-486-5p, and since the lncRNAs seems to be poorly conserved at the sequence level, which makes the target prediction on lncRNAs a bit difficult job. Integrating more than one algorithm is a promising strategy to select true targets than using a single algorithm alone (Li Y. et al., 2013. Wang et al., 2015). Taking these considerations into account, we used MiRanda-3.3a (Enright A.J. et al., 2003) and RNAhybrid-2.1.2 (Krüger J. et al., 2006) for predicting miRNA targets on lncRNAs. MiRanda uses a weighted dynamic programming algorithm (Smith - Watermann) for predicting targets between a set of mature miRNA and mRNA. While the target prediction method for RNAhybrid is based on calculations of mRNA secondary structure and energetically favorable hybridization between miRNA and target mRNA. The miRNA – lncRNAs targets having a MiRanda score>= 130 and Energy <= -25 kcal/mol were selected for downstream analysis (Figure 9B). The analysis predicted 14 different lncRNAs targeted by our selected miRNA, from which LINC02802 had the highest MiRanda binding Score and the lowest Energy/Kcal.Mol., which thus signifies that this interaction is likely to be more stable (Figure 9C).

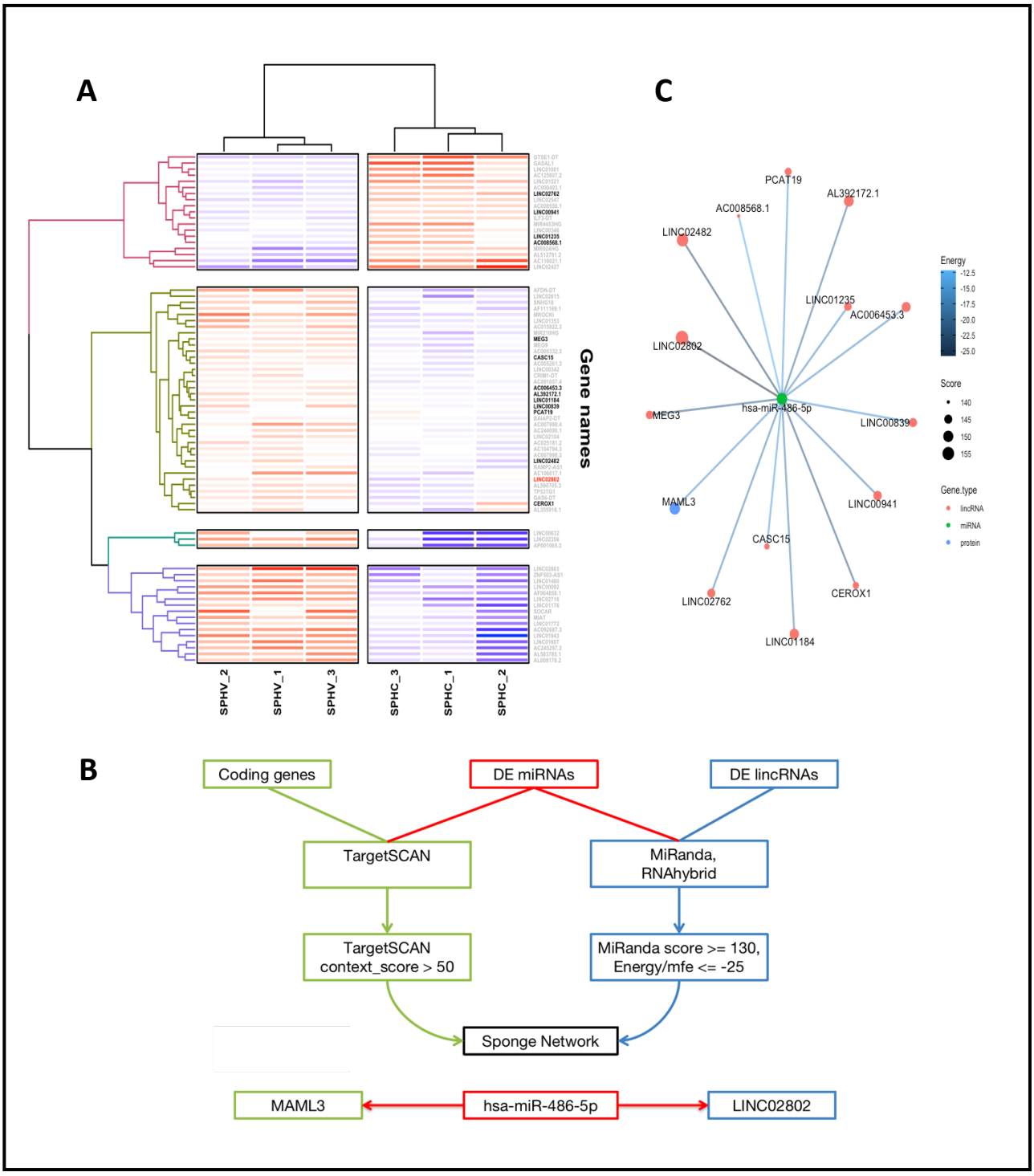

Figure 9. Expression of LINC02802 and miRNA target prediction pipeline.

(A) Differentially expressed lncRNAs in SPHV versus SPHC, 14 lncRNAs targeted by miR-486-5p are highlighted in black and LINC02802 in red. (B) Schematic representation of the computational pipeline used in miRNA target prediction analysis. (C) mRNA-miRNA-lncRNA interaction (MMLI) network, node size represents MiRanda score, edge color represents the Energy/Kcal.Mol, and node color represents the gene type.

To confirm our bioinformatic prediction, dual luciferase assay was performed to validate the direct interaction between LINC02802 and miR-486-5p. The sequence of LINC02802 was point-mutated to disrupt the binding site for miR-486-5p. Then, the wild type sequence and the mutated one were cloned downstream to the luciferase gene into a *pmirGLO Dual-Luciferase Vector*. As showed on (Figure 10A) miR-486-5p over-expression resulted in a decreased luciferase activity only when ECs cells were co-transfected with pMIR_LINC02802-WT. On the contrary, in cells co-transfected with the mutated form the inhibitory effect on luciferase was lost.

Direct interaction is also confirmed at molecular level by evaluation of the impact of miR-486-5p modulation on LINC02802 expression levels. We found that miR-486-5p over-expression significant decreased LINC02802 (Figure 10B) while specific knocked-down of miR-486-5p increased LINC02802 expression significantly (Figure 10C). Collectively, the results confirmed the interaction between LINC02802 and miR-486-5p and demonstrated that miR-486-5p negatively regulate LINC02802 expression level.

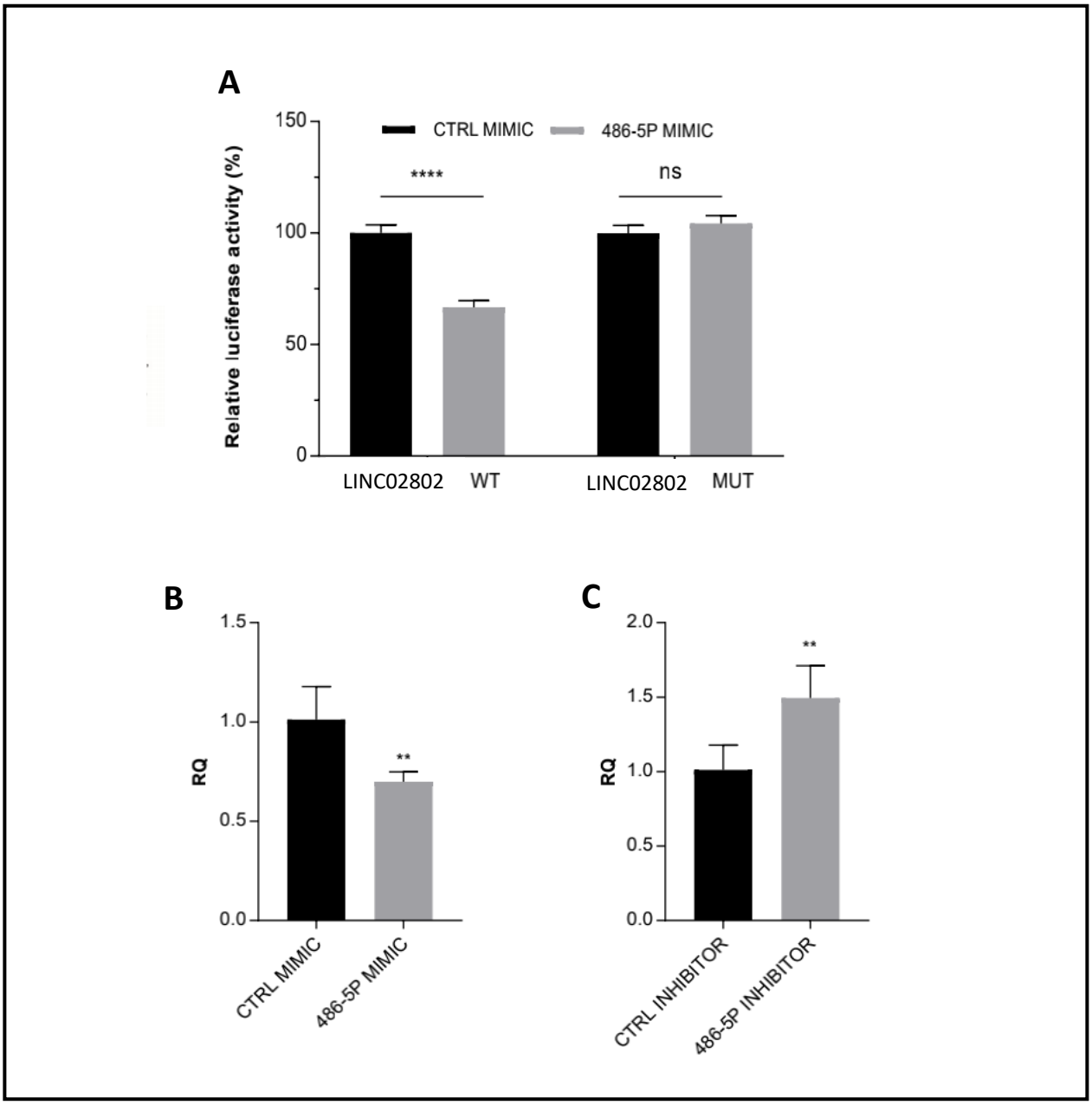

Figure 10. LINC02802 acts as ceRNA for miR-486-5p.

(A) Luciferase reporter assay in HUVECs co-transfected with miR-486-5p mimic together with wild-type LINC02802 or the mutated form in which miR-486-5p binding site has been disrupted.

(B) Sprouting assay performed with cells transfected with miR-486-5p mimic, and relative quantification.

(C) Sprouting assay performed with cells transfected with miR-486-5p mimic, and relative quantification.

3.4 LINC02802 modulate MAML3 expression.

Finally, to test if the interaction between LINC02802 and miR-486-5p, has as consequence the modulation of MAML3 expression, confirming the ceRNA hypothesis, we examined MAML3 expression subsequent to forced manipulation of LINC02802.

We found that over-expression of LINC02802 resulted in an increased expression of MAML3 but only if miR-486-5p binding site is present (Figure 11A). On the contrary, knockdown of lincRNA LINC02802 resulted in decreased expression of MAML3 (Figure 11B). Overall, these results indicate that lincRNA LINC02802 acting as a competitive endogenous RNA for miR-486-5p, controls miR-486-5p expression and as consequence impact on MAML3 expression.

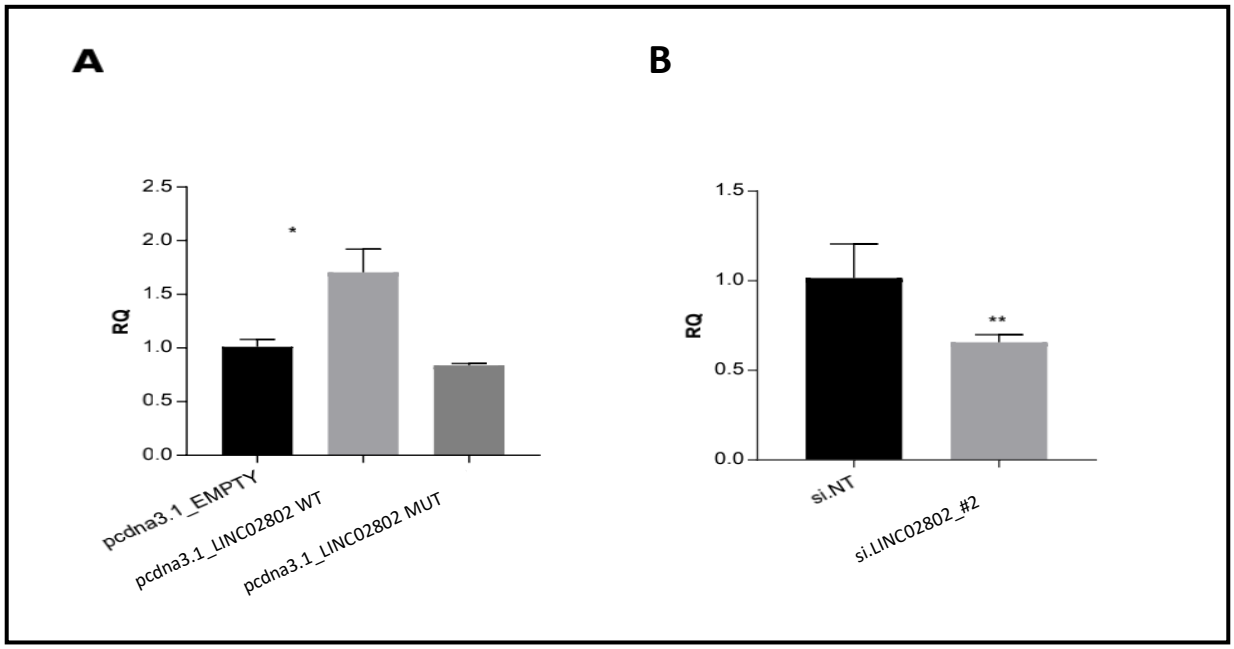

Figure 11. LINC02802 regulates MAML3 expression.

(A) Effect of LINC02802 over-expression an MAML3.

(B) Effect of LINC02802 knockdown on MAML3.

3.5 Discussion:

In this work, using a more traditional single-gene approach, we characterized the expression of the unknown lincRNA LINC02802 and we validated its function in the context of the competitive-endogenous RNA (ceRNA) hypothesis. In fact, we demonstrated that lincRNA LINC02802 act as a sponge for miR-486-5p in the fine regulation of the expression of the protein-coding gene MAML3. As reported before, MAML3 is an essential co-activator for the signal transduction of Notch pathway. Previous studies demonstrated that MAML3 has a particular affinity for the intracellular portion of the Notch 4 receptor and therefore it could be involved in its downstream signaling. This information is coherent with our model; were the expression of notch 1 is down regulated in the comparison between SPHC and SPHV while notch 4 is strongly upregulated. Thus we can speculate that during SA the Notch pathway rely mostly on Notch 4 activation, rather than Notch 1, and that the circuit involving LINC02802 and miR-486-5p could take part in the fine tuning of the regulation of Notch 4 downstream effectors. This is very interesting since the function of notch 4 receptor in SA has not been completely elucidated so far.

4. A subset of miRNA targeting only lncRNA's in endothelial cells.

The annotation of lncRNA expression and the characterization of their function in the vasculature is only at the beginning and very few examples were reported. The Tie-1 antisense lncRNA have a role in the control of ECs homeostasis and cell-to-cell junctions (Li et al., 2010). The endothelial-enriched lncRNA MALAT1 is known to control the migration and sprouting of ECs (Michalik et al., 2014). Another antisense lncRNA, SENCR, was identified in human artery smooth muscle cells and is involved in migration of this type of vascular cells (Bell et al., 2014). A limited number of lncRNAs has been described to act as "miRNA sponges" also in endothelial cells. It is the case of the transforming growth factor beta 2 overlapping transcript 1 (TGFβ2-OT1). TGFβ2-OT1 expression is regulated through lipopolysaccharide 31 and oxidized low-density lipoprotein, the central mediator involved in the initiation and progression of atherosclerosis. TGFβ2-OT1 has found to act as an endogenous competing RNA for miR-3960, miR-4488, and miR-4459. The down regulation of these microRNAs mediated by TGFβ2-OT1 results in up regulation of their targets CERS1 (ceramide synthase 1), NAT8L (N-acetyltransferase 8-like), and LARP1 (La ribonucleoprotein domain family, member 1). All three targets are involved in endothelial cell autophagy and inflammation, that are central processes involved in endothelial injury (Huang et al., 2015). Another example is linc-p21 that has been shown to act as an endogenous sponge for miRNA-130b in both vascular endothelial and smooth muscle cells. In ECs, miR-130 modulates apelin-miR-424/503-FGF2 signaling (Bertero et al., 2014).

Results

4.1 Transcriptomic analysis of lncRNA's and correlation of expression with protein coding genes.

Transcriptomic analysis on mRNA data allowed us to predict 723 non-coding RNAs (ncRNAs) as expressed with a TPM > 1 (in every sample), out of which 168 were lncRNAs in ECs. Differential expression analysis (DEA) by DESeq2 (Love et al., 2014) identified 78 lncRNAs (log2FC > 0.5, pval < 0.05) with altered expression in our experimental condition (SPHV vs SPHC) (Figure 12A).

To predict the molecular functions and the biological pathway in which these lncRNAs could be involved, we applied a co-expression approach (like chapter 2.4) based on Pearson correlation analysis and GSEA algorithm. After a clusterization process, the genes belonging to the main groups were subjected to GO analysis. We found that some groups of lncRNAs are positively or negatively enriched in particular biological process, such as cell adhesion and migration, glucose metabolic process, cell cycle, etc. (Figure 12B). Hence, these observations signifies that there are some lncRNAs which could be involved in modulating certain biological pathways which play an important role in SA. Performing a miRNA target prediction study would help to build a post transcriptional network, which then could highlight the functional roles of these lncRNAs.

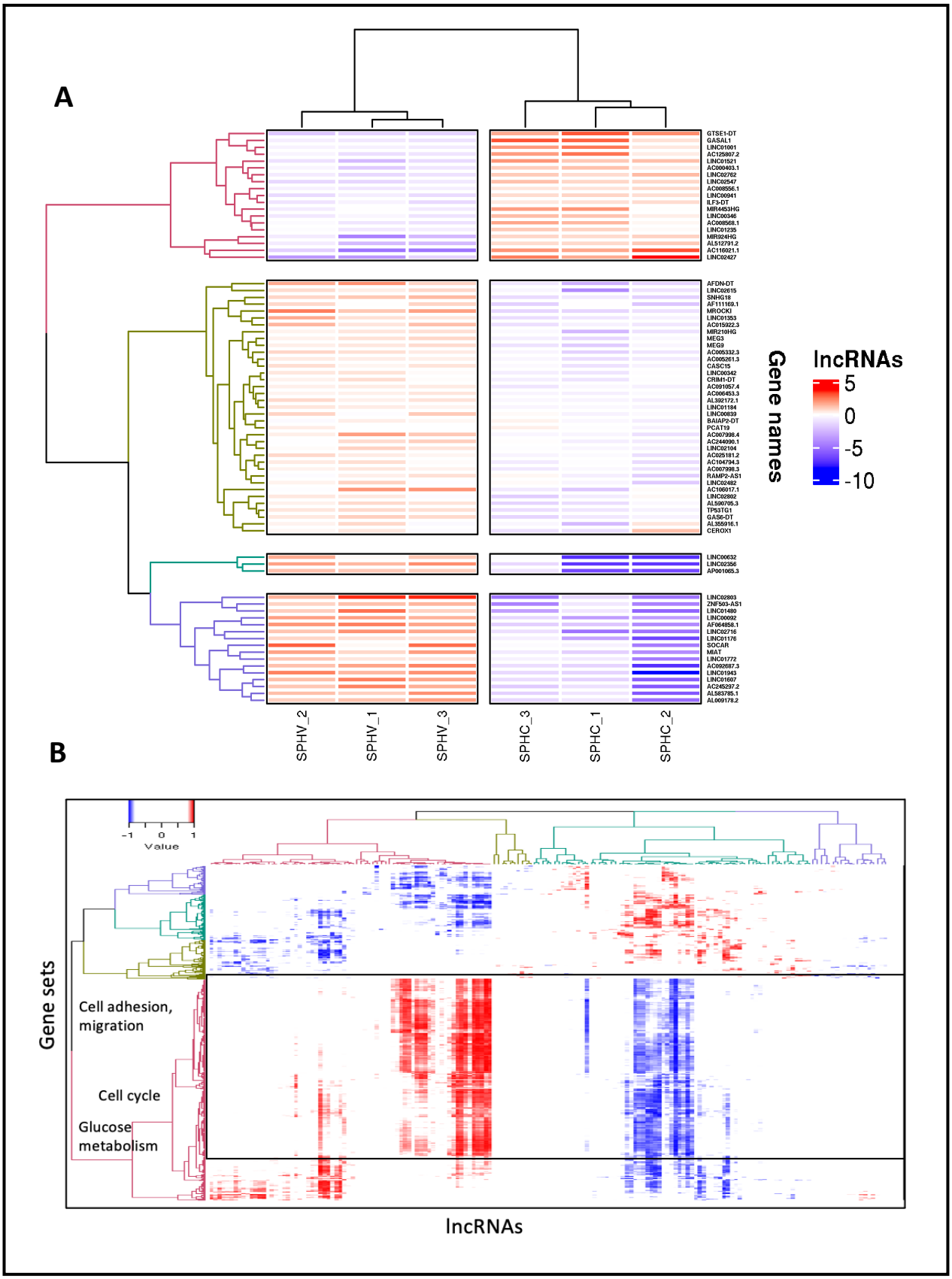
A
GTSE1-DT
GASAL1
LINC01001
AC125807.2
LINC01521
AC000403.1
LINC02762
LINC02547
AC008556.1
LINC00941
ILF3-DT
MIR44S3HG
LINC00346
AC008568.1
LINC01235
MIR924HG
AL512791.2
AC116921.1
LINC02427
AFDN-DT
LINC02615
SNHG18
AF111169.1
MROCK1
LINC01353
AC015922.3
MIR210HG
MEG3
MEG9
AC005332.3
AC005261.3
CASC15
LINC00342
CRIM1-DT
AC091057.4
AC006453.3
AL392172.1
LINC01184
LINC00839
BAIAP2-DT
PCAT19
AC007998.4
AC244090.1
LINC02104
AC025181.2
AC104794.3
AC007398.3
RAMP2-AS1
LINC02462
AC106017.1
LINC02802
AL590705.3
TP53TG1
GAS6-DT
AL355916.1
CEROX1
LINC00632
LINC02356
AP001065.3
LINC02803
ZNF503-AS1
LINC01480
LINC00092
AF064858.1
LINC02716
LINC01176
SOCAR
MIAT
LINC01772
AC092687.3
LINC01943
LINC01607
AC245297.2
AL583785.1
AL009178.2
SPHV_2
SPHV_1
SPHV_3
SPHC_3
SPHC_1
SPHC_2
Gene names
lncRNAs
5
0
-5
-10
B
-1
0
1
Value
Gene sets
Cell adhesion, migration
Cell cycle
Glucose metabolism
lncRNAs

Figure 12. Analysis of lncRNAs in the 3D model of sprouting angiogenesis.

(A) Heatmap of differentially expressed lncRNAs in SA. Red and blue color of the gene (rows) indicates the upregulation and downregulation respectively. (B) GSEA coexpression analysis between lncRNA profiles (columns) and functional gene sets (rows). Significant associations (FDR < 0.05) are shown in red (positive) or blue (negative). White, not significant. Biologically relevant clusters are highlighted with different colors.

4.2 miRNA target prediction on non-coding RNAs.

The current understanding of lncRNA functions is still limited, but it has been revealed that they act as key regulators in multiple biological process through a complex mechanism in which they interact with proteins and other ncRNAs (Wapinski and Chang et al, 2011). While on the other hand, miRNAs are known to post-transcriptionally regulate the expression of their target genes. Both of these two types of ncRNA influence many aspects of biology (Lu et al., 2005). And also, the deviating expression level of ncRNAs appears to be one of the initiating factors of different types of disease including cancers (Lewis et al., 2003; Calin and Croce, 2006).

Some efforts have been already made to design a number of computational methods and algorithms for an accurate prediction of miRNA-lncRNA interactions on a large scale. Most of these computational tools are based on matching seed sequences, algorithms like TargetSCAN, miRanda and RNAhybrid, aim at predicting miRNA targets by selecting evolutionarily conserved miRNA binding site (Zheng et al., 2017). However, the prediction results by these methods on lncRNAs could be of high false positives and often biologically irrelevant (Pinzòn et al., 2017). Since, lncRNAs show poor evolutionary conservation, this makes it even more difficult to find “true miRNA-lncRNA interactions”.

Taking these observations into considerations and not relying only on the results produced by the computational tools, we decided to go ahead with an integrated approach (like chapter 2.4). Where the target prediction results from the computational tools are integrated with the expression data of both these

ncRNAs (miRNAs and lncRNAs). A miRNA-target prediction database, StarBase (Li JH, et al., 2014) is an open-source platform for studying the miRNA-ncRNA and miRNA-mRNA interactions from CLIP-seq, degradome-seq and RNA-RNA interactome data. From StarBase, we extracted MTIs for coding and non-coding genes (lncRNAs). And then performed a Pearson correlation on both these datasets, plotting a distribution correlator (Figure 13). The distribution correlator showed a significant negative enrichment for the interactions between miRNA and PCGs (Figure 13A), confirming our previous observations from TargetSCAN. While on the other hand, there was no positive/negative enrichment observed in case of miRNA-lncRNA interactions. These observations raised few questions about the crosstalk between ncRNAs, such as, whether the miRNAs have a different regulatory effect on lncRNAs as compared to the PCGs or probably no significant effect at all? And also, whether the lncRNAs are targeted by the most represented miRNAs that target PCGs or by a different subset?

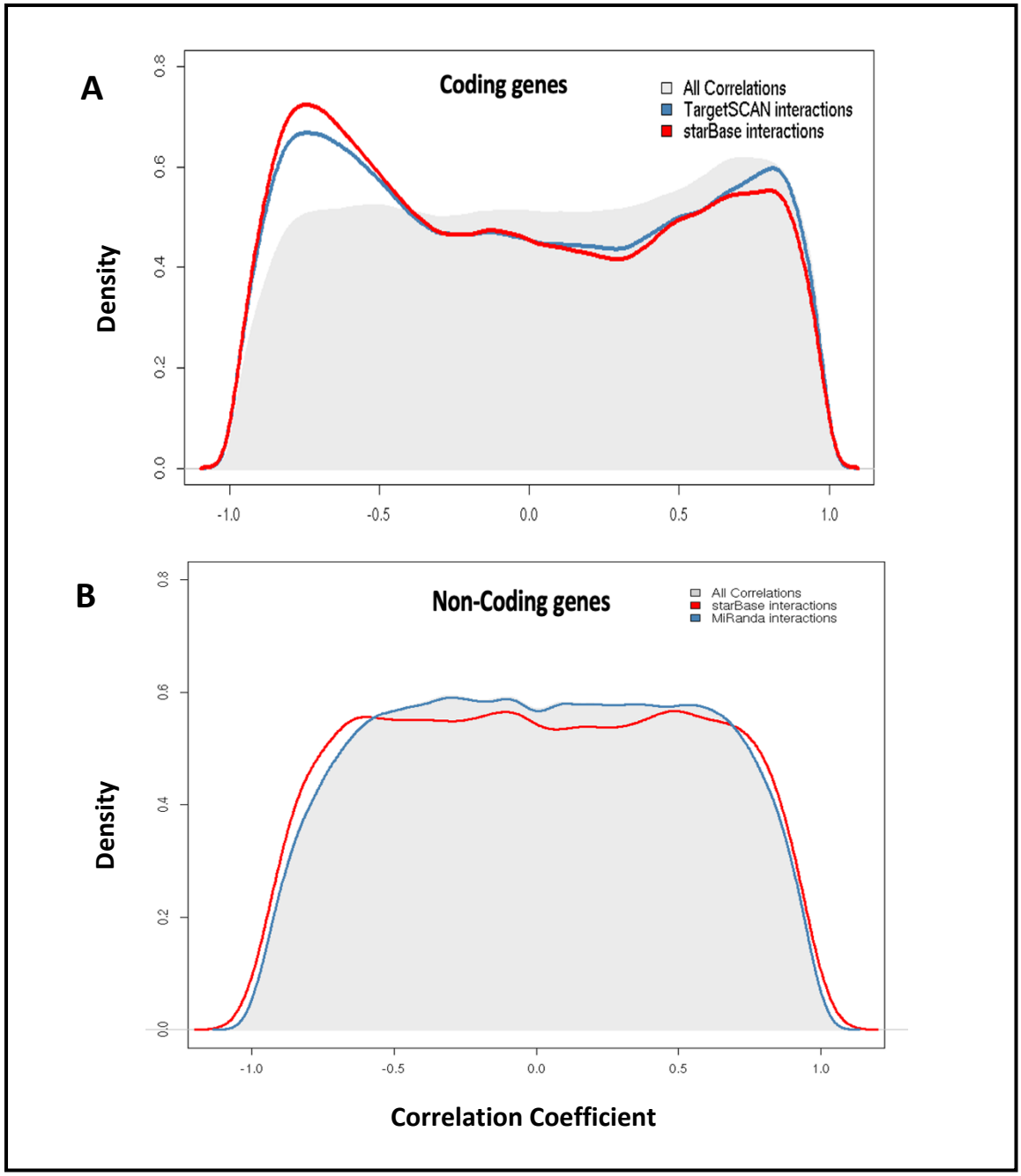

Figure 13. Coexpression analysis of miRNA target prediction results.

(A) Distribution correlator of the pairwise analysis between miRNA and PCGs. Blue curve represents MTIs predicted from TargetSCAN and red curve represents MTIs predicted by StarBase. (B) Distribution correlator of the pairwise analysis between miRNA and lncRNAs. Blue curve represents MTis predicted by MIRanda, and red curve represents MTI's predicted by StarBase.

4.3 Subset of miRNAs targeting only lncRNAs.

Both lncRNAs and miRNAs interact with each other forming a huge complex regulatory network that controls the gene expression at transcriptional and post-transcriptional levels (Karreth Pandolfi, 2013). Taking part in almost all aspects of cell cycles including cell divison, senescence, differentiation, stress response, immune activation, and apoptosis (Shi et al., 2013), thus attracting a widespread attention in medical research (Huan et al., 2016). But since in our sprouting model, we did not observe the miRNAs showing a similar effect on lncRNAs as compared to the PCGs (Figure 13), we hypothesized that there is a different crosstalk happening between the miRNAs and lncRNAs. Which can also lead to a finding that there are some subsets of miRNAs which target only the lncRNAs and not PCGs.

The miRNA – lncRNA interactions predicted by StarBase in our sprouting model, were also confirmed by MiRanda algorithm having a good binding potential (MiRanda score) and likely to be stable (MiRanda pvalue). Some of these interactions are also validated in DIANA-LncBase (Paraskevopoulou et al., 2013) by a HITS-CLIP method. To find a subset of miRNAs which target only lncRNAs in ECs, we filtered and removed the miRNAs which target PCGs using TS and StarBase (miRNA-PCG interactions). The resulting miRNA – lncRNA network consists of 10 miRNAs targeting 6 lncRNAs. (Figure 14).

The functions of some lncRNA transcripts such as XIST and MEG3 are very well known, were XIST (Gonton et al., 2011) acts by silencing the expression of specific gene clusters by making them inaccessible to the transcription machinery.

However, the network still needs a further validation by luciferase assay or a PCR report to support the findings. But studying such a crosstalk between the ncRNAs would be interesting, such type of interactions might be designed to neutralize miRNAs, which can eventually counteract their negative post-transcriptional regulatory effect.

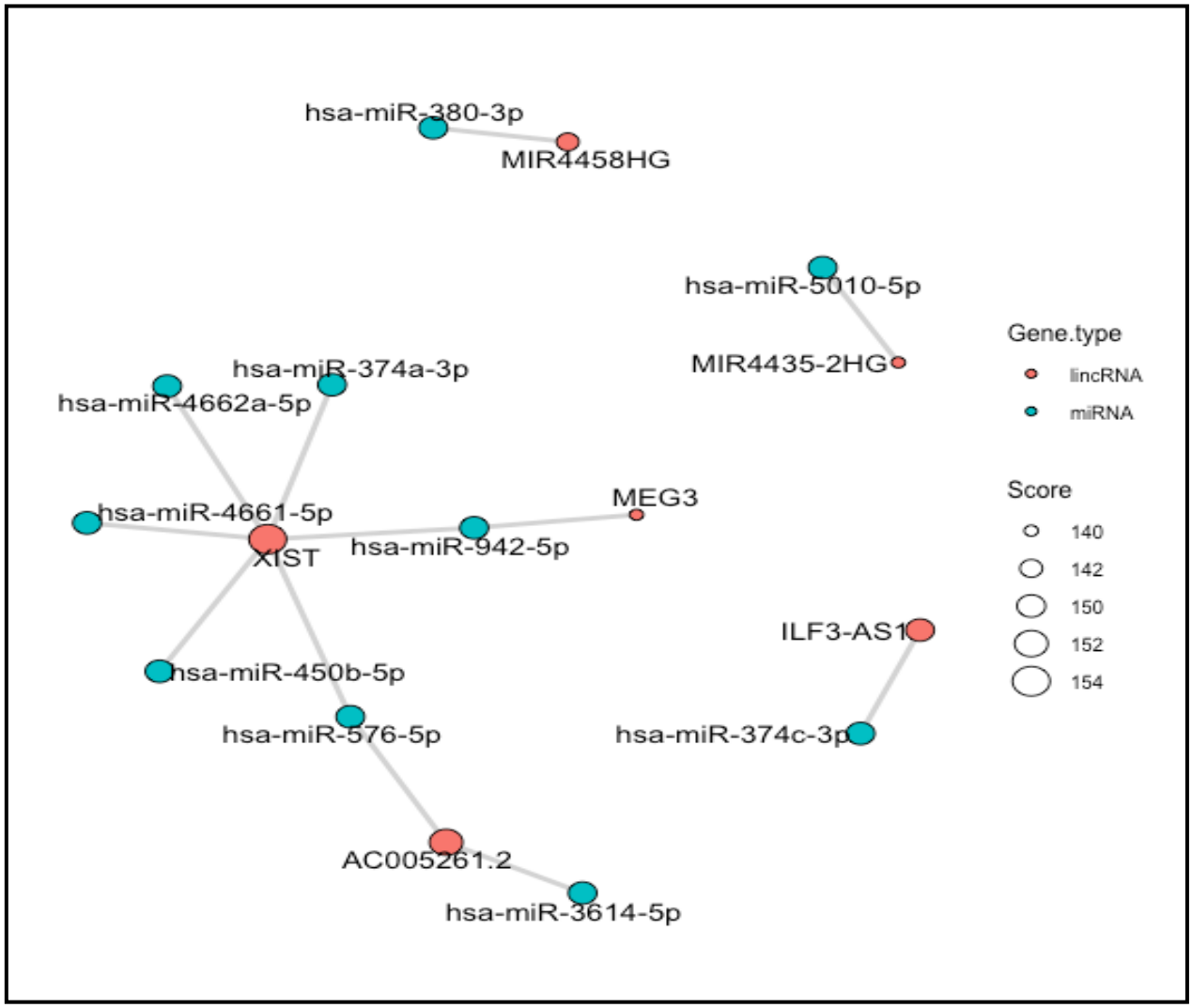

Figure 14. Graphical representation of the miRNA – lncRNA regulatory network. The network represents the crosstalk between a subset of miRNAs targeting lncRNAs only, the node size represents MiRanda score, and the node color represents the gene type.

4.4 Discussion

Understanding the lncRNA-miRNA interaction networks governing the initiation and development of diverse diseases is essential but remains largely uncompleted (Karreth and Pandolfi, 2013). Such evidence shows that miRNAs and lncRNAs collaborate to form a network for gene regulation. However, little effort has been made to develop computational approaches to predict miRNA-lncRNA interaction on a large scale. The main challenges come from the small number of known interactions between lncRNA and miRNA and the limited understanding pattern on lncRNA-miRNA interaction. But studying such types of crosstalk's between ncRNAs will provide great insights into understanding the molecular mechanism of the initiation and development of various types of complex diseases.

5. Discussion

In this project, we used an innovative approach to study the process of SA. Here, we combined several bioinformatics tools with wet biology approach in order to describe the different biological functions that sustain SA, using a multi-gene systems view rather than the single gene/single function paradigm. Emerging evidences suggest that the global approach could overcome the limitations and the issues derived from the reductionist approach. To this end, our workaddressed these issues with an innovative approach to provide new information useful for targeting angiogenesis.

In this work, first we focused our attention on the global transcriptional dynamics that sustain the sprouting process. We exploited, by the use of RNA Sequencing technology, a three dimensional model of SA that in vitro recapitulates the angiogenic program. By the sequencing of the RNAs derived from HUVEC cells and spheroids, we generated a complete annotation of all protein coding genes and non-coding RNAs expressed by endothelial cells in different conditions, included a 3D model of SA. We provided complete information about the genes expressed by spheroid in a quiescent state, that mimic the normal endothelium, and also during the sprouting process after the VEGF-A stimulation. This kind of data is completely new, and our annotation provides a precise and global picture of the transcriptional and post-transcriptional programs activated during SA; this is a really powerful information that provide an important starting point to dissect the intricated regulation of SA.

Gene expression analysis revealed dramatic changes in the global transcriptomic profile in control spheroids compared to the stimulated ones, and mirrored the intrinsic phenotypic remodeling of the spheroids. The GSEA highlighted that migration has a prevalent role in the ongoing process and showed also the activation of several collateral pathways functional to cell migration. As described in the introduction, VEGF stimulation on ECs is able to induce several biological functions including cell migration and cell proliferation. Unexpectedly, GSEA analysis revealed a strong down regulation in genes related to cell proliferation. We largely validated this bioinformatics indication by functional assays, and this was further supported by the observation of a general downregulation of genes involved in nucleotides synthesis. GSEA also revealed a strong positive enrichment in genes related to different metabolic pathways (Figure 2).

Furthermore, the transcriptomic analysis and functional annotation identified the most relevant biological pathways and molecules that are engaged in the initial phase of SA, we asked which could be the impact of the post-transcriptional layer of regulation, and in particular the microRNAs activity on the expression of their target genes. It is already known that microRNAs act as regulators of gene expression and several data demonstrated that they can regulate different aspects of vascular physiology and angiogenesis. We found that 643 mature miRNAs are expressed by ECs across all the experimental condition, and that after VEGF stimulation in 3D conditions 128 miRNAs were differentially expressed, indicating that also this class of molecules could be strongly involved in the regulation of the angiogenic process. It is important to highlight that among the 63 microRNA differentially expressed, only a third of them have been previously related to the vascular or cardio-vascular system. This indicates that microRNAs in the vascular system are still largely unexplored.

The primary focus of our work fits in this context, as we were able to assess the impact of miRNA-mediated post-transcriptional activity in the regulation of the main pathways that are involved in SA. To dissect this issue, we developed a specific bioinformatics pipeline based on the co-expression between all pairs of protein-coding genes and microRNAs, and on the prediction of microRNA interactions on the 3'-UTR of protein-coding genes. When considering only pairs containing predicted microRNA-target gene interactions, we observed a significant enrichment in negative correlations, indicating that expression analysis combined with prediction of microRNA target genes was able to highlight the effect of microRNAs on target genes expression and to identify functional interactions that more likely are affected by microRNAs activity. By selecting only negative correlation between miRNAs and protein-coding genes contained in clusters identified by the GSEA analysis we generated a global-miRNA-centered- network that includes all the most relevant miRNAs those expression is modulated during SA. Thanks to this network we can describe the post-transcriptional layer of regulation in SA. We demonstrated that the hub miRNAs identified in our network analysis are extremely relevant in the SA process. However the interesting thing is that, thanks to our global approach, we can show how the direct targeting of a specific target gene by a microRNA can impact globally a specific biological function.

In this work we generated a complete annotation of all lncRNAs expressed by ECs and modulated during the process of SA. A complete annotation of all lncRNA expressed by ECs was still missing so far, therefore it represents is an essential starting point to dissect the functions of this complex class of regulatory molecules in the process of SA. We found that the large majority of lncRNAs annotated in our model are completely uncharacterized.

At the beginning we used a more traditional single-gene approach, as reported before, MAML3 is an essential co-activator for the signal transduction of Notch pathway. Previous studies demonstrated that MAML3 has a particular affinity for the intracellular portion of the Notch 4 receptor and therefore it could be involved in its downstream signaling. This information is coherent with our model; in fact, based on the expression data from our RNAseq analysis we know that, in ECs, two Notch receptors are expressed, such as notch 1 and notch 4. The expression of notch 1 is down regulated in the comparison between SPHC and SPHV while notch 4 is strongly up-regulated. We demonstrated that an unknown lincRNA, LINC02802 act as a sponge for miR-486-5p in the fine regulation of the expression of the protein-coding gene MAML3. We showed that sequestration of miR-486-5p mediated by LINC02802 affects MAML3 expression and that a balanced expression of all players is essential to sustain the process of SA. Thus we can speculate that during SA the Notch pathway rely on mostly on Notch 4 activation, rather than Notch 1, and that the circuit involving LINC02802 and miR-486-5p could take part in the fine tuning of the regulation of Notch 4 downstream effectors. This is very interesting since the function of notch 4 receptor in SA has not been completely elucidated so far.

The transcriptomic analysis annotated 168 lncRNAs expressed in our SA model. However, which made us speculate what role these lncRNAs might be playing in the post-transcriptional regulatory network. Target prediction and coexpression analysis between the miRNA and lncRNAs, suspected a different regulatory effect as compared to the protein coding genes (Figure 13). Hence, we focused our attention on some subsets of miRNAs which target lncRNAs only. This analysis resulted in a network of 10 miRNAs targeting 6 lncRNAs out of which some are also differentially expressed in our experimental condition (SPHV vs

SPHC). Most of the lncRNAs from the network are unknown but the functions of other lncRNAs like XIST and MEG3 are very well known. For example, XIST acts as silencer for the expression of specific gene clusters by making them inaccessible to the transcription machinery. We suspect that such types of networks could be designed to neutralize the effect of miRNAs and so to counteract their negative post-transcriptional effect. Even though, there is a very limited understanding on such crosstalk's of ncRNAs, we speculate that such type networks/interactions might provide greater insights into understanding the complex mechanisms of various types of diseases.

6. Materials and Methods

Cell cultures

Human umbilical vein endothelial cells (HUVECs) were freshly isolated from different donors as previously described (264), and used between passage 1 and 3. Collection of cord blood is governed by an agreement between Università degli Studi di Torino and the "Ordine Mauriziano di Torino" hospital; signature of an informed consent is required. To minimize experimental variability, cells from at least 3 different donors were pooled. HUVECs were cultured in M199 medium (Sigma) supplemented with 20% fetal bovine serum (FBS) (Sigma), 0.2% brain extract, 0.05 μg/ml porcine heparin (Sigma) and 2% penicillin streptomycin solution (Sigma).

Spheroid capillary sprouting assay

To generate EC spheroids, HUVECs were cultured in hanging drops for 10 hours in M199 medium containing 10% FBS and 0.4% methylcellulose (Sigma-Aldrich). Spheroids were then collected and mixed with a solution containing 15% FBS, 0.5% methylcellulose, collagen (Roche) 1mg/ml, 30 mM HEPES and 10X concentrated M199 medium. This solution was then induced to polymerize by pH neutralization with NaOH and incubation at 37 °C as described (251). EC sprouting was induced by addition, at the moment of the embedding, of medium containing 20 ng/ml of recombinant human VEGF125 (R&D Systems). Spheroids were collected or analyzed at given time points as indicated further.

RNA extraction

Total RNA was isolated from HUVECs by using Trizol reagent (Life Technologies) and miRNeasy Mini Kit (Qiagen). Residual DNA was removed by treatment with

RNase-Free Dnase Set (Qiagen). Quality and concentration of RNAs were assessed with a Nanodrop ND-100 (Nanodrop Technologies). To isolate ECs after the sprouting assay, collagen matrix was removed by incubation with 0.25% Collagenase A from *Clostridium histolyticum* (Roche) in M199 medium. 92 Quality of RNA samples that were subsequently processed for RNA-Seq was assessed with Qubit RNA HS Assay Kit (Thermo Fisher Scientific) and Agilent RNA 6000 Nano Kit (Agilent Technologies).

RNA-sequencing analysis

Total RNA from spheroids exposed to VEGF-A for 18 hr (SPHV) and control spheroids (SPHC) that were not exposed to VEGF-A were subjected to high throughput sequencing for poly-A+ RNAs by an external next generation sequencing (NGS) facility (Fasteris, Geneva, Switzerland). Three biological replicates from each biological condition were analyzed. RNA sequencing was performed on a HiSeq 2000 sequencer (Illumina, San Diego, CA, USA), obtaining a mean of 100 million paired-end reads of 100 bps per sample. Reads to counts conversion and differential expression analysis were performed using the software implementation described by (Beccuti et al., 2018). In brief, fastq files were mapped with STAR-2.5 to the reference genome (hg19 assembly) and gene counts were generated using RSEM-1.3.0 and ENSEMBL annotation. Differential expression analysis was performed using DESeq2 version 1.14.1 to detect modulated genes (| log2FC |>0.5 and FDR < 0.05). Data were deposited in the GEO database, with accession number GSE115817.

For miRNAs, the same external NGS facility (Fasteris, Geneva, Switzerland) was used to perform small-RNA sequencing profiling on the same matched samples as those used for mRNA sequencing. Sequencing was performed on a HiSeq

2000 sequencer (Illumina), obtaining a mean of 8 million 50bps single-end reads per sample. From the raw data, adaptors were first trimmed by the FASTXToolkit. Then, inserts were mapped by the BWA tool (Li and Durbin, 2010) on mature miRNA sequences from miRBase v22 (Kozomara and Griffiths-Jones, 2014), thus producing an expression level for all annotated miRNAs. Data were deposited in the GEO database, with accession number GSE115954.

Gene set enrichment analysis

Gene Set Enrichment Analysis (GSEA) was run on the dataset of protein-coding genes in SPHV versus SPHC against the canonical pathway genesets collection (c2.cp.v5.2) by using 1000 permutations on the genesets. Only genesets with FDR q value < 0.05 were considered.

Post-Transcriptional Network

Correlation analysis between PCGs and miRNAs was performed by implementing the GSEA algorithm. Briefly, miRNAs expression data were used as phenotype to calculate the Pearson correlation coefficient between each pair of miRNA and PCGs and to find association with biological processes. Genesets with FDR < 0.05 that positively or negatively correlated with miRNAs expression were extracted and used to generate a matrix that was subsequently clusterized by using GenePattern (Broad Institute). Genes constituting the core enrichment were extracted from significant genesets and subjected to functional annotation by using the online David platform. To find associations between miRNA and their protein-coding target genes, we extracted data from TargetScan database focusing only on conserved interactions with a weighted context++ score percentile > 50. Network graphical representation and analysis were performed by using Cytoscape software, version 3.3 (Shannon et al., 2003).

On the other hand, the interactions between miRNA and lncRNAs were predicted by StarBase and then confirmed by MiRanda and RNAhybrid. A network for the subset of miRNA's targeting only lncRNAs in our sprouting model was represented by igraph package (Csardi and Nepusz, 2006) in R.

Luciferase assays

$3x10^5$ cells were co-transfected with 100 ng of luciferase reporter vector (MAML3 3'-UTR WT, MAML3 3'-UTR Mut, LINC02802 WT or LINC02802 Mut), together with miR-486-5p miRNA mimic or miRNA Mimic Negative Control #1 90 nmol/L using RNAiMAX lipofectamine. Lysates were collected 24 h after transfection and luciferase activity was measured with Dual Luciferase Reporter Assay System (Promega) in a Bio-Tek Synergy HT Multi-Detection Microplate Reader (MTX Labsystems). When indicated the 3'UTRs were mutagenized at the miR-486-5p recognition site/s using the QuickChange Site-Directed Mutagenesis kit (Stratagene, Cedar Creek, TX) according to the manufacturer‟s instructions.

7. References

1. Abbott AL et al. The let-7 MicroRNA family members mir-48, mir-84, and mir-241 function together to regulate developmental timing in Caenorhabditis elegans. Dev Cell. 2005;9(3):403–14.
2. Adair TH, Montani JP. San Rafael (CA): Morgan & Claypool Life Sciences; 2010.
3. Adams RH1, Alitalo K Molecular regulation of angiogenesis and lymphangiogenesis.Nat Rev Mol Cell Biol. 2007 Jun;8(6):464-78.
4. Agarwal V, Bell GW, Nam J-W, Bartel DP. 2015. Predicting effective microRNA target sites in mammalian mRNAs. eLife 4:e05005. DOI: https://doi.org/10.7554/eLife.05005.
5. ALBERT-LÁSZLÓ BARABÁSI THE SCALE-FREE PROPERTY NETWORK SCIENCE
6. Ambros V (2004). The Functions of Animal microRNAs. Nature., doi: 10.1038/nature02871.
7. Ana Kozomara, Maria Birgaoanu, Sam Griffiths-Jones, miRBase: from microRNA sequences to function, *Nucleic Acids Research*, Volume 47, Issue D1, 08 January 2019, Pages D155–D162, https://doi.org/10.1093/nar/gky1141.
8. Ausprunk DH, Folkman J.Migration and proliferation of endothelial cells in preformed and newly formed blood vessels during tumor angiogenesis. Microvasc Res. 1977 Jul;14(1):53-65.
9. Barabàsi A-L, Pòsfai M. 2016. Network Science. Cambridge, United Kingdom: Cambridge University Press.
10. Bartel DP. MicroRNAs: genomics, biogenesis, mechanism, and function. Cell. 2004;116(2):281–97.

11. Beccuti M, Cordero F, Arigoni M, Panero R, Amparore EG, Donatelli S, Calogero RA. 2018. SeqBox: rnaseq/ ChIPseq reproducible analysis on a consumer game computer. Bioinformatics 34:871–872. DOI: https://doi.org/10.1093/bioinformatics/btx674.
12. Beck L Jr, D'Amore PA. Beck and D'Amore, Vascular development: cellular and molecular regulation. FASEB J. 1997 Apr;11(5):365-73.
13. Behm-Ansmant I, Rehwinkel J, Doerks T, Stark A, Bork P, Izaurralde E. mRNA degradation by miRNAs and GW182 requires both CCR4:NOT deadenylase and DCP1:DCP2 decapping complexes. Genes Dev. 2006 Jul 15;20(14):1885-98.
14. Bell R.D., Long X., Lin M. Identification and initial functional characterization of a human vascular cell-enriched long noncoding RNA. Arterioscler Thromb Vasc Biol. 2014;34:1249–1259.
15. Bentley K, Mariggi G, Gerhardt H, Bates PA. Tipping the balance: robustness of tip cell selection, migration and fusion in angiogenesis. PLoS Comput Biol. 2009 Oct;5(10):e1000549.
16. Berezikov, E.; Guryev, V.; van de Belt, J.; Wienholds, E.; Plasterk, R. H.; Cuppen, E. Phylogenetic shadowing and computational identification of human microRNA genes. Cell, 2005, 120, 21-24.
17. Bertero T, Lu Y, Annis S, Hale A, Bhat B, Saggar R, Saggar R, Wallace WD, Ross DJ, Vargas SO, Graham BB, Kumar R, Black SM, Fratz S, Fineman JR, West JD, Haley KJ, Waxman AB, Chau BN, Cottrill KA, Chan SY.. Systems-level regulation of microRNA networks by miR-130/301 promotes pulmonary hypertension. J. Clin. Invest. 124(8), 3514–3528 (2014).
18. Berthod F. Fibroblasts and endothelial cells: the basic angiogenic unit. In: Santulli G, editor. Angiogenesis: Insights from a systematic overview. New York, NY: Nova Science Publisher; 2013. pp. 145–158.

19. Biyashev D, Veliceasa D, Topczewski J, Topczewska JM, Mizgirev I, Vinokour E, Reddi AL, Licht JD, Revskoy SY, Volpert OV. 2012. miR-27b controls venous specification and tip cell fate. Blood 119:2679–2687. DOI: https://doi.org/10.1182/blood-2011-07-370635.
20. Boccaletti S, Latora V, Moreno Y, Chaves M and Hwang DU (2006) Complex networks: Structure and dynamics. Physics Rep 424:175-308.
21. Bray SJ. Notch signalling: a simple pathway becomes complex. Nat Rev Mol Cell Biol. 2006 Sep;7(9):678-89. Review.
22. Burri PH, Tarek MR. A novel mechanism of capillary growth in the rat pulmonary microcirculation. Anat Rec 228: pp. 35–45, 1990.
23. Bussolino F, Di Renzo MF, Ziche M,Bocchietto E, Olivero M, Naldini L, Gaudino G, Tamagnone L, Coffer A, Comoglio PM (Hepatocyte growth factor is a potent angiogenic factor which stimulates endothelial cell motility and growth.. J Cell Biol. 1992 Nov;119(3):629-41.).
24. C alin GA et al. Human microRNA genes are frequently located at fragile sites and genomic regions involved in cancers. Proc Natl Acad Sci U S A. 2004;101(9):2999–3004.
25. Cabili MN, Trapnell C, Goff L, et al. Integrative annotation of human large intergenic noncoding RNAs reveals global properties and specifific subclasses. Genes Dev 2011;25(18): 1915
26. Cabili, M.N. et al. Integrative annotation of human large intergenic noncoding RNAs reveals global properties and specific subclasses. Genes Dev. 25, 1915–1927 (2011).
27. Caduff JH, Fischer LC, Burri PH. Scanning electron microscope study of the developing microvasculature in the postnatal rat lung. Anat Rec 216: pp. 154–64, 1986.

28. Calin, G. A., Croce, C. M. J. N. R. C. (2006). MicroRNA signatures in human cancers. *Nat. Rev. Cancer.* 6, 857. doi: 10.1038/nrc1997.
29. Carmeliet P, Jain RK. 2011. Molecular mechanisms and clinical applications of angiogenesis. Nature 473:298–307. DOI: https://doi.org/10.1038/nature10144, PMID: 21593862.
30. Carmeliet P., Angiogenesis in life, disease and medicine. Nature. 2005 Dec 15;438(7070):932-6. Review.
31. Carninci, P. et al. The transcriptional landscape of the mammalian genome. Science 309, 1559–1563 (2005).
32. Cesana M et al. A long noncoding RNA controls muscle differentiation by functioning as a competing endogenous RNA. Cell. (2011) 147(2):358-69 108.
33. Chamorro-Jorganes A, Araldi E, Penalva LO, Sandhu D, Fernández-Hernando C, Suárez Y. 2011. MicroRNA-16 and microRNA-424 regulate cell-autonomous angiogenic functions in endothelial cells via targeting vascular endothelial growth factor receptor-2 and fibroblast growth factor receptor-1. Arteriosclerosis, Thrombosis, and Vascular Biology 31:2595–2606. DOI: https://doi.org/10.1161/ATVBAHA.111.236521, PMID: 21885851.
34. Chamorro-Jorganes A1, Lee MY1, Araldi E1, Landskroner-Eiger S1, Fernández-Fuertes M1, Sahraei M1, Quiles Del Rey M1, van Solingen C1, Yu J1, Fernández-Hernando C1, Sessa WC1, Suárez Y2.VEGF-Induced Expression of miR-17-92 Cluster in Endothelial Cells Is Mediated by ERK/ELK1 Activation and Regulates Angiogenesis.Circ Res. 2016 Jan 8;118(1):38-47.
35. Chem. 2000;275(9):6059-62. 29. Takahashi T, Yamaguchi S, Chida K, Shibuya M. A single autophosphorylation site on KDR/Flk-1 is essential for

VEGF-A-dependent activation of PLC gamma and DNA synthesis in vascular endothelial cells. EMBO J. 2001;20(11):2768-78.

36. Chen G., Wang Z., Wang D., Qiu C., Liu M., Chen X. et al. 2013 LncRNA disease: a database for long-non-coding RNAassociateddiseases.NucleicAcidsRes.41,D983–D986
37. Chou CH, Shrestha S, Yang CD, Chang NW, Lin YL, Liao KW, Huang WC, Sun TH, Tu SJ, Lee WH, Chiew MY, Tai CS, Wei TY, Tsai TR, Huang HT, Wang CY, Wu HY, Ho SY, Chen PR, Chuang CH, et al. 2018. miRTarBase update 2018: a resource for experimentally validated microRNA-target interactions. Nucleic Acids Research 46: D296–D302. DOI: https://doi.org/10.1093/nar/gkx1067, PMID: 29126174.
38. Claesson-Welsh L, Welsh M. VEGFA and tumour angiogenesis. J Intern Med. 2013;273(2):114-27.
39. Claxton S1, Fruttiger M. Periodic Delta-like 4 expression in developing retinal arteries. Gene Expr Patterns. 2004 Nov;5(1):123-7.
40. Cora' D, Re A, Caselle M, Bussolino F. 2017. MicroRNA-mediated regulatory circuits: outlook and perspectives. Physical Biology 14:045001. DOI: https://doi.org/10.1088/1478-3975/aa6f21, PMID: 28586314.
41. Costa LF, Rodrigues FA, Travieso G and Boas PRV (2007) Characterization of complex networks: A survey of measurements. Adv Physics 56:167-242.
42. Csardi G, Nepusz T (2006). "The igraph software package for complex network research." *InterJournal*, Complex Systems, 1695. https://igraph.org.
43. D. Ribatti, Angiogenesis, Editor(s): Stanley Maloy, Kelly Hughes, Brenner's Encyclopedia of Genetics (Second Edition), Academic Press, 2013, Pages 130-132, ISBN 9780080961569, https://doi.org/10.1016/B978-0-12-374984-0.00065-6.

44. Dang LT, Lawson ND, Fish JE. 2013. MicroRNA control of vascular endothelial growth factor signaling output during vascular development. Arteriosclerosis, Thrombosis, and Vascular Biology 33:193–200. DOI: https://doi.org/10.1161/ATVBAHA.112.300142, PMID: 23325476.
45. Dayanir V, Meyer RD, Lashkari K, Rahimi N. Identification of tyrosine residues in vascular endothelial growth factor receptor-2/FLK-1 involved in activation of phosphatidylinositol 3-kinase and cell proliferation. J Biol Chem. 2001;276(21):17686-92.
46. Derrien T., Guigó R. and Johnson R. 2011 The long non-coding RNAs:anewplayerinthe“darkmatter”.Front.Genet.2,107.
47. Derrien T., Johnson R., Bussotti G., Tanzer A., Djebali S., Tilgner H. et al. 2012 The GENCODE v7 catalog of human long noncoding RNAs: analysis of their gene structure, evolution, and expression.GenomeRes.22,1775–1789.
48. Dieci, G., Fiorino, G., Castelnuovo, M., Teichmann, M. & Pagano, A. The expanding RNA polymerase III transcriptome. Trends Genet. 23, 614–622 (2007)
49. Dinger ME, Pang KC, Mercer TR and Mattick IJ. Differentiating protein-coding and noncoding RNA: challenges and ambiguities. PLOS Comput Biol. (2008) 4(11)e1000176
50. Djonov V, Baum O, Burri PH. Vascular remodeling by intussusceptive angiogenesis. Cell Tissue Res 314: pp. 107–17, 2003.
51. Duscha BD, Robbins JL, Kontos CD, Kraus WD, Annex BH. Angiogenesis in peripheral artery disease: an emerging therapy targeting skeletal muscle. In: Santulli G, editor. Angiogenesis: Insights from a systematic overview. New York, NY: Nova Science Publisher; 2013. pp. 99–134.

52. Eilken HM, Adams RH. Dynamics of endothelial cell behavior in sprouting angiogenesis. Curr Opin Cell Biol. 2010 Oct;22(5):617-25. Review.

53. Eilken HM, Adams RH. Turning on the angiogenic microswitch. Nat Med. 2010 Aug;16(8):853-4.

54. Enright, A.J., John, B., Gaul, U. et al. (2003). MicroRNA targets in Drosophila. Genome Biol 5, R1. doi:10.1186/gb-2003-5-1-r1.

55. F.A. Karreth, Y. Tay, D. Perna, U. Ala, S.M. Tan, A.G. Rust, et al. In vivo identification of tumor suppressive PTEN ceRNAs in an oncogenic BRAF-induced mouse model of melanoma Cell, 147 (2011), pp. 382–395

56. Fasanaro P, D'Alessandra Y, Di Stefano V, Melchionna R, Romani S, Pompilio G, Capogrossi MC, Martelli F.MicroRNA-210 modulates endothelial cell response to hypoxia and inhibits the receptor tyrosine kinase ligand Ephrin-A3. J Biol Chem. 2008 Jun 6;283(23):15878-83.

57. Ferrara N, Gerber HP, LeCouter J. The biology of VEGF and its receptors. Nat Med. 2003;9(6):669- 76.

58. Fish JE, Santoro MM, Morton SU, Yu S, Yeh RF, Wythe JD, Ivey KN, Bruneau BG, Stainier DY, Srivastava D. 2008. miR-126 regulates angiogenic signaling and vascular integrity. Developmental Cell 15:272–284. DOI: https://doi.org/10.1016/j.devcel.2008.07.008, PMID: 18694566.

59. Friedman RC, Farh KK, Burge CB, Bartel DP. 2009. Most mammalian mRNAs are conserved targets of microRNAs. Genome Research 19:92–105. DOI: https://doi.org/10.1101/gr.082701.108, PMID: 18955434.

60. Gerhardt H, Golding M, Fruttiger M, Ruhrberg C, Lundkvist A, Abramsson A, Jeltsch M, Mitchell C, Alitalo K, Shima D, Betsholtz C. VEGF guides angiogenic sprouting utilizing endothelial tip cell filopodia. J Cell Biol. 2003 Jun 23;161(6):1163-77. Epub 2003 Jun 16.

61. Geudens I., Gerhardt H. Coordinating cell behaviour during blood vessel formation Development. 2011 Nov;138(21):4569-83.

62. Giraldez A.J., Mishima Y., Rihel J., Grocock R.J., Van Dongen S., Inoue K., Enright A.J., Schier A.F., Mishima Y., Rihel J., Grocock R.J., Van Dongen S., Inoue K., Enright A.J., Schier A.F., Rihel J.,Grocock R.J., Van Dongen S., Inoue K., Enright A.J., Schier A.F., Grocock R.J., Van Dongen S., Inoue K., Enright A.J., Schier A.F., Van Dongen S., Inoue K., Enright A.J., Schier A.F., Inoue K., Enright A.J., Schier A.F., Enright A.J., Schier A.F., Schier A.F. Z. Zebrafish MiR-430 promotes deadenylation and clearance of maternal mRNAs. Science. 2006 Apr 7;312(5770):75-9.

63. Gontan C, Jonkers I, Gribnau J. Long Noncoding RNAs and X Chromosome Inactivation. Prog Mol Subcell Biol. 2011;51:43-64. doi: 10.1007/978-3-642-16502-3_3.

64. Guo H, Ingolia NT, Weissman JS, Bartel DP. 2010. Mammalian microRNAs predominantly act to decrease target mRNA levels. Nature 466:835–840. DOI: https://doi.org/10.1038/nature09267.

65. Guttman M, Amit I, Garber M, French C, Lin MF, Feldser D, Huarte M, Zuk O, Carey BW, Cassady JP, Cabili MN, Jaenisch R, Mikkelsen TS, Jacks T, Hacohen N, Bernstein BE, Kellis M, Regev A, Rinn JL, Lander ES. Chromatin signature reveals over a thousand highly conserved large non-coding RNAs in mammals. Nature (2009) 458(7235):223–27

66. Guy Eelen, Pauline de Zeeuw, Michael Simons, and Peter Carmeliet Endothelial cell metabolism in normal and diseased vasculature Circ Res. 2015 Mar 27; 116(7): 1231–1244.

67. Ha M, Kim VN. 2014. Regulation of microRNA biogenesis. Nature Reviews Molecular Cell Biology 15:509–524. DOI: https://doi.org/10.1038/nrm3838, PMID: 25027649.

68. He L et al. A microRNA polycistron as a potential human oncogene. Nature. 2005;435(7043):828–33.
69. Heiss M, Hellström M, Kalén M, May T, Weber H, Hecker M, Augustin HG, Korff T. 2015. Endothelial cell spheroids as a versatile tool to study angiogenesis in vitro. The FASEB Journal 29:3076–3084. DOI: https://doi.org/10.1096/fj.14-267633, PMID: 25857554.
70. Holmqvist K, Cross MJ, Rolny C, Hägerkvist R, Rahimi N, Matsumoto T, et al. The adaptor protein shb binds to tyrosine 1175 in vascular endothelial growth factor (VEGF) receptor-2 and regulates VEGF-dependent cellular migration. J Biol Chem. 2004;279(21):22267-75.
71. Huang S, Lu W, Ge D, Meng N, Li Y, Su L, Zhang S, Zhang Y, Zhao B, Miao J. A new microRNA signal pathway regulated by long noncoding RNA TGFB2-OT1 in autophagy and inflflammation of vascular endothelial cells. Autophagy 11, 2172–2183 (2015).
72. Huang, Y.-A., You, Z.-H., Chen, X., Yan, G.-Y. J. B. S. B. (2016a). Improved protein-protein interactions prediction via weighted sparse representation model combining continuous wavelet descriptor and PseAA composition. *BMC Syst Biol* 10, 120. doi: 10.1186/s12918-016-0360-6.
73. Humphreys DT, Westman BJ, Martin DI, Preiss T. MicroRNAs control translation initiation by inhibiting eukaryotic initiation factor 4E/cap and poly(A) tailfunction. Proc Natl Acad Sci U S A. 2005 Nov 22;102(47):16961-6.
74. Hutvágner G, Zamore PD. A microRNA in a multiple-turnover RNAi enzyme complex. Science. 2002 Sep 20;297(5589):2056-60.

75. Izabella Slezak-Prochazka, Selvi Durmus, Bart-Jan Kroesen, and Anke van den Berg MicroRNAs, macrocontrol: Regulation of miRNA processing NA. 2010 Jun; 16(6): 1087–1095.

76. J.M. Franco-Zorrilla, A. Valli, M. Todesco, I. Mateos, M.I. Puga, I. Rubio-Somoza, et al.Target mimicry provides a new mechanism for regulation of microRNA activity Nat Genet, 39 (2007), pp. 1033–1037

77. Jackson RJ, Standart N. How do microRNAs regulate gene expression? Sci STKE. 2007 Jan 2;2007(367):re1. Review.

78. Jakobsson L1, Franco CA, Bentley K, Collins RT, Ponsioen B, Aspalter IM, Rosewell I, Busse M, Thurston G, Medvinsky A, Schulte-Merker S, Gerhardt H. Endothelial cells dynamically compete for the tip cell position during angiogenic sprouting. Nat Cell Biol. 2010 Oct;12(10):943-53.

79. Jan Krüger, Marc Rehmsmeier (2006). RNAhybrid: microRNA target prediction easy, fast and flexible, *Nucleic Acids Research,* Volume 34, Issue suppl_2, 1 July 2006, Pages W451–W454, doi:10.1093/nar/gkl243.

80. Kapranov, P. et al. RNA maps reveal new RNA classes and a possible function for pervasive transcription. Science 316, 1484–1488 (2007).

81. Kapranov, P. et al. RNA maps reveal new RNA classes and a possible function for pervasive transcription. Science 316, 1484-8 (2007).

82. Karagkouni D, Paraskevopoulou MD, Chatzopoulos S, Vlachos IS, Tastsoglou S, Kanellos I, Papadimitriou D, Kavakiotis I, Maniou S, Skoufos G, Vergoulis T, Dalamagas T, Hatzigeorgiou AG. 2018. DIANA-TarBase v8: a decade-long collection of experimentally supported miRNA-gene interactions. Nucleic Acids Research 46: D239–D245. DOI: https://doi.org/10.1093/nar/gkx1141, PMID: 29156006.

83. Karreth, F. A., Pandolfi, P. P. J. C. D. (2013). ceRNA cross-talk in cancer: when ce-bling rivalries go awry. 3, 1113–1121. doi: 10.1158/2159-8290.CD-13-0202.

84. Kasza Z, Fredlund Fuchs P, Tamm C, Eriksson AS, O'Callaghan P, Heindryckx F, Spillmann D, Larsson E, Le Jan S, Eriksson I, Gerwins P, Kjellén L, Kreuger J.MicroRNA-24 suppression of N-deacetylase/N-sulfotransferase-1 (NDST1) reduces endothelial cell responsiveness to vascular endothelial growth factor A (VEGFA). J Biol Chem. 2013 Sep 6;288(36):25956-63.

85. Kendall RL, Rutledge RZ, Mao X, Tebben AJ, Hungate RW, Thomas KA. Vascular endothelial growth factor receptor KDR tyrosine kinase activity is increased by autophosphorylation of two activation loop tyrosine residues. J Biol Chem. 1999;274(10):6453-60.

86. Koch, S., S. Tugues, X. Li, L. Gualandi, and L. Claesson-Welsh, 2011, Signal transduction by vascular endothelial growth factor receptors: Biochem J, v. 437, p. 169-83.

87. Korff, T., Krauss, T. & Augustin, H. G. Three-dimensional spheroidal culture of cytotrophoblast cells mimics the phenotype and differentiation of cytotrophoblasts from normal and preeclamptic pregnancies. Exp. Cell Res. 297, 415–423 (2004).

88. KornienkoA.E.,GuenzlP.M.,BarlowD.P.andPaulerF.M.2013 Gene regulation by the actof long non coding RNA transcription. BMCBiol.11,59.

89. Kozomara A, Griffiths-Jones S. 2014. miRBase: annotating high confidence microRNAs using deep sequencing data. Nucleic Acids Research 42:D68–D73. DOI: https://doi.org/10.1093/nar/gkt1181, PMID: 24275495.

90. Kuehbacher A, Urbich C, Zeiher AM, Dimmeler S. 2007. Role of dicer and drosha for endothelial microRNA expression and angiogenesis. Circulation

Research 101:59–68. DOI: https://doi.org/10.1161/CIRCRESAHA.107.153916, PMID: 17540974.

91. Kume T. Novel insights into the differential functions of Notch ligands in vascular formation. J Angiogenes Res. 2009 Nov 16;1:8.
92. Kurz H, Burri PH, Djonov VG. Angiogenesis and vascular remodeling by intussusception: From form to function. News Physiol Sci 18: pp. 65–70, 2003.
93. L. Poliseno, L. Salmena, J. Zhang, J. Carver, J. Haveman, P.P. Pandolfi, et al. A coding-independent function of gene and pseudogene mRNAs regulates tumor biology Nature, 465 (2010), pp. 1033–1038
94. L. Salmena, L. Poliseno, Y. Tay, PP. Pandolfi The ceRNA hypothesis: the Rosetta stone of a hidden RNA languag Cell, 146 (2011), pp. 353–358
95. Lagos-Quintana M et al. Identififi cation of novel genes coding for small expressed RNAs. Science. 2001;294(5543):853–8.
96. Lamalice L, Houle F, Huot J. Phosphorylation of Tyr1214 within VEGFR-2 triggers the recruitment of Nck and activation of Fyn leading to SAPK2/p38 activation and endothelial cell migration in response to VEGF. J Biol Chem. 2006;281(45):34009-20.
97. Lau NC et al. An abundant class of tiny RNAs with probable regulatory roles in Caenorhabditis elegans. Science. 2001;294(5543):858–62.
98. Leigh-Ann MacFarlane and Paul R. Murphy MicroRNA: Biogenesis, Function and Role in Cancer Curr Genomics. 2010 Nov; 11(7): 537–561.
99. Lewis, B. P., Shih, I.-H., Jones-Rhoades, M. W., Bartel, D. P., Burge, C. B. J. C. (2003). Prediction of mammalian microRNA targets. *Cell* 115, 787–798. doi: 10.1016/S0092-8674(03)01018-3.

100. Li H, Durbin R. 2010. Fast and accurate long-read alignment with Burrows-Wheeler transform. Bioinformatics 26: 589–595. DOI: https://doi.org/10.1093/bioinformatics/btp698, PMID: 20080505.

101. Li JH, et al.starBase v2.0: decoding miRNA-ceRNA, miRNA-ncRNA and protein-RNA interaction networks from large-scale CLIP-Seq data , Nucleic Acids Res. 2014 Jan;42:D92-7.

102. Li JH, Liu S, Zhou H, Qu LH, Yang JH. 2014. starBase v2.0: decoding miRNA-ceRNA, miRNA-ncRNA and protein–RNA interaction networks from large-scale CLIP-Seq data. Nucleic Acids Research 42:D92–D97. DOI: https://doi.org/10.1093/nar/gkt1248, PMID: 24297251.

103. Li K., Blum Y., Verma A. A noncoding antisense RNA in tie-1 locus regulates tie-1 function in vivo. Blood. 2010;115:133–139.

104. Li Y, Xu J, Chen H, et al. Comprehensive analysis of the functional microRNA-mRNA regulatory network identifies miRNA signatures associated with glioma malignant progression. *Nucleic Acids Res*. 2013;41(22):e203. doi:10.1093/nar/gkt1054.

105. Liu J, Carmell MA, Rivas FV, Marsden CG, Thomson JM, Song JJ, Hammond SM, Joshua-Tor L, Hannon GJ. Argonaute2 is the catalytic engine of mammalian RNAi. Science. 2004 Sep 3;305(5689):1437-41.

106. Liu, W.; Mao, S. Y.; Zhu, W. Y. Impact of tiny miRNAs on cancers.World J. Gastroenterol., 2007, 13, 497-502.

107. Love MI, Huber W, Anders S (2014). “Moderated estimation of fold change and dispersion for RNA-seq data with DESeq2.” *Genome Biology*, 15, 550. doi: 10.1186/s13059-014-0550-8.

108. Lu ZZ, Wang LS, Wu CT., Sheng Li Ke Xue Jin Zhan. Progress in Notch signaling. 2004 Apr;35(2):135-8. Review

109. Lu, J., Getz, G., Miska, E. A., Alvarez-Saavedra, E., Lamb, J., Peck, D., et al. (2005). MicroRNA expression profiles classify human cancers. *Nature* 435, 834. doi: 10.1038/nature03702.

110. M.T. Chen, H.S. Lin, C. Shen, Y.N. Ma, F. Wang, H.L. Zhao, et al.PU.1-regulated long noncoding RNA lnc-MC controls human monocyte/macrophage differentiation through interaction with microRNA 199a-5pvMol Cell Biol, 35 (2015), pp. 3212–3224

111. Martinez J, Tuschl T. RISC is a 5' phosphomonoester-producing RNA endonuclease. Genes Dev. 2004 May 1;18(9):975-80.

112. Matsumoto T, Bohman S, Dixelius J, Berge T, Dimberg A, Magnusson P, et al. VEGF receptor-2 Y951 signaling and a role for the adapter molecule TSAd in tumor angiogenesis. EMBO J. 2005;24(13):2342-53. 28.

113. McColl, B. K., M. E. Baldwin, S. Roufail, C. Freeman, R. L. Moritz, R. J. Simpson, K. Alitalo, S. A. Stacker, and M. G. Achen, 2003, Plasmin activates the lymphangiogenic growth factors VEGF-C and VEGF-D: J Exp Med, v. 198, p. 863-8.

114. Meister G, Landthaler M, Patkaniowska A, Dorsett Y, Teng G, Tuschl T. Human Argonaute2 mediates RNA cleavage targeted by miRNAs and siRNAs. Mol Cell. 2004 Jul 23;15(2):185-97.

115. Mercer TR and Mattick JS. Structure and function of long noncoding RNAs in epigenetic regulation. Nat Struct Mol Biol. (2013) 20(3):300-7

116. Mercer TR, Dinger ME, Mattick JS. Long non-coding RNAs: insights into functions. 2009. Nat Rev Genetics 10:155-159.

117. Michalik K.M., You X., Manavski Y. Long noncoding RNA MALAT1 regulates endothelial cell function and vessel growth. Circ Res. 2014;114:1389–1397.

118. Miska EA et al. Most Caenorhabditis elegans microRNAs are individually not essential for development or viability. PLoS Genet. 2007;3(12):e215.

119. Misook Ha, Mingxiong Pang, Vikram Agarwal and Z. Jeffery Chen (2008). Intespecies Regulation of MicroRNAs and their Targets. Biochim Biophys Acta., doi: 10.1016/j.bbagrm.2008.03.004.

120. Molnar A et al. miRNAs control gene expression in the single-cell alga Chlamydomonasreinhardtii. Nature. 2007;447(7148):1126–9.

121. Nature. (2014) 505(7483):344-52

122. Newman MEJ (2003) Structure and function of complex networks. SIAM Review 45:167-256.

123. Niazi F. and Valadkhan S. 2012 Computational analysis of functional long noncoding RNAs reveals lack of peptidecoding capacity and parallels with 3# UTRs. RNA 18, 825– 843.

124. Nicoli S, Knyphausen CP, Zhu LJ, Lakshmanan A, Lawson ND. 2012. miR-221 is required for endothelial tip cell behaviors during vascular development. Developmental Cell 22:418–429. DOI:https://doi.org/10.1016/j.devcel.2012.01.008, PMID: 22340502.

125. Nottrott S, Simard MJ, Richter JD. Human let- 7a miRNA blocks protein production on actively translating polyribosomes. Nat Struct Mol Biol. 2006 Dec;13(12):1108-14

126. Nowak-Sliwinska P, Alitalo K, Allen E, Anisimov A, Aplin AC, Auerbach R, Augustin HG, Bates DO, van Beijnum JR, Bender RHF, Bergers G, Bikfalvi A, Bischoff J, Böck BC, Brooks PC, Bussolino F, Cakir B, Carmeliet

P, Castranova D, Cimpean AM, et al. 2018. Consensus guidelines for the use and interpretation of angiogenesis assays. Angiogenesis 21:425–532. DOI: https://doi.org/10.1007/s10456-018-9613-x, PMID: 29766399.

127. Okamura K, Ishizuka A, Siomi H, Siomi MC. Distinct roles for Argonaute proteins in small RNA directed RNA cleavage pathways. Genes Dev. 2004 Jul 15;18(14):1655-66.

128. Olsson AK, Dimberg A, Kreuger J, Claesson-Welsh L. VEGF receptor signalling - in control of vascular function. Nat Rev Mol Cell Biol. 2006;7(5):359-71.

129. Paraskevopoulou MD, Georgakilas G, Kostoulas N, Reczko M, Maragkakis M, Dalamagas TM, Hatzigeorgiou AG. DIANA-LncBase: experimentally verified and computationally predicted microRNA targets on long non-coding RNAs. Nucl. Acids Res. (2013) 41 (D1).

130. Patel-Hett S, D'Amore PA. Signal transduction in vasculogenesis and developmental angiogenesis. Int J Dev Biol. 2011;55(4-5):353-63. Review.

131. Pauli A, Valen E, Lin MF, Garber M, Vastenhouw NL, Levin JZ, Fan L, Sandelin A, Rinn JL, Regev A, Schier AF. Systematic identification of long noncoding RNAs expressed during zebrafish embryogenesis. Genome Res. 2012 Mar;22(3):577-91.

132. Petersen CP, Bordeleau ME, Pelletier J, Sharp PA. Short RNAs repress translation after initiation in mammalian cells. Mol Cell. 2006 Feb 17;21(4):533- 42.

133. Pinzón, N., Li, B., Martinez, L., Sergeeva, A., Presumey, J., Apparailly, F., et al. (2017). microRNA target prediction programs predict many false positives. *Genome Res.* 27, 234–245. doi: 10.1101/gr.205146.116.

134. Poliseno L et al. A coding-independent function of gene and pseudogene mRNAs regulates tumour biology. Nature. (2010) 465(7301):1033-8

135. Ponting CP, Oliver PL, Reik W. Evolution and Functions of Long Noncoding RNAs. 2009. Cell 136: 629-641.

136. Potente M, Gerhardt H, Carmeliet P Basic and therapeutic aspects of angiogenesis.Cell. 2011 Sep 16; 146(6):873-87.

137. Rajewsky, N. L(ou)sy miRNA targets? Nat. Struct. Mol. Biol., 2006, 13, 754-755.

138. Rajewsky, N. microRNA target predictions in animals. Nat. Genet., 2006, 38(Suppl), S8-13.

References:

139. Rodriguez A et al. Identifification of mammalian microRNA host genes and transcription units. Genome Res. 2004;14(10A):1902–10.

140. Salmena L, Poliseno L, Tay Y, Kats L and Pandolfi PP. The ceRNA hypothesis: the Rosetta stone of a hidden RNA language. Cell. (2011) 146:353–358

141. Santulli G, Cipolletta E, Sorriento D, Del Giudice C, Anastasio A, Monaco S, Maione AS, Condorelli G, Puca A, Trimarco B, Illario M, Iaccarino G. CaMK4 Gene Deletion Induces Hypertension. J Am Heart Assoc. 2012 Aug; 1(4):e001081.

142. Santulli G. Angiopoietin-like proteins: a comprehensive look. Front Endocrinol (Lausanne). 2014 Jan23; 5():4.

143. Schmidt T, Carmeliet P., Blood-vessel formation: Bridges that guide and unite. Nature. 2010 Jun10;465(7299):697-9.

144. Shane P. Herbert and Didier Y.R. Stainier Molecular control of endothelial cell behaviour during blood vessel morphogenesis Nat Rev Mol Cell Biol. 2011 Aug 23; 12(9): 551–564.

145. Shannon P, Markiel A, Ozier O, Baliga NS, Wang JT, Ramage D, Amin N, Schwikowski B, Ideker T. Cytoscape: a software environment for integrated models of biomolecular interaction networks. Genome Res. 2003 Nov;13(11):2498-504. doi: 10.1101/gr.1239303. PMID: 14597658; PMCID: PMC403769.

146. Shi, X., Sun, M., Liu, H., Yao, Y., Song, Y. J. C. L. (2013). Long non-coding RNAs: a new frontier in the study of human diseases. *Cancer Lett.* 339, 159–166. doi: 10.1016/j.canlet.2013.06.013.

147. Siekmann AF, Lawson ND. Notch signalling and the regulation of angiogenesis. Cell Adh Migr. 2007 Apr-Jun;1(2):104-6.

148. Smalheiser NR, Torvik VI. Mammalian microRNAs derived from genomic repeats. Trends Genet. 2005;21(6):322–6.

149. Stanczyk, J.; Pedrioli, D. M.; Brentano, F.; Sanchez-Pernaute, O.; Kolling, C.; Gay, R. E.; Detmar, M.; Gay, S.Kyburz, D. Altered expression of MicroRNA in synovial fibroblasts and synovial tissue in rheumatoid arthritis. Arthritis Rheum., 2008, 58, 1001-1009

150. Stratman AN, Davis GE. Endothelial cell-pericyte interactions stimulate basement membrane matrix assembly: influence on vascular tube remodeling, maturation, and stabilization. Microsc Microanal. 2012 Feb;18(1):68-80. Review.

151. Suárez Y, Fernández-Hernando C, Yu J, Gerber SA, Harrison KD, Pober JS, Iruela-Arispe ML, Merkenschlager M, Sessa WC. 2008. Dicer-dependent endothelial microRNAs are necessary for postnatal

angiogenesis. PNAS 105: 14082–14087. DOI: https://doi.org/10.1073/pnas.0804597105, PMID: 18779589.

152. Subramanian A1, Tamayo P, Mootha VK, Mukherjee S, Ebert BL, Gillette MA, Paulovich A, Pomeroy SL, Golub TR, Lander ES, Mesirov JP.Gene set enrichment analysis: a knowledge-based approach for interpreting genome-wide expression profiles.Proc Natl Acad Sci U S A. 2005 Oct 25;102(43):15545-50. Epub 2005 Sep 30.

153. Suchting S, Freitas C, le Noble F, Benedito R, Bréant C, Duarte A, Eichmann A. The Notch ligand Delta-like 4 negatively regulates endothelial tip cell formation and vessel branching. Proc Natl Acad Sci U S A. 2007 Feb 27;104(9):3225-30

154. Takahashi T, Ueno H, Shibuya M. VEGF activates protein kinase C-dependent, but Ras-independent Raf-MEK-MAP kinase pathway for DNA synthesis in primary endothelial cells. Oncogene. 1999;18(13):2221-30

155. Tay Y, Rinn JL and Pandolfi PP1. The multilayered complexity of ceRNA crosstalk and competition.

156. Thurston G1, Kitajewski J.VEGF and Delta-Notch: interacting signalling pathways in tumour angiogenesis.Br J Cancer. 2008 Oct 21;99(8):1204-9. doi: 10.1038/sj.bjc.6604484. Epub 2008 Sep 30.

157. Tischer, E., R. Mitchell, T. Hartman, M. Silva, D. Gospodarowicz, J. C. Fiddes, and J. A. Abraham, 1991, The human gene for vascular endothelial growth factor. Multiple protein forms are encoded through alternative exon splicing: J Biol Chem, v. 266, p. 11947-54.

158. W. Peng, S. Si, Q. Zhang, C. Li, F. Zhao, F. Wang, et al.Long non-coding RNA MEG3 functions as a competing endogenous RNA to regulate gastric cancer progression j Exp Clin Cancer Res, 34 (2015), pp. 79–89

159. Wacker A, Gerhardt H. Endothelial development taking shape Curr Opin Cell Biol. 2011 Dec;23(6):676-85.

160. Wang J et al. CREB up-regulates long non-coding RNA, HULC expression through interaction with microRNA-372 in liver cancer. Nucleic Acids Res. (2010) 38(16):5366.

161. Wang J, Zhang J, Zheng H, et al. Mouse transcriptome: neutral evolution of 'non coding'complementary DNAs. Nature 2004;431(7010):757

162. Wang P, Ning S, Zhang Y, et al. Identification of lncRNA-associated competing triplets reveals global patterns and prognostic markers for cancer. *Nucleic Acids Res*. 2015;43(7):3478-3489. doi:10.1093/nar/gkv233.

163. Wang Y et al. Endogenous miRNA sponge lincRNA-RoR regulates Oct4, Nanog, and Sox2 in human embryonic stem cell self-renewal. Dev Cell. (2013) 25(1):69-80

164. Wapinski, O., Chang, H. Y. J. T. I. C. B. (2011). Long noncoding RNAs and human disease. *Cell Biol.* 21, 354–361. doi: 10.1016/j.tcb.2011.04.001.

165. Warner AJ, Lopez-Dee J, Knight EL, Feramisco JR, Prigent SA. The Shc-related adaptor protein, Sck, forms a complex with the vascular-endothelial-growth-factor receptor KDR in transfected cells. Biochem J. 2000;347(Pt 2):501-9. 33

166. Weidemann A, Breyer J, Rehm M, Eckardt K-U, Daniel C, Cicha I, Giehl K, Goppelt-Struebe M. 2013. HIF-1a activation results in actin cytoskeleton reorganization and modulation of Rac-1 signaling in endothelial cells. Cell Communication and Signaling 11:80. DOI: https://doi.org/10.1186/1478-811X-11-80.

167. Welten SM, Bastiaansen AJ, de Jong RC, de Vries MR, Peters EA, Boonstra MC, Sheikh SP, La Monica N, Kandimalla ER, Quax PH, Nossent AY.Inhibition of 14q32 MicroRNAs miR-329, miR-487b, miR-494, and miR-495 increases neovascularization and blood flow recovery after ischemia. Circ Res. 2014 Sep 26;115(8):696-708.

168. Wu L., Fan J., Belasco J.G., Fan J., Belasco J.G., Belasco J.G. MicroRNAs direct rapid deadenylation of mRNA. Proc Natl Acad Sci U S A. 2006 Mar 14;103(11):4034-9.

169. Wu LW, Mayo LD, Dunbar JD, Kessler KM, Ozes ON, Warren RS, et al. VRAP is an adaptor protein that binds KDR, a receptor for vascular endothelial cell growth factor. J Biol Chem. 2000;275(9):6059-62.

170. Xu K, Cleaver O. Tubulogenesis during blood vessel formation. Semin Cell Dev Biol. 2011 Dec;22(9):993-1004. Review.

171. Xu K, et al. Blood vessel tubulogenesis requires Rasip1 regulation of GTPase signaling. Dev Cell. 2011;20:526–539.

172. Y. Tay, L. Kats, L. Salmena, D. Weiss, S.M. Tan, U. Ala, et al.Coding-independent regulation of the tumor suppressor PTEN by competing endogenous mRNAs Cell, 147 (2011), pp. 344–357.

173. Yin KJ, Olsen K, Hamblin M, Zhang J, Schwendeman SP, Chen YE. 2012. Vascular endothelial cell-specific microRNA-15a inhibits angiogenesis in hindlimb ischemia. Journal of Biological Chemistry 287:27055–27064. DOI: https://doi.org/10.1074/jbc.M112.364414, PMID: 22692216.

174. Yoontae Lee, Minju Kim, Jinju Han, Kyu-Hyun Yeom, Sanghyuk Lee, Sung Hee Baek, and V Narry Kim MicroRNA genes are transcribed by RNA polymerase II EMBO J. 2004 Oct 13; 23(20): 4051– 4060.

175. Zhao T et al. A complex system of small RNAs in the unicellular green alga Chlamydomonas reinhardtii. Genes Dev. 2007;21(10):1190–203.

176. Zheng, Y., Liu, L., Shukla, G. C. J. C. L. (2017). A comprehensive review of web-based non-coding RNA resources for cancer research. *Cancer Lett* 407, 1–8. doi: 10.1016/j.canlet.2017.08.015

177. Zhou KR, Liu S, Cai L, Bin L, et al. ENCORI: The Encyclopedia of RNA Interactomes.

178. Zovein AC, et al. β1 integrin establishes endothelial cell polarity and arteriolar lumen formation via a Par3-dependent mechanism. Dev Cell. 2010;18:39–51.

eLIFE elifesciences.org

RESEARCH ARTICLE

A regulatory microRNA network controls endothelial cell phenotypic switch during sprouting angiogenesis

Stefania Rosano[1,2], Davide Corà[3,4], Sushant Parab[1,2], Serena Zaffuto[1,2], Claudio Isella[1,2], Roberta Porporato[2], Roxana Maria Hoza[1,2], Raffaele A Calogero[5], Chiara Riganti[1], Federico Bussolino[1,2†*], Alessio Noghero[1,2†‡*]

[1]Department of Oncology, University of Turin, Candiolo, Italy; [2]Candiolo Cancer Institute FPO-IRCCS, Candiolo, Italy; [3]Department of Translational Medicine, Piemonte Orientale University, Novara, Italy; [4]Center for Translational Research on Autoimmune and Allergic Diseases - CAAD, Novara, Italy; [5]Molecular Biotechnology Center, Department of Biotechnology and Health Sciences, University of Turin, Turin, Italy

Abstract Angiogenesis requires the temporal coordination of the proliferation and the migration of endothelial cells. Here, we investigated the regulatory role of microRNAs (miRNAs) in harmonizing angiogenesis processes in a three-dimensional in vitro model. We described a microRNA network which contributes to the observed down- and upregulation of proliferative and migratory genes, respectively. Global analysis of miRNA–target gene interactions identified two sub-network modules, the first organized in upregulated miRNAs connected with downregulated target genes and the second with opposite features. miR-424–5p and miR-29a-3p were selected for the network validation. Gain- and loss-of-function approaches targeting these microRNAs impaired angiogenesis, suggesting that these modules are instrumental to the temporal coordination of endothelial migration and proliferation. Interestingly, miR-29a-3p and its targets belong to a selective biomarker that is able to identify colorectal cancer patients who are responding to anti-angiogenic treatments. Our results provide a view of higher-order interactions in angiogenesis that has potential to provide diagnostic and therapeutic insights.

***For correspondence:** federico.bussolino@unito.it (FB); anoghero@lrri.org (AN)

†These authors contributed equally to this work

Present address: ‡Lovelace Biomedical Research Institute, Albuquerque, United States

Competing interests: The authors declare that no competing interests exist.

Funding: See page 23

Received: 30 April 2019
Accepted: 07 January 2020
Published: 24 January 2020

Reviewing editor: Stefania Nicoli, Yale University School of Medicine, United States

Introduction

The expansion of a vascular network through the sprouting angiogenesis (SA) process requires a coordinated control of many cellular functions, including the activation of quiescent endothelial cells (ECs), cell protrusion, basal lamina and extracellular matrix degradation, cell migration and proliferation, deposition of new basement membrane, cell junctions and cell polarity alteration (***Carmeliet and Jain, 2011***). In response to an angiogenic stimulus, activated ECs acquire distinct specialized phenotypes to accomplish these different tasks (***Jakobsson et al., 2010***), ultimately leading to the formation of a new functional vascular network. In particular, during SA, ECs dynamically switch from a tip phenotype, which guides the network expansion, to a stalk cell state that is characterized by active proliferation.

Vascular Endothelial Growth Factor-A (VEGF-A) is the most prominent cytokine that activates a genetic program that sustains this morphogenetic process (***Simons et al., 2016***). Transcriptomic analysis of tip and stalk cells isolated from the retinal vascular plexus showed differential expression of molecular determinants, represented by genes that are involved in extracellular matrix remodeling for tip cells and that encode components of the Notch signaling pathway for stalk cells (***del Toro***

et al., 2010; *Strasser et al., 2010*). It also has been proposed that the EC fate decision towards the tip or stalk cell phenotype is affected by VEGF-A gradient concentration in the surrounding extracellular matrix and by VEGF receptors expression levels (*Gerhardt et al., 2003*). Nevertheless, the gene expression regulatory events that sustain the initial transition from quiescent to activated ECs in response to an angiogenic stimulus have not yet been fully elucidated. We hypothesized that such phenotypic transition would require profound transcriptomic alterations that are brought about through the coordination of multiple regulation layers, including microRNA-mediated post-transcriptional regulation.

MicroRNAs (miRNAs) are a class of small non-coding RNAs that extensively modulate gene expression at the post-transcriptional level by targeting the mRNAs of protein-coding genes, directing their repression through mRNA degradation or (to a lesser extent) inhibition of protein translation (*Guo et al., 2010*). Interestingly, one of the first functions attributed to miRNAs was the control of developmental processes in which a morphogen gradient directs cell fate by activating specific genetic programs (*Inui et al., 2012*; *Ivey and Srivastava, 2015*). In this scenario, miRNAs are an integral part of the regulatory network that allows transitions between different cell states (*Hornstein and Shomron, 2006*). A role for miRNAs in ECs biology and vascular development has been established in vitro and in vivo by inhibition of two endonucleases that are required for mature miRNAs generation, namely Dicer and Drosha (*Ha and Kim, 2014*). The consequent reduction in the level of miRNAs resulted in alteration of several key properties of ECs, including their sprouting ability (*Kuehbacher et al., 2007*), and impaired postnatal angiogenesis (*Suárez et al., 2008*).

The activity of specific miRNAs in connection with the VEGF signaling pathway components has been studied more extensively (*Dang et al., 2013*). Several studies have demonstrated that miR-15a and miR-16, among other miRNAs, repress VEGF expression (*Chamorro-Jorganes et al., 2011*; *Yin et al., 2012*), whereas miR-126 promotes VEGF signaling by targeting the downstream effector *PIK3R2* (*Fish et al., 2008*). Furthermore, miR-27b and miR-221 are required for tip cell specification (*Biyashev et al., 2012*; *Nicoli et al., 2012*). Recently, RNA-sequencing (RNAseq) technology allowed the generation of a complete annotation of the miRNAs that are expressed by two-dimensional cultured human ECs in normal (*Kuosmanen et al., 2017*) or hypoxic (*Voellenkle et al., 2012*) conditions. Yet, the extent to which miRNAs could affect ECs phenotypic specification during SA has not been fully captured to date. Using RNAseq technology and network analysis, we exploited a three-dimensional model of SA that specifically describes the lateral inhibition-driven tip cell selection (*Heiss et al., 2015*; *Nowak-Sliwinska et al., 2018*), which is considered to be the first step in capillary nascence (*Eilken and Adams, 2010*). The information obtained was used to generate a co-expression network encompassing the post-transcriptionally regulated interactions between modulated miRNAs and their predicted protein-coding gene targets. Here, we show that in the initial step of SA, miRNAs act cooperatively to give robustness to the specification of the tip cell phenotype by reducing the expression of genes that are associated with cell-cycle progression and of members of the mitogen-associated protein kinase (MAPK) cascade that sustains VEGF-A-mediated cell proliferation, while de-repressing genes that are involved in cell migration and extracellular matrix remodeling.

Results

VEGF-A induces the tip phenotype of endothelial cells in a 3D model of sprouting angiogenesis

To study the activation of quiescent endothelial cells induced by an angiogenic stimulus, and the impact that miRNAs may exert on this process, we exploited a three-dimensional (3D) model that mimics the initial phase of SA in vitro (*Heiss et al., 2015*; *Nowak-Sliwinska et al., 2018*). ECs were induced to form 3D spheroids that are characterized by mature EC–EC junctions that are responsible for quiescent proliferation state (*Weidemann et al., 2013*). Spheroids were then embedded in a 3D collagen matrix and exposed to VEGF-A to trigger SA and to stimulate the formation of capillary-like structures (*Figure 1A*). Spheroids that had been exposed to VEGF-A for 18 hr (SPHV) and control spheroids (SPHC) were then processed for long- and small-RNAseq. Expression analysis of protein-coding genes identified 3071 differentially expressed (DE) genes in SPHV compared to SPHC (*Figure 1—figure supplement 1A*), revealing dramatic changes in the global transcriptomic profile

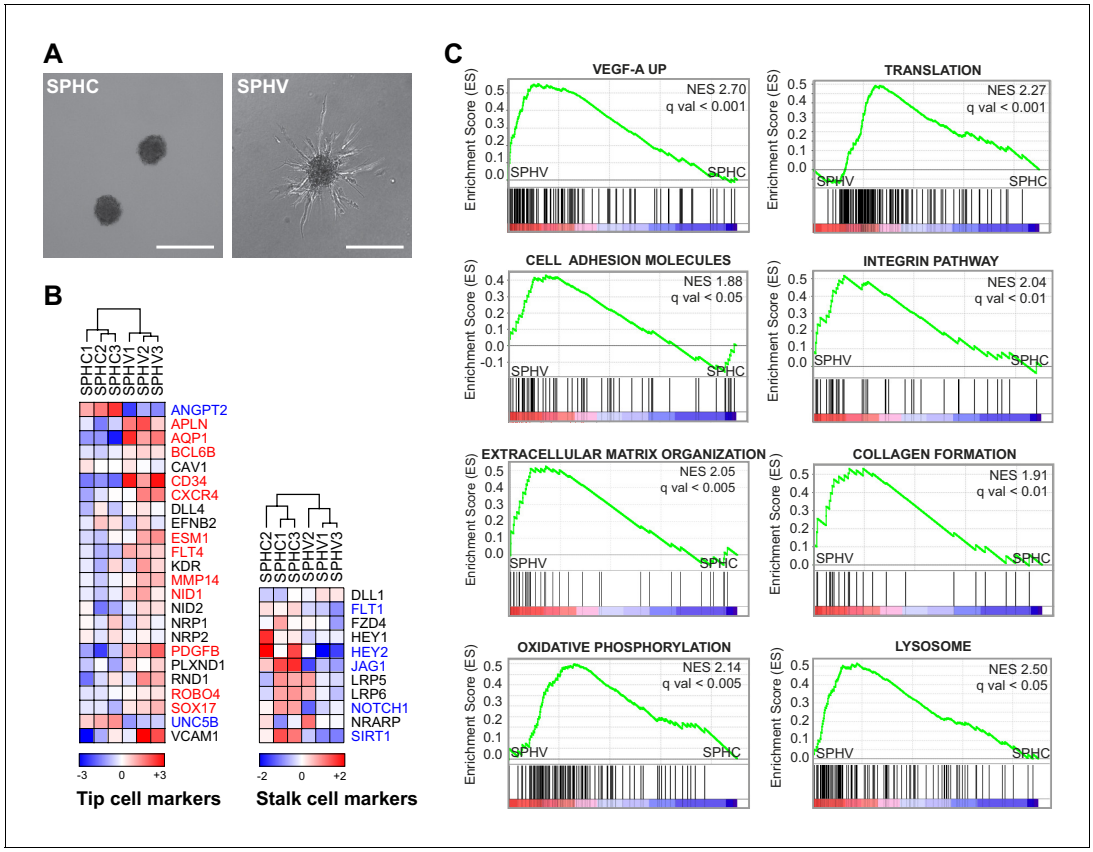

Figure 1. VEGF-A induces the tip phenotype of endothelial cells in a 3D model of sprouting angiogenesis. (**A**) EC spheroids were embedded in a collagen matrix and stimulated with VEGF-A to induce endothelial cell sprouting. RNA-sequencing analysis was performed on control spheroids (SPHC) not stimulated with VEGF-A, and on spheroids after 18 hr from stimulus (SPHV). Scale bars, 200 μm. (**B**) Heatmaps showing the expression of tip and stalk cell markers in SPHC and SPHV. Color bars indicate log_2(fold change) (log_2FC) in the comparison SPCV versus SPHC. (**C**) Positively enriched gene sets identified by the GSEA study in the genesets collection for canonical pathways. False discovery rate (FDR) was accepted when q value <0.05.
The online version of this article includes the following figure supplement(s) for figure 1:

Figure supplement 1. Expression profile of protein-coding genes annotated from the RNA-sequencing data.
Figure supplement 2. Organization of tip and stalk cells and the effect of Notch pathway manipulation in EC spheroids.

during the early phase of sprouting. Upregulation of VEGFR2, the major VEGF signal transducer, was validated by real-time PCR and Western blot analysis (***Figure 1—figure supplement 1B–D***). By looking at the expression of known tip and stalk cell markers (***De Bock et al., 2013***; ***del Toro et al., 2010***; ***Strasser et al., 2010***), we observed a general upregulation of tip marker genes and a downregulation of stalk marker genes in the comparison between SPHV and SPHC (***Figure 1B***). To visualize the organization of tip and stalk cells in this model, we analyzed the tip cell markers DLL4 and CXCR4 by immunofluorescence, or we transduced ECs with a fluorescent reporter of Notch activity to visualize stalk cells (***Figure 1—figure supplement 2A***). Although the EC sprouts strongly expressed DLL4 and CXCR4, cells in which the Notch reporter was activated were present only occasionally, so ECs largely acquired a tip-cell phenotype. Furthermore, manipulation of the Notch pathway by the γ-secretase inhibitor DAPT or by exogenous DLL4 resulted in increased or reduced sprouting, respectively (***Figure 1—figure supplement 2B***). Altogether, these observations indicate that this sprouting model can be used, at this specific developmental time point, to represent the early phase of VEGF-A response that involves activation of quiescent ECs and differentiation to tip cells.

To identify key biological pathways or that set of genes that is relevant to the sprouting process, the gene expression dataset was interrogated by taking advantage of Gene Set Enrichment Analysis (GSEA) (***Subramanian et al., 2005***). When comparing SPHV with SPHC, this analysis confirmed the upregulation of known VEGF-A responder genes ('VEGF-A UP'), and revealed a positive enrichment

of gene sets that are representative of several biological pathways and classes of molecules, including 'Translation', 'Cell adhesion molecules', 'Integrin pathway', 'Extracellular matrix organization', and 'Collagen formation'. Altogether, these alterations in gene expression mirror the transcriptional landscape that allows the migratory process. Other representative enriched pathways included 'Oxidative phosphorylation' and 'Lysosome' (***Figure 1C***).

Early VEGF-A response does not involve cell proliferation

Activation of the VEGF pathway through VEGF receptors initiates a signaling cascade that promotes the proliferation of ECs, among other actions (***Simons et al., 2016***). Nonetheless, and in agreement with the non-proliferating tip cell phenotype, GSEA showed a strongly negative enrichment score (ES) for cell-cycle-controlling genes (***Figure 2A***). Indeed, when looking at the expression levels of genes belonging to the 'cell cycle' KEGG pathway (***Kanehisa et al., 2016***), expression analysis showed that 52 genes out of 113 were DE in SPHV compared to SPHC, of which 50 were downregulated (***Figure 2B***). Hypergeometric test confirmed a statistically significant over-representation of this subset of genes among all the DE genes ($P = 7.40x10^{-5}$). Only cyclin D2 (CCND2) and cyclin E1 (CCNE1), two genes belonging to the cyclin family and participating in the G_1phase of the cell cycle, were upregulated. The finding that VEGF-A did not activate the proliferation of ECs and the accompanying DNA synthesis was also confirmed by the negative ES of gene sets that are representative of pyrimidine metabolism (***Figure 2C***) and, to a lesser extent, purine metabolism (***Figure 2D***). Indeed, we observed a general downregulation of genes involved in de novo synthesis of nucleotides (***Figure 2—figure supplement 1A***). Downregulations of the cyclin B1 gene and of IMPDH2, the rate-limiting enzyme in de novo guanine nucleotide biosynthesis, were validated by a real-time PCR assay (***Figure 2—figure supplement 1B,C***). We then measured the activities of the enzymes PPAT and CAD, which are considered to be indices of de novo synthesis of purine and pyrimidine nucleotides and of ATIC, which catalyzes the last step of purine synthesis, respectively. VEGF-A stimulation decreased the activity of these three enzymes in the 3D model (***Figure 2E***) indicating that, in this condition, de novo nucleotide synthesis is not required. On the contrary, their activity significantly increased in a control experiment performed with ECs cultured in 2D conditions (***Figure 2—figure supplement 1D***). Measurement of the percentage of cells that entered the S phase of the cell cycle confirmed that SPHC displayed a quiescent, non-proliferative status, and that VEGF-A was not able to trigger cell proliferation in spheroids significantly within an 18-hr time frame (***Figure 2F***). By contrast, VEGF-A activity on cell proliferation was well evident in cells cultured in standard 2D conditions, both in a proliferation assay and in a GSEA of the corresponding microarray data (***Figure 2—figure supplement 1E,F***). Furthermore, ECs that were mitotically inactivated by mitomycin C treatment maintained the ability to migrate and to form endothelial sprouts (***Figure 2G***). Taken together, these observations indicate that, in 3D conditions, early VEGF-A activity is primarily directed towards cell migration rather than towards cell proliferation.

A miRNA-dependent regulatory network sustains acquisition of the tip cell phenotype

Analysis of the small-RNAs sequencing data allowed the annotation of 639 mature miRNAs that were expressed by ECs across the two experimental conditions (SPHC and SPHV), at levels above a fixed cutoff (raw counts = 5) (***Figure 3—source data 1***). To assess the impact of endogenous miRNAs on the phenotypic differentiation that occurs during SA, we applied a bioinformatics pipeline based on the co-expression analysis of miRNAs and protein-coding genes, the prediction of miRNA target genes, and the association of miRNAs with biological pathways, followed by network analysis (***Figure 3A***). We first performed pair-wise correlation analysis between miRNAs and the expression of protein-coding expression, and plotted the distribution of the correlator (***Figure 3B***). We then isolated the subset of pairs that contained evolutionarily conserved or non-conserved miRNA–target gene interactions, based on TargetScan predictions (***Agarwal et al., 2015***). The frequency distribution of the correlator for the conserved interactions subset showed a significant enrichment in negative correlations compared to that for the entire dataset (***Figure 3B***, blue line). This is indicative of the repressive activity exerted by miRNAs on their targets; that is, when a miRNA is upregulated, its protein-coding gene target is downregulated and vice-versa. By contrast, the

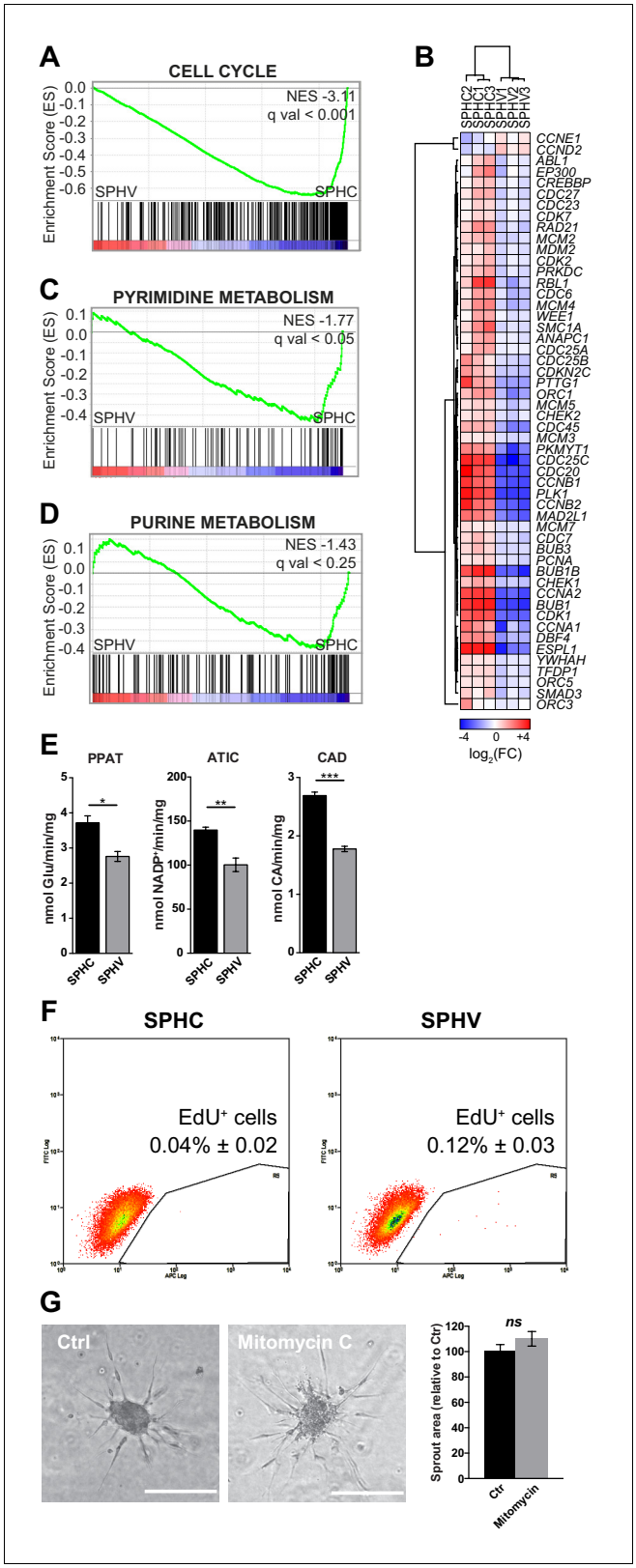

Figure 2. Early VEGF-A response does not involve cell proliferation. (**A**) GSEA plot showing negative association with the 'cell cycle' gene set in SPHV compared to SPHC. (**B**) Heatmap representing the expression of genes that are included in the KEGG pathway 'cell cycle' and are differentially expressed with a $\log_2$(Fold Change)>0.5, FDR < 0.05 when comparing SPHV versus SPHC. Color bar indicates $\log_2$(fold change). (**C, D**) GSEA plots showing,

Figure 2 continued on next page

Figure 2 continued

respectively, negative association with 'pyrimidine metabolism' and 'purine metabolism' gene sets in SPHV compared to SPHC. FDR was accepted when q value < 0.05. (**E**) Measure of the VEGF-A-induced enzymatic activity of three enzymes involved in de novo nucleotide synthesis in SPHC and SPHV. PPAT, phosphoribosyl pyrophosphate amidotransferase; ATIC, 5-aminoimidazole-4-carboxamide ribonucleotide formyltransferase/IMP cyclohydrolase; CAD, carbamoyl-phosphate synthetase 2/aspartate transcarbamylase/dihydroorotase. Data are represented as mean ± SEM of n = 3 experiments. (**F**) Cell proliferation rate analysis in SPHC and SPHV performed by evaluation of EdU incorporation into the newly synthetized DNA. Representative plots of n = 3 experiments. Data represent the mean percentage of proliferating cells ± SEM of n = 3 experiments. $p<0.05$ in the comparison between SPHC and SPHV. (**G**) Sprouting assay performed with ECs pre-treated with the cell replication blocker mitomycin C, and the corresponding quantification of sprout area. Data are represented as mean ± SEM from n = 3 experiments. ***, $p<0.001$; **, $p<0.01$; *, $p<0.05$; *ns*, not significant.

The online version of this article includes the following figure supplement(s) for figure 2:

Figure supplement 1. Expression profile of genes involved in nucleotide synthesis and cell proliferation assays.

non-conserved interactions subset did not show any significant alteration in the correlator frequency distribution (***Figure 3—figure supplement 1A***). Considering that target-site conservation is believed to be an indication of functional repression for mammalian miRNAs (***Friedman et al., 2009***), the integration of the SA gene expression dataset with information about evolutionarily conserved miRNA–target gene interactions provides information on the global activity of miRNAs taking place during the early sprouting phase. Therefore, this strategy permits the identification of target genes and biological processes that are more likely to be affected by miRNA-mediated post-transcriptional regulation.

GSEA-based analysis of correlation between miRNA expression and groups of genes participating in the regulation of specific biological pathways, represented as gene sets, was also used to support our findings (***Figure 3C***). This analysis identified five clusters of genesets representing distinct biological functions that are modulated during SA, together with their associated miRNAs. Gene ontology-based enrichment analysis performed on the genes contained in each cluster showed the following classes: 1) extracellular matrix remodeling and cell migration, 2) protein translation and metabolic processes, 3) intracellular signaling pathways, 4) RNA and protein processing, and, 5) cell cycle, DNA repair and MAPK cascade (***Figure 3D***). Clusters 1 and 2 contained genes that are mostly upregulated in SPHV compared to SPHC, whereas clusters 3, 4 and 5 contained genes that are mostly downregulated. To generate the global post-transcriptional regulatory network that sustains SA, the results from the above analyses were integrated. The resulting miRNA-centered co-expression network is composed of 149 miRNAs and 717 protein-coding genes connected by 1713 edges (***Figure 4*** and ***Figure 4—source data 1***). This network is essentially characterized by two individual components: one representing upregulated miRNAs connected with downregulated target genes, and one representing downregulated miRNAs connected with upregulated target genes. Degree distribution for both miRNAs (out-degree) and protein-coding genes (in-degree) observed a power-law behavior (***Figure 3—figure supplement 1B,C***), indicating that this network is compatible with the scale-free hypothesis, a typical feature of biological networks (***Barabási and Pósfai, 2016***).

The ERK gene module is under the control of a miRNA network in sprouting angiogenesis

VEGF-mediated EC proliferation and migration recognize the ERK pathway (***Wong and Jin, 2005***) and p38 MAP kinase activity (***Rousseau et al., 2000***), respectively, as master signaling modules (***Simons et al., 2016***). The data shown so far demonstrate that genes controlling cell proliferation were strongly downregulated (***Figure 2***), as were the expression levels of miRNAs correlated with genes associated with cell division and the MAPK cascade (***Figure 3D***). On these bases, we asked whether miRNAs have a role in suppressing the proliferative signal downstream VEGF-A through ERK pathway inhibition, while supporting cell migration in a 3D context. To this purpose, we interrogated the previously defined global post-transcriptional network (***Figure 4—source data 1***), and extracted the nodes corresponding to genes that encode known MAP kinases (***Craig et al., 2008***) together with their targeting miRNAs. Mapping of these interactions generated a network composed of one major component, which represents the inhibitory activity of miRNAs over several

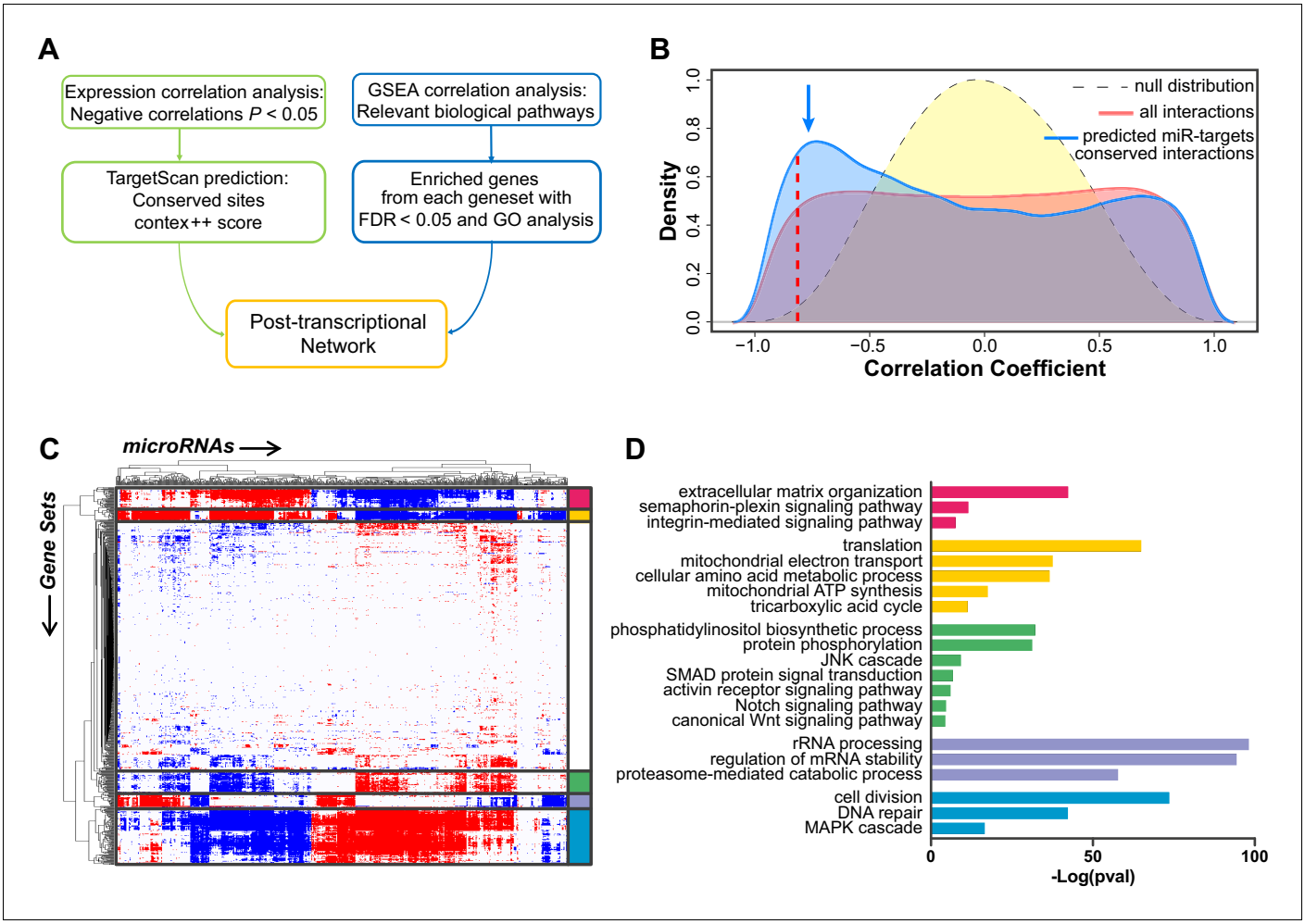

Figure 3. Construction of the post-transcriptional regulatory network that sustains acquisition of the tip cell phenotype. (**A**) Schematic view of the computational approach used to generate the post-transcriptional regulatory network. (**B**) Distribution of the correlator (Pearson coefficient) of the pair-wise analysis that considered the expression profile of all miRNAs and of protein-coding genes expressed in SPCH and SPHV. The gray dashed curve represents the null hypothesis distribution (uncorrelated miRNA–protein coding gene pairs) obtained by sample randomization with 1000 permutations; the red curve represents all pair-wise miRNA–protein-coding gene interactions; the blue curve represents the subset of miRNA–protein-coding gene pairs containing an evolutionarily conserved interaction as predicted by the TargetScan database. The blue arrow points to the enrichment in negative correlations. The red dashed line indicates the statistical significance threshold chosen for the correlator ($P < 0.05$). (**C**) Association matrix of the expression profiles of miRNAs (columns) with functional gene sets (rows) representing canonical pathways. Significant associations (FDR < 0.05) are shown in red (positive) or blue (negative). White, not significant. Biologically relevant clusters are highlighted with different colors. (**D**) For each cluster in (**C**), genes contributing to enrichment in the correlated gene sets were analyzed by functional annotation. Graph shows –Log(*P* value) of representative gene ontology terms.

The online version of this article includes the following source data and figure supplement(s) for figure 3:

Source data 1. miRNAs annotation.

Figure supplement 1. Non-conserved miRNA-target gene interactions analysis and network degree analysis.

MAP kinases (***Figure 5A***). These MAP kinases showed reduced expression in SPHV compared to SPHC. The *TAOK1* gene, whose protein product is a kinase that activates stress response (***Raman et al., 2007***), and *MAPK1*, whose protein product is ERK2, were the most targeted genes in this sub-network, being targeted by 11 and 7 different miRNAs, respectively. Notably, all components constituting the ERK module, namely C-Raf (*RAF1*), MEK (*MAP2K1*) and ERK2 (*MAPK1*), were represented. Among the four members composing the p38MAPK family (p38α, -β, -γ and -δ), only p38α (*MAPK14*) was present, but this gene was not connected with the major component of the network because its expression is increased in SPHV compared to SPHC. Downregulation of *RAF1*, *MAP2K1*, *MAPK1* and *TAOK1*, and upregulation of *MAPK14* in SPHV compared to SPHC, was

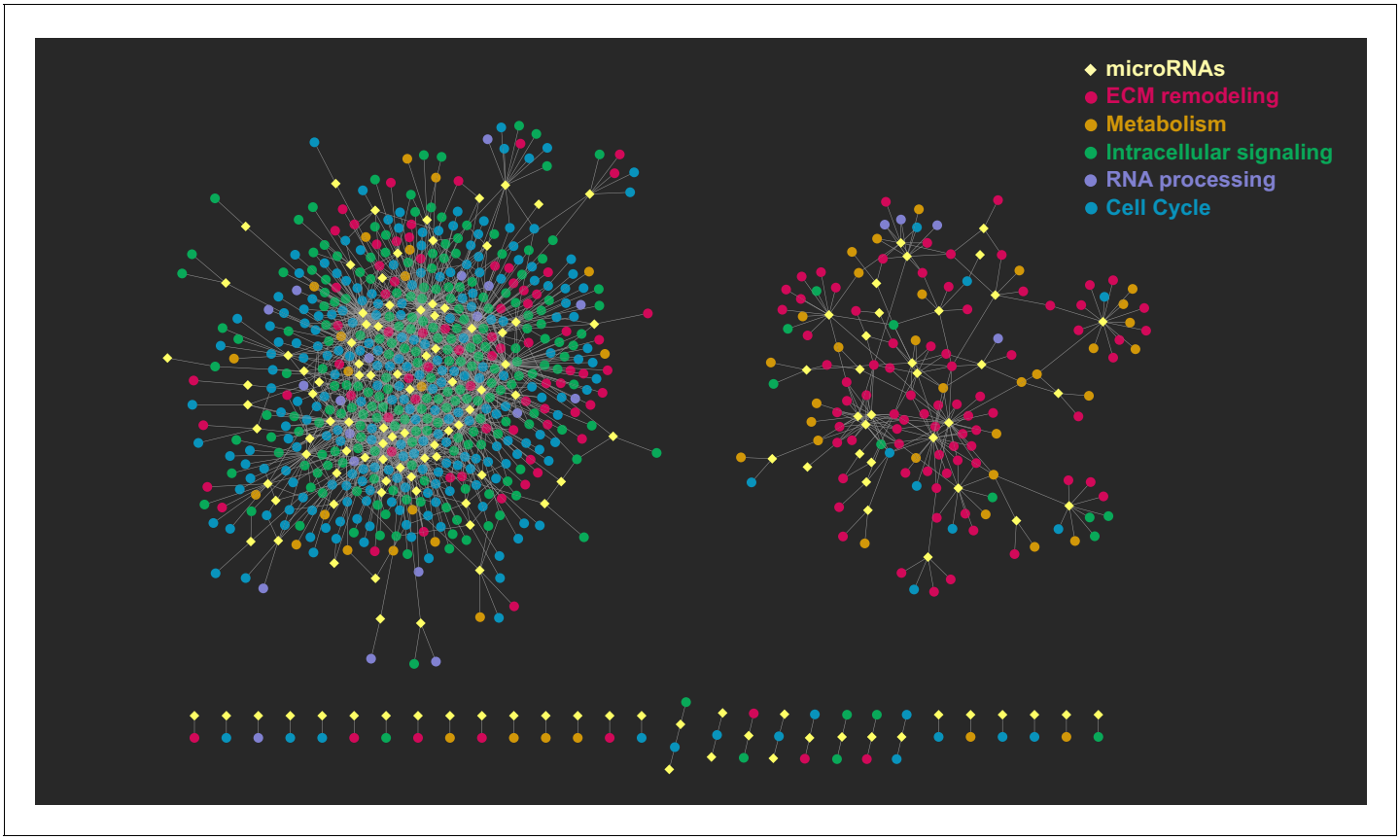

Figure 4. Graphical representation of the post-transcriptional network. The network consists of two major, independent components. The component on the left includes the interactions between upregulated miRNAs and their respective downregulated target genes; the component on the right includes the interactions between downregulated miRNAs and their respective upregulated target genes. Yellow diamonds represent miRNAs, circles represent their target genes, colored on the basis of the gene ontology cluster to which they belong. Edges are the miRNA–target gene pairs with a predicted direct interaction and a significant negative correlation.
The online version of this article includes the following source data for figure 4:

Source data 1. Co-expression network edges.

validated by real-time PCR (***Figure 5B***). Furthermore, ERK activity was measured in SPHC and SPHV by Meso Scale Technology (MSD) and expressed as P-ERK/total ERK ratio in order to take variations in total ERK expression into account. ***Figure 5C*** shows that ERK activity decreases after VEGF treatment. We also analyzed the effect in the sprouting model of SHC 772984 or SB 202190 compounds, which inhibit ERK1/2 and p38MAPK, respectively. Effective inhibitor concentrations were assessed by evaluating the inhibitory activity on VEGF-A-induced enzyme phosphorylation (***Figure 5—figure supplement 1***). As shown in ***Figure 5D***, treatment with the ERK inhibitor SCH 772984 did not have any effect on sprouting, confirming that ERK activity is not required, and in agreement with the observed low proliferation rate (***Figure 2***). By contrast, treatment with p38MAPK inhibitor SB 202190 completely abrogated the ability of ECs to migrate and to form sprouts.

DICER knock-down rescues the proliferative effect of VEGF-A

To demonstrate a regulatory role exerted by miRNAs on their predicted target genes and, more generally, to confirm the involvement of miRNAs in the control of the sprouting process, we removed mature miRNAs from the system by inactivating DICER, one of the endonucleases responsible for the generation of mature miRNAs from their precursors (***Ha and Kim, 2014***). This approach, which investigated the effects of miRNAs on the global post-transcriptional network, was preferred over the inhibition of individual miRNAs. Cells in which *DICER* expression was knocked-down by a short-hairpin RNA ($DICER^{KD}$) showed a reduction of sprouting to about 50% of that seen in cells

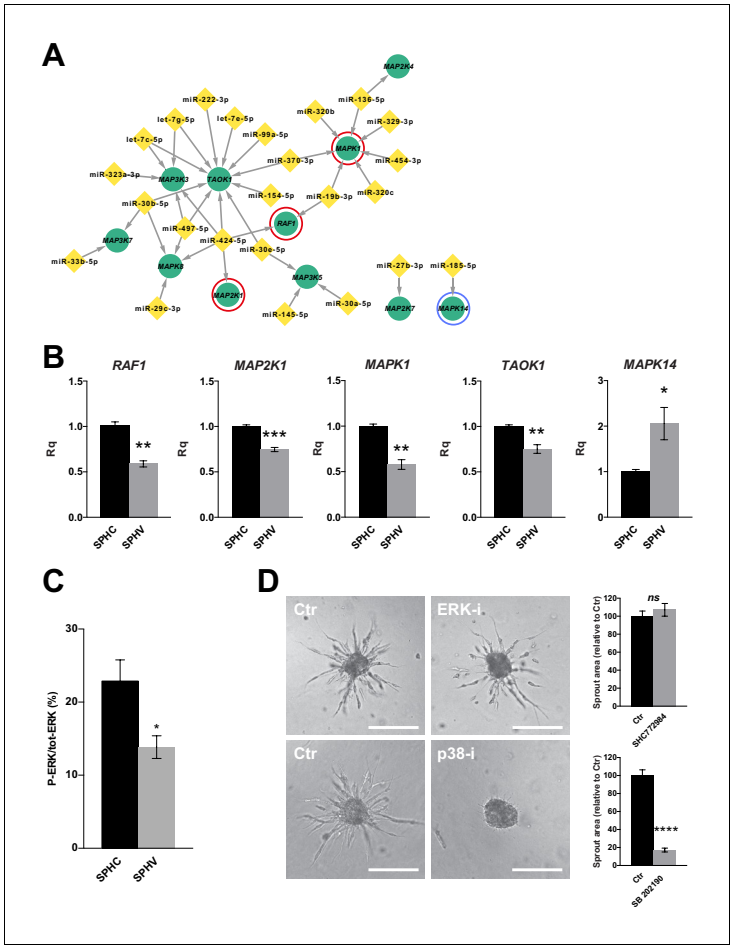

Figure 5. ERK activation is not required for sprouting and the ERK module is repressed by miRNAs. (**A**) Sub-network representing miRNAs targeting MAPK genes, derived from the global post-transcriptional network. The ERK module, consisting of *RAF1* (C-Raf), *MAP2K1* (MEK) and *MAPK1* (ERK2), is highlighted by red circles. *MAPK14* (p38α) is highlighted by a blue circle. (**B**) Real-time PCR validations of the RNA-sequencing data for some of the MAPK sub-network members, in SPHC and SPHV. Data are represented as mean ± SEM for n = 3 experiments. (**C**) ERK activity in SPHC and SPHV measured by Meso Scale Discovery (MSD) technology and expressed as the ratio of P-ERK/total ERK. Data are represented as mean ± SEM from n = 4 experiments. (**D**) Sprouting assay performed in the presence of the ERK inhibitor SHC 772984 or in the presence of the p38 inhibitor SB 202190, and the corresponding quantification of sprout area. Scale bars, 200 µm. ****, p<0.0001; ***, p<0.001; **, p<0.01; *, p<0.05; *ns*, not significant.

The online version of this article includes the following figure supplement(s) for figure 5:

Figure supplement 1. Assessment of the effective concentrations of ERK and p38 inhibitors in ECs.

transduced by non-targeting shRNA (*DICER*^{WT}) (***Figure 6—figure supplement 1A***), in agreement with previous observations (***Kuehbacher et al., 2007***). Effective *DICER* knock-down was verified by real-time PCR (***Figure 6—figure supplement 1B***). Then, we measured *RAF1*, *MAP2K1*, *MAPK1*, *TAOK1*, and *MAPK14* expression in SPHV generated with *DICER*^{WT} or *DICER*^{KD} cells by real-time PCR. All of these genes were upregulated in the *DICER*^{KD} condition (***Figure 6A***), indicating that their expression is subjected to a miRNA-mediated post-transcriptional control. The amount of P-ERK also increased in *DICER*^{KD} spheroids (***Figure 6B***). We repeated the sprouting assay with *DICER*^{KD} spheroids in the presence of the ERK inhibitor SCH 772984. *DICER*^{WT} spheroids were not affected by ERK inhibition, as shown previously in ***Figure 5D***. Nonetheless, *DICER*^{KD} spheroids that were treated with the ERK inhibitor showed a further reduction of sprouting (***Figure 6C,D***), confirming that removal of miRNAs by *DICER* knock-down restored ERK pathway activity and thus sensitizing cells to the ERK inhibitor SCH 772984.

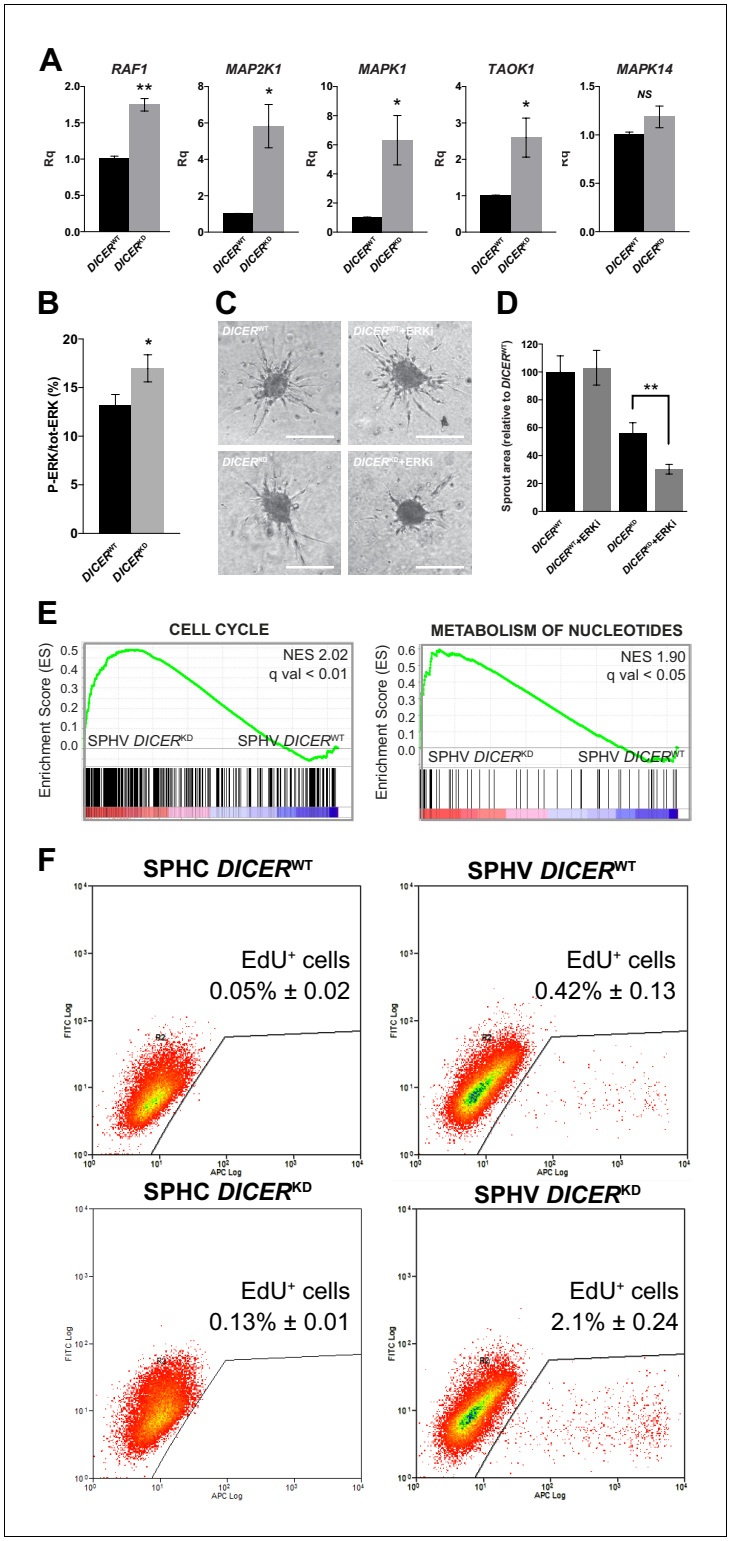

Figure 6. *DICER* knock-down rescues VEGF-A proliferative effect. (**A**) Real-time PCR analysis of *RAF1*, *MAP2K1*, *MAPK1*, *TAOK1*, and *MAPK14* in SPHV generated with *DICER*^{WT} cells or *DICER*^{KD} cells. Data are represented as mean ± SEM from n = 3 experiments. (**B**) ERK activity in SPHV generated with *DICER*^{WT} cells or *DICER*^{KD} cells measured by MSD and expressed as the ratio of P-ERK/total ERK. Data are represented as mean ± SEM from n = 3 experiments. (**C**) Sprouting assay performed with spheroids generated with *DICER*^{WT} cells or *DICER*^{KD} cells, in the presence of the ERK inhibitor SHC 772984. Scale bars, 200 µm. (**D**) Quantification of sprouts area for the

Figure 6 continued on next page

Figure 6 continued

cells shown in panel (**C**). Data are represented as mean ± SEM from n = 3 experiments. (**E**) GSEA study performed against the canonical pathways gene sets collection showed positive enrichment in the 'cell cycle' and 'metabolism of nucleotides' gene sets, in the comparison between *DICER*^{KD} and *DICER*^{WT} stimulated spheroids (SPHV). FDR was accepted when q value < 0.05. (**F**) Cell proliferation assessed by cytofluorimetric analysis of EdU incorporation into the DNA in spheroids generated from *DICER*^{WT} cells or *DICER*^{KD} cells that were either not stimulated (SPHC) or stimulated (SPHV) with VEGF-A. Representative plots of n = 3 experiments. Data represent mean percentages of proliferating cells ± SEM from n = 3 experiments. **, p<0.01; *, p<0.05.
The online version of this article includes the following figure supplement(s) for figure 6:

Figure supplement 1. *DICER* knock-down.

Furthermore, we performed a microarray study to analyze the gene expression profiles of *DICER*^{WT} and *DICER*^{KD} spheroids. GSEA comparison showed levels of expression of 'cell cycle'- and 'metabolism of nucleotides'-related genes in *DICER*^{KD}spheroids that were higher than those in *DICER*^{WT} spheroids stimulated with VEGF-A (***Figure 6E***), but no higher than those in control spheroids (***Figure 6—figure supplement 1C***). These findings indicate that the activity of miRNAs can restrain the expression of genes that promote cell proliferation following VEGF-A stimulation, in agreement with the network analysis (***Figure 3***) and the results shown in ***Figure 2***. This observation was further validated by measuring proliferation rate in SPHC and SPHV (***Figure 6F***). *DICER*^{KD} spheroids displayed a VEGF-A-dependent increase of cell proliferation compared to *DICER*^{WT} spheroids, confirming that the removal of miRNAs allows activation of the proliferative pathway downstream of VEGF-A. Interestingly, when the proliferation assay was performed on ECs cultured in 2D, *DICER*^{KD} cells showed a reduced proliferative response to VEGF compared to *DICER*^{WT} cells, suggesting that different miRNA activities are involved in the 2D or 3D environments (***Figure 6—figure supplement 1D***).

Biological validation of the miRNA hub network regulating sprouting angiogenesis

As previously shown, network analysis indicates that only few miRNAs are predicted to target a large number of protein-coding genes (***Figure 4—source data 1***), in agreement with the scale-free hypothesis that describes real networks. These hub miRNAs therefore should be pivotal to the network architecture and to the post-transcriptional regulatory activity that sustains the sprouting process. To validate the accuracy of the network analysis, and the relevance of the predicted miRNA-mediated post-transcriptional control of the genetic program sustaining SA, we subjected two miRNAs to further investigations. To validate the network, we selected miR-424–5p and miR-29a-3p, which are well-known miRNAs involved in angiogenesis regulation, and showed a high number of interactions with coding genes. miR-424–5 p was upregulated and targeted 98 genes, which were mainly related to intracellular signaling, including the MAPK pathway (***Figure 5A***) and cell cycle control (***Figure 7A*** and ***Figure 4—source data 1***). miR-29a-3p was downregulated and controlled the post-transcriptional regulation of 25 genes, mostly related to extracellular matrix remodeling (***Figure 7B*** and ***Figure 4—source data 1***). These miRNA–target interactions are also reported in the publicly available databases miRTarBase (***Chou et al., 2018***), TarBase (***Karagkouni et al., 2018***) and starBase (***Li et al., 2014***), which store miRNA–mRNA interactions supported by experimental evidence. In particular, for miR-424–5 p, 97 out of 98 interactions were present in these databases (24 of them in all three databases, and 73 in one or two); for miR-29a-3p, 23 out of 25 interactions were present in the databases (7 of them in all three databases, 16 in one or two) (***Figure 7—source data 1***). RNAseq expression data for miR-424–5p and miR-29a-3p in SPHC and SPHV were confirmed by real-time PCR analysis (***Figure 7—figure supplement 1A, B***). The expression of these two miRNAs can also be altered when the Notch pathway is manipulated. In fact, inhibition of the Notch pathway with DAPT, which increases sprouting (***Figure 1—figure supplement 2B***), increased the expression of miR-424–5p and reduced the expression of miR-29a-3p; the opposite effect was obtained when spheroids were treated with exogenous DLL4 (***Figure 7C,D***).

To assess the role of miR-424–5p and miR-29a-3p in the sprouting process, we altered their expression in ECs by using miRNA mimics or inhibitors (***Figure 7—figure supplement 1D,E***), and

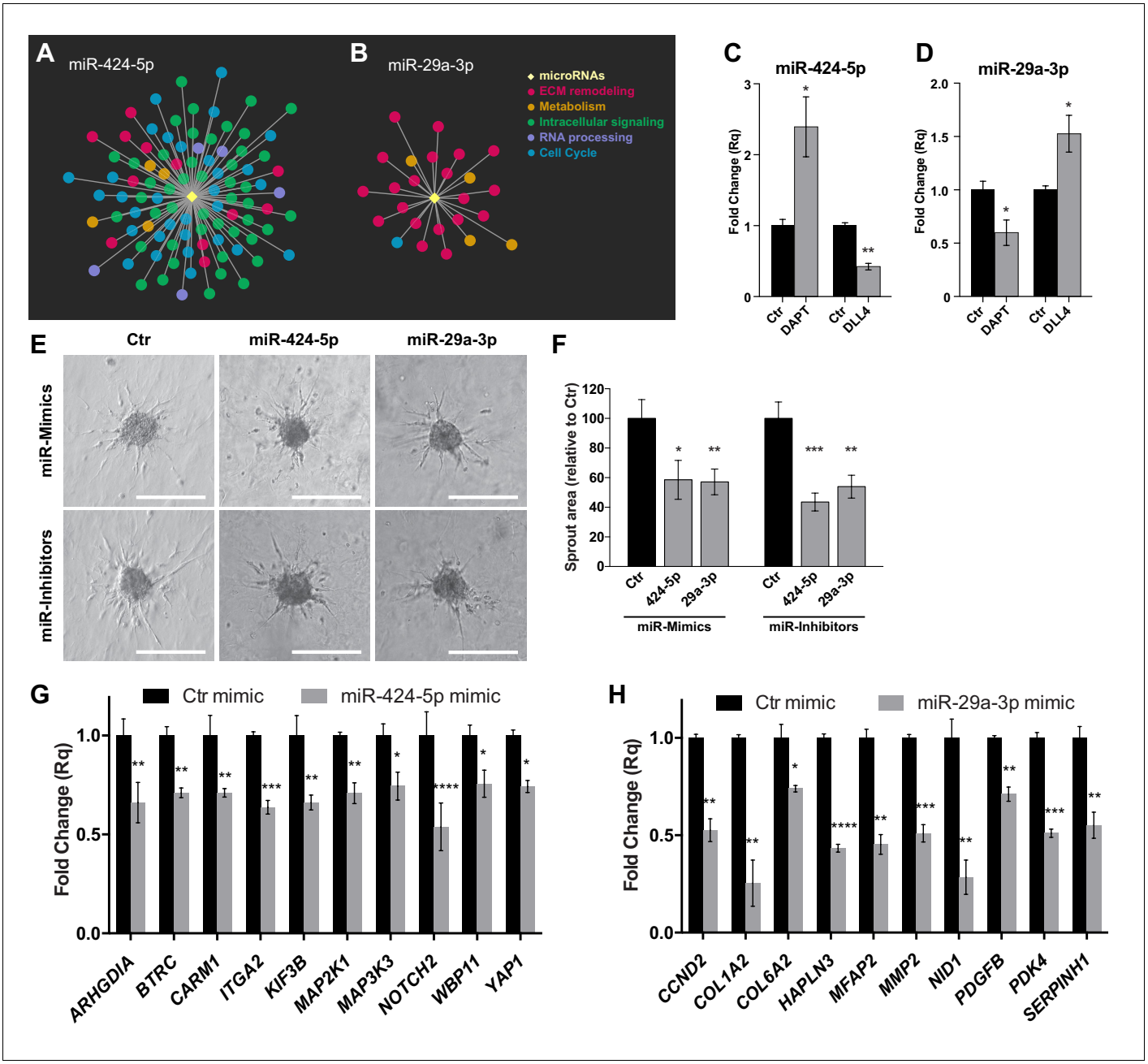

Figure 7. Hub miRNAs are essential to the sprouting process. Graphical representation of miR-424–5p (**A**) and miR-29a-3p (**B**) sub-networks, characterized by different patterns of functional classes target genes. (**C**) Real-time PCR analysis of miR-424–5p expression in SPHV treated with DAPT or with exogenous DLL4. Data are represented as mean ± SEM from n = 3 experiments. (**D**) Real-time PCR analysis of miR-29a-3p expression in SPHV treated with DAPT or with exogenous DLL4. Data are represented as mean ± SEM for n = 3 experiments. (**E**) Sprouting assay performed with ECs transfected with miR-424–5p or miR-29a-3p mimics and inhibitors. Scale bars, 200 µm. (**F**) Quantification of sprout area for the cells shown in panel (**E**). Data are represented as mean ± SEM from n = 4 experiments. (**G**) Real-time PCR assays in EC transfected with miR-424–5p mimic detecting the expression of miR-424–5p targets predicted from the network analysis. Data are represented as mean ± SEM from n = 3 experiments. (**H**) Real-time PCR assays in EC transfected with miR-29a-3p mimic detecting the expression of miR-29a-3p targets predicted from the network analysis. Data are represented as mean ± SEM from n = 3 experiments. ****, p<0.0001; ***, p<0.001; **, p<0.01; *, p<0.05.
The online version of this article includes the following source data and figure supplement(s) for figure 7:

Source data 1. Hub miRNA interactions supported by experimental evidence.
Figure supplement 1. miR-424–5p, miR-29a-3p and miR-16–5 p gain of function and loss of function.
Figure supplement 2. Tip competition assay.
Figure supplement 3. Assessment of VEGF-A-induced cell proliferation and migration upon modulation of miR-424–5p or miR-29a-3p.
Figure 7 continued on next page

Figure 7 continued

Figure supplement 4. Gene expression analysis of miR-424–5p and miR-29a-3p target genes upon miRNA inhibition.

performed the sprouting assay (***Figure 7E***). Quantification of sprout areas (***Figure 7F***) indicated that both upregulation by miRNA mimics and downregulation by miRNA inhibitors of miR-424–5p and miR-29a-3p impaired the ability of ECs to sprout, suggesting that the equilibrium of the network architecture requires that the expression of these two hub miRNAs is maintained at controlled levels. In a tip competition assay, spheroids were generated by mixing an equal number of ECs expressing the fluorescent protein DsRed with ECs transfected with miR-424–5p or miR-29a-3p mimics or inhibitors. Fluorescent or non-fluorescent cells occupying the tip position of the sprouts were counted. ***Figure 7—figure supplement 2*** shows that cells with altered expression of miR-424–5p or miR-29a-3p were impaired in reaching the tip cell position. To ascertain the robustness of the gain-of-function/loss-of-function approach, we also altered the expression of miR-16–5 p, which belongs to the same family as miRNA-424–5p, with which it putatively shares the same subset of target genes. However, our network analysis, which integrates target predictions with expression data, predicted a different subset of target genes for miR-424–5p and miR-16–5 p in the spheroid model (***Figure 4—source data 1***), and miR-16–5 p appeared to be a more peripheral miRNA that had only 16 predicted target genes. Indeed, miR-16–5 p modulation did not affect sprouting (***Figure 7—figure supplement 1F,G***). miR-424–5p and miR-29a-3p expression was significantly reduced in *DICER*^{KD} spheroids compared to *DICER*^{WT} spheroids (***Figure 7—figure supplement 1H***), suggesting that impaired expression of these two miRNAs could account, at least in part, for the sprouting defects observed in spheroids after *DICER* knock-down and in agreement with their role in network hierarchy. Furthermore, modulation of miR-424–5p, which is involved in the MAPK sub-network shown in ***Figure 5A***, resulted in the alteration of P-ERK activity according to the bioinformatics prediction, whereas modulation of miR-29a-3p, which is not involved in this network, was not effective (***Figure 7—figure supplement 1I***).

The effect of modulation of miR-424–5p and miR-29a-3p on cell proliferation was also tested in the spheroid model, the limitation of this assay being that the inhibition of cell proliferation cannot be evaluated as it is already close to zero. Indeed, none of the treatments could significantly increase cell proliferation (***Figure 7—figure supplement 3A***). In a 2D VEGF-dependent cell proliferation assay, however, treatment with the miR-424–5p mimic was able to reduce cell proliferation by 50% (***Figure 7—figure supplement 3B***). When tested in a 2D VEGF-dependent cell migration experiment, the miR-424–5p mimic had a positive effect on cell migration, whereas the miR-29a-3p mimic had a negative effect, the latter in agreement with its predicted role as a negative regulator of cell migration. miRNA inhibitors, however, did not show any significant effect (***Figure 7—figure supplement 3C***).

To further validate miR-424–5p and miR-29a-3p activity in the different biological pathways identified by the network analysis, we used real-time PCR to analyze the expression of 10 predicted target genes for miR-424–5p and 10 for miR-29a-3p. The targets investigated included genes involved in cell proliferation control (*MAP2K1*, *CCND2*), as well as genes involved in cell migration and extracellular remodeling (*ITGA2*, *NID1*), whose alteration could account for the phenotype observed. Indeed, we were able to verify a reduction in the expression of target genes when the corresponding miRNA mimic was overexpressed (***Figure 7H,I***). The effect of the miRNA inhibitors on the selected targets was, however, less pronounced, and we were able to observe upregulation for only three target genes for each condition (***Figure 7—figure supplement 4A,B***). Therefore, we analyzed the expression of other miR-424–5p and miR-29a-3p targets that are present in their respective miRNA subnetworks and that were not previously analyzed. For most of these target genes, we observed a significant upregulation upon inhibition of miRNAs (***Figure 7—figure supplement 4C,D***).

Modulation of miRNA hubs alters network architecture

The data showed above indicate, for some of the experiments performed, a non-symmetrical effect of miRNA upmodulation and downmodulation. This might be explained by the existence of a broader effect on the network architecture that would involve indirect miRNA–miRNA interactions. To gain more insights into the impact that modulation of a hub miRNA can have on the global

network architecture, we analyzed the expression of a large panel of miRNAs (of which 127 are represented in the SA network) by TaqMan array microRNA cards when miR-424–5p or miR-29a-3p were either upregulated or downregulated. The results indicate that 76 miRNAs showed altered expression ($|\Delta\Delta Ct| > 2$) upon up- or downmodulation of miR-424–5p or miR-29a-3p in at least two conditions (***Figure 8A***). In particular, when the analysis was restricted to the subset of miRNAs that share common target genes with miR-424–5p or miR-29a-3p in the SA network, 27 of these miRNAs showed altered expression (***Figure 8B***). Interestingly, several miRNAs showed increased expression under the effect of miR-424–5p or miR-29a-3p inhibitors. Altogether, these data indicate that that miR-424–5p and miR-29a-3p modulations induce a deep rewiring of the global miRNA network in addition to the modulation of their target coding genes, which can also account for the differences observed when comparing the effects of miRNA mimics and miRNA inhibitors.

Upregulation of genes that are targeted by miRNAs during sprouting angiogenesis correlates with tumor angiogenesis

To extend the results derived from the SA model in a human setting, and to identify possible implications of our findings in tumor biology, we evaluated the expression of the global upregulated and downregulated gene modules extracted from the network analysis, as well as the expression of single miRNA targets, in a collection of colorectal cancers (CRC). This type of tumor was chosen because angiogenesis plays an important role in its progression (***Battaglin et al., 2018***), and some of the patients benefit from anti-angiogenic therapy with the VEGF blocker bevacizumab. 450 CRC samples were first ranked by their endothelial gene signature or endothelial score, a parameter that takes into account the expression of 35 EC-specific genes, not expressed by CRC or other stromal components, and that correlates with ongoing angiogenesis (***Isella et al., 2015***). When GSEA was used to correlate the different miRNA-target gene subsets obtained from the network analysis (***Figure 4—source data 1***) with CRC samples, we observed a significant positive enrichment for the miR-29a-3p-targets subset (***Figure 9A***), meaning that expression of miR-29a-3p targets is higher in CRCs that have a high endothelial score. Furthermore, average expression in CRC samples of the genes that were present in the network analysis and that are upregulated in SPHV (upregulated module, ***Figure 9—source data 1***) also showed a significant positive correlation with endothelial score (***Figure 9B***). Likewise, GSEA analysis in which the endothelial score was used as phenotype classifier revealed a significant enrichment of the upregulated module (***Figure 9C***) and allowed the identification of a core gene set of 58 genes that are coherently regulated in vitro and in vivo (***Figure 9—source data 1***). This gene subset was further challenged in a dataset from CRC patients treated with the VEGF inhibitor bevacizumab (***Pentheroudakis et al., 2014***). Indeed, the core subset of the upregulated gene module was significantly enriched in bevacizumab-responding patients (***Figure 9D***), thus confirming the involvement of the genes within this module during pathological angiogenic remodeling.

Discussion

The spheroid model as a tool to study tip cell selection

In this study, we generated protein-coding gene and miRNAs RNAseq data from a VEGF-A dependent, well-established three-dimensional model of SA (***Korff and Augustin, 1998***; ***Nowak-Sliwinska et al., 2018***). We showed that initial response to VEGF-A in ECs consists of a profound remodeling of the transcriptome, which allows differentiation toward the tip phenotype. This includes the activation of genes that regulate extracellular matrix remodeling, which is essential to the migratory process, and the repression of genes that promote cell proliferation and nucleotide de novo synthesis (***Figure 1B*** and ***Figure 2***). The observation that these two fundamental VEGF-A downstream pathways might not be synchronous in tip cells is in agreement with earlier studies on pathophysiological angiogenesis, in which it was demonstrated that the onset of vascular sprouting depends on the migration of existing ECs and does not require EC proliferation (***Ausprunk and Folkman, 1977***; ***Sholley et al., 1984***). The spheroid model described here cannot, however, recapitulate all of the molecular events that lead to the formation of a more complex vascular bed. Furthermore, it cannot allow the analysis of tip-stalk cell dynamics because of the inability to differentiate stalk cells properly. This can be attributed to the intrinsic short life of the model

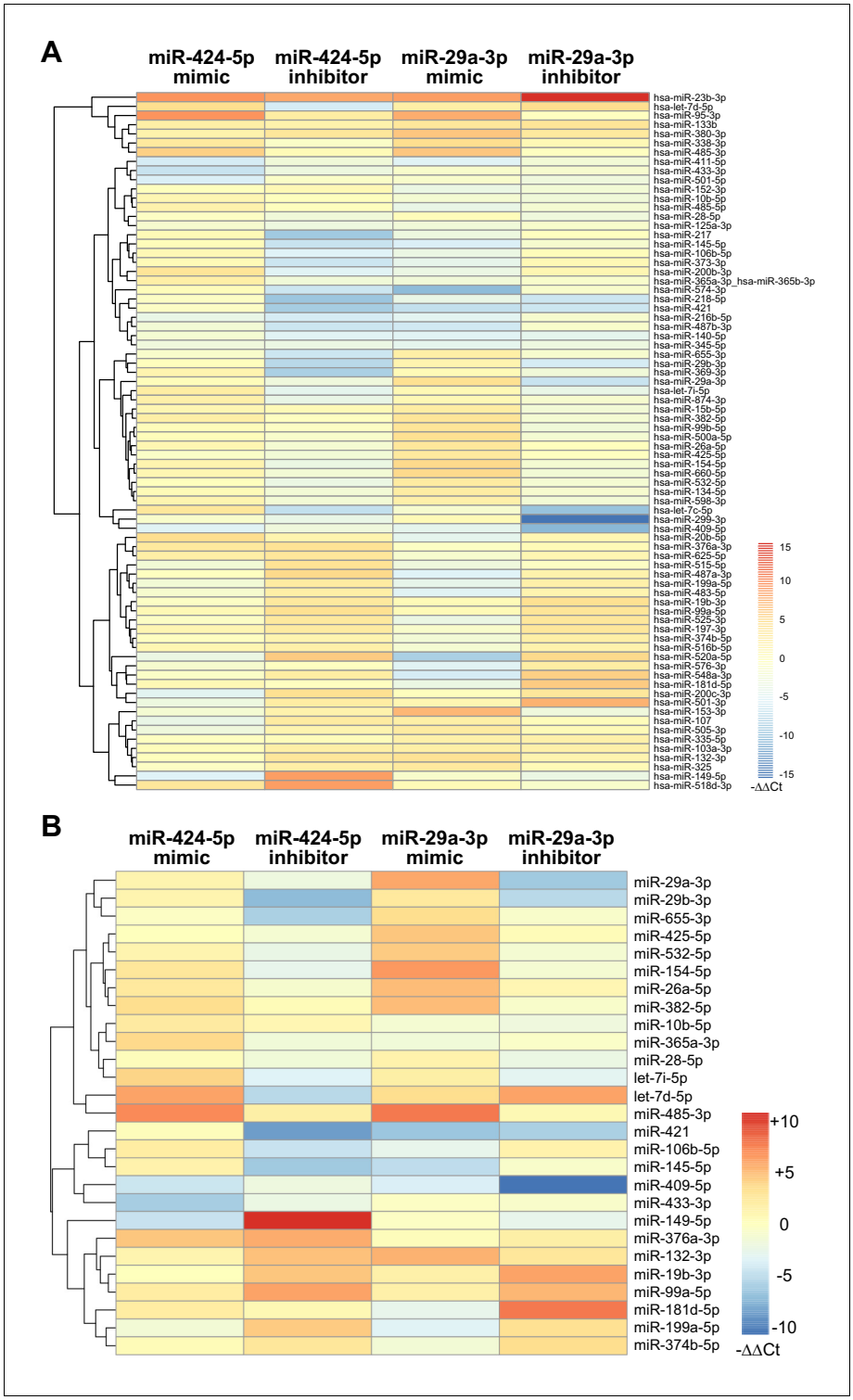

Figure 8. Modulation of miRNA hubs alters network architecture. (**A**) Heatmap showing the result of a differential gene expression analysis of a panel of miRNAs upon up- or downmodulation of miR-424–5p or miR-29a-3p. Only miRNAs with |ΔΔCt| > 2 are represented. Color bar indicates –ΔΔCt values. (**B**) Heatmap showing only those differentially expressed miRNAs that have predicted target genes in common with miR-424–5p or miR-29a-3p. Color bar indicates –ΔΔCt values.

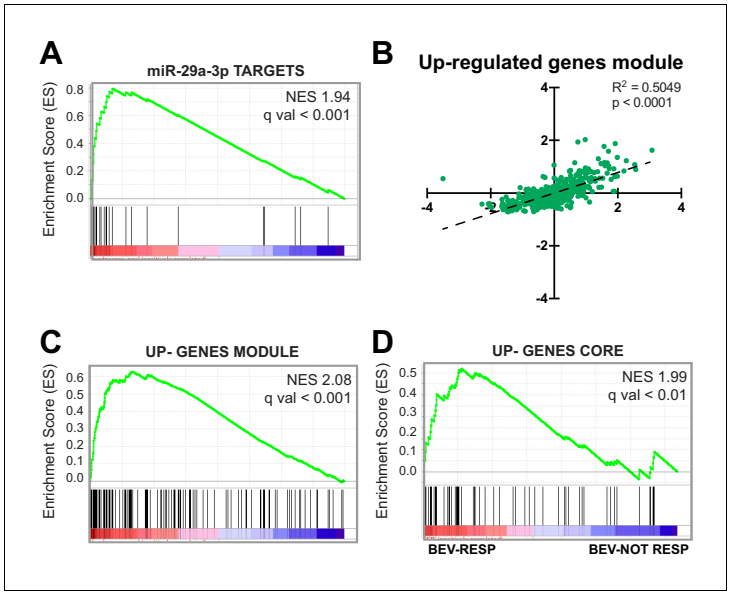

Figure 9. Upregulation of genes that are targeted by miRNAs during SA correlates with tumor angiogenesis. (**A**) GSEA plot showing significant positive association for miR-29a-3p target genes in CRC samples stratified by their endothelial score. (**B**) Scatter plot showing correlation, in CRC samples, between the expression of genes that constitute the upregulated gene module from the network analysis and endothelial score. (**C**) GSEA plot showing significant positive association for the up-gene module with CRC samples stratified by their endothelial score. (**D**) GSEA plot showing significant positive association for the upregulated genes core, extracted from panel (**B**), with a cohort of bevacizumab-responding CRC patients (bev-resp), compared to not-responding patients (bev-not resp). FDR was accepted when q value < 0.05.

The online version of this article includes the following source data for figure 9:

Source data 1. Genes constituting the upregulated gene module and the enrichment core in CRC.

compared to the mouse retina model and to the absence of other co-regulatory events, such as the generation of a VEGF gradient by neurons (***Okabe et al., 2014***). Nonetheless, the specificity of this model in the generation of tip cells allowed the analysis, at a molecular level, of the post-transcriptional regulation that sustains tip cells selection.

Functions of miRNA in the context of regulatory networks

Here, information about the expression of miRNAs was used to generate a global post-transcriptional regulatory network based on co-expression between miRNAs and their predicted protein-coding target genes. Using this unbiased approach, we were able to emphasize a role of miRNAs in repressing genes that regulate cell proliferation and other signaling pathways downstream of VEGF. Such pathways include the MAPKs signaling cascade, which is mainly involved in transducing the VEGF-A mitogenic signal. Meanwhile, miRNAs also promoted the expression of genes that are involved in extracellular matrix remodeling.

Several studies have highlighted the importance of both transcriptional and post-transcriptional interactions in the shaping of global regulatory networks. The connections involving both transcription factors and miRNAs can be described in terms of small regulatory patterns (***Hornstein and Shomron, 2006***; ***Tsang et al., 2007***). Some circuits topologies, in their incoherent form, can be associated with positive correlation patterns between the expression of miRNAs and their predicted target genes, and are generally thought to have a buffering function on transcriptional noise. On the other hand, the coherent form of miRNA-target circuits is thought to mediate a post-transcriptional reinforcement of transcriptional regulation and is associated with negative correlation schemes of gene expression (***Cora' et al., 2017***). Our experimental setup intrinsically highlights and selects such negative correlations (***Figure 3B***). In this context, miRNA activity is meant to reinforce the transcriptional program and to facilitate phenotypic transitions by precisely shaping a genetic program that is triggered by external cues (***Ebert and Sharp, 2012***). In principle, however, we cannot

preclude the presence, among the miRNA–gene network presented, of a later layer of indirect interactions between miRNAs and their targets or between the miRNAs themselves that is able to fine-tune the behavior of the network elements.

Regulation of MAP kinase activity by miRNAs

To demonstrate carefully the robustness of the post-transcriptional regulatory network described here at a system level, we performed a series of experimental validation by envisaging two different approaches: 1) removal of mature miRNAs by *DICER* knock-down to evaluate the global effects of miRNA-mediated post-transcriptional activity on SA, and 2) validation of predicted targets for two miRNAs identified as hubs from the network analysis. For the first validation approach, we focused on a MAPK-specific subnetwork, due to its role in cell proliferation control, that pinpointed a coordinated miRNA inhibitory activity on the ERK module, represented by the *RAF1*, *MAP2K1* and *MAPK1* genes (***Figure 5A***). Removal of mature miRNAs by means of *DICER* knock-down reverted the downregulation of these genes that was observed after VEGF-A stimulus (***Figure 5B*** and ***Figure 6A***), increased P-ERK activity (***Figure 6B***), and restored a proliferative response (***Figure 6F***). Although the process that is triggered by a mitogenic stimulus depends on subsequent substrate phosphorylation throughout the MAPK cascade, it has been shown that the final outcome can also be influenced by miRNA-mediated post-transcriptional regulation of MAPK genes themselves. In particular, and in accordance with the interactions presented in this work, *RAF1* targeting by miR-497 inhibits breast cancer cell growth (***Li et al., 2011***), whereas downregulation of miR-424 leads to aberrant cell proliferation through MEK1 (*MAP2K1*) upregulation in senile hemangioma (***Nakashima et al., 2010***). Here, we also identified novel miRNA–MAPK interactions, such as miR-424–5p targeting *MAP2K1* and *MAP3K3*, or miR-19b-3p and miR-320b/c targeting *MAPK1*, although more specific experimental validations are required to demonstrate the function of these interactions.

Our data also indicate that the effect of miRNA activity in ECs is highly context-dependent. In fact, previous studies attributed the angiogenesis defects induced by *DICER* inhibition to a reduction of VEGF-induced proliferation (***Suárez et al., 2007***; ***Suárez et al., 2008***). However, the mechanistic demonstration of this hypothesis was limited to in vitro experiments that used 2D-cultured ECs only. Although we confirmed the reported effects of *DICER* inhibition in 2D cultures, we also demonstrated that the activation of ECs that enables tip cell selection and migration (the first step in SA [***Carmeliet and Jain, 2011***]) benefits from a miRNA-mediated inhibition of cell proliferation. Therefore, in the more complex in vivo scenario, in which different ratios of migratory (tip) and proliferating (stalk) ECs exist simultaneously, miRNAs could have different effects depending on the EC phenotype considered. Nevertheless, owing to its broad effect on the expression of miRNAs, *DICER* inhibition could also have affected regulatory pathways other than ERK, and thus could have contributed to the observed phenotype.

Role of two hub miRNAs in the post-transcriptional regulatory network

For the second validation approach, we focused on two hub miRNAs: miR-424–5p and miR-29a-3p, which belong to the network component containing up- and downregulated miRNAs, respectively. Their expression could be further modulated when the Notch pathway is either repressed or activated (***Figure 7C,D***), supporting the concept that their regulation promotes tip cell specification. Earlier studies in two-dimensional EC cultures reported that miR-424–5p upregulation reduced VEGF-induced proliferation (***Chamorro-Jorganes et al., 2011***), or indirectly modulated HIF-α expression thus promoting angiogenesis (***Ghosh et al., 2010***), whereas miR-29a inhibition impaired cell-cycle progression (***Yang et al., 2013***). However, it is also known that a widespread feature of miRNA activity toward a specific target is context-dependency, which also highlights the importance of target validation under physiological conditions (***Erhard et al., 2014***). In our three-dimensional model, integration of expression data with target prediction allowed the identification of context-specific targets. In fact, miR-424–5p showed preferential targeting activity towards genes that are associated with cell-cycle progression and intercellular signaling, whereas miR-29a-3p activity was more specific to genes involved in extracellular matrix remodeling (***Figure 7A,B***). A similar targeting pattern, for both miRNAs, has been described in previous evidence-based computational studies in different cellular models (***Tsang et al., 2010***). Our independent analyses in ECs support

the concept that a single miRNA can act on different targets belonging to the same pathway to reinforce its biological effect.

Finally, our unbiased approach disclosed an unpredicted hierarchical role of miR-424–5p and miR-29a-3p in a complex process such as SA. In fact, perturbation of miR-424–5p and miR-29a-3p expression levels propagated throughout the network, causing alterations in the expression levels of a large number of other miRNAs, including miRNAs that share coding targets with miR-424–5p or mir-29a-3p. Considering that each gene in the network is targeted by several different miRNAs, such broad network rearrangement could explain why inhibition of a single miRNA did not result in a significant increase in the expression of all its targets in a predictable way, and why inhibition of miR-424–5p alone was not as effective as removal of miRNAs by DICER knock-down in rescuing cell proliferation upon VEGF-A stimulus.

Signature of the activity of miRNAs in tumor angiogenesis

To prove the strength of our experimental design and extend our findings to clinical data, we investigated the angiogenic post-transcriptional activity in human tumors. Indeed, in a collection of 450 CRC, we successfully challenged the correlation between gene modules that constitute a signature of the activity of miRNAs and ongoing angiogenesis in the stromal compartment. A significant correlation was, however, not detected for the downregulated gene modules, which mostly included cell-proliferation-associated genes. This can be explained by the fact that, in whole tumor transcriptomic data, the signal from the highly proliferating epithelial cancer cells overcome the signal coming from the less represented ECs. In addition, a signature composed of 58 sprouting-associated genes, which also included miR-29a-3p targets, was able to identify patients who benefitted from anti-angiogenic treatment with the VEGF-A blocking agent bevacizumab. On one side, this strengthens the evidence of the involvement of post-transcriptional regulation in tumor angiogenesis, and on the other side, it paves the way for future development of predictive markers for VEGF-A blocking agents. This analysis could also be extended to other cancer types, such as ovarian, cervical, non-small cell lung cancer or glioblastoma, in which angiogenesis is recognized to support tumor growth and in which bevacizumab is an approved therapeutic option. In summary, network analysis of whole transcriptomic data obtained from an in vitro SA model identified miRNA-mediated regulatory modules that fine-tune the response of ECs to VEGF-A and that could be exploited to identify new druggable biomarkers in angiogenesis-related diseases.

Materials and methods

Primary cell cultures

Human umbilical vein endothelial cells (HUVECs) were isolated from the cords of newborns by collagenase digestion of the interior of the umbilical vein, as previously described (***Nowak-Sliwinska et al., 2018***). To reduce the experimental variability that results from the different genetic backgrounds of individuals, each HUVEC batch was composed of cells derived from three to five different cords. HUVECs were cultured in M199 medium supplemented with 20% fetal bovine serum (FBS), 0.05 µg/ml porcine heparin, 2% penicillin-streptomycin solution (all from Sigma-Aldrich, St. Louis, MO, USA) and 0.2% brain extract. HUVECs were used for experiments until the third passage. Collection of umbilical cords for the isolation of HUVECs is governed by an agreement between Università degli Studi di Torino and the Azienda Ospedaliera Ordine Mauriziano di Torino, protocol number 1431 02/09/2014. Informed consent was obtained from all subjects involved.

Spheroid capillary sprouting assay

EC spheroids were generated as described previously (***Nowak-Sliwinska et al., 2018***) with minor modifications. HUVECs within the third passage were trypsinized and cultured in hanging drops (800 cells/drop) in M199 containing 10% FBS and 0.4% (w/v) methylcellulose (Sigma-Aldrich). After 10 hr or overnight incubation, spheroids were collected and embedded in a solution containing 15% FBS, 0.5% (w/v) methylcellulose, 1 mg/ml rat tail collagen I solution, 30 Mm HEPES and M199 from 10X concentrate (all from Sigma-Aldrich). 0.1M NaOH was added to adjust the pH to 7.4 to induce collagen polymerization. After 30 min incubation at 37˚C, polymerized gel was overlaid with M199 medium. Sprouting was induced by addition of 20 ng/ml recombinant human VEGF-A (R and D

Systems, Minneapolis, MN, USA) to the collagen solution and to the overlaying medium. After 18 hr incubation at 37˚C in a 5% CO_2 incubator, spheroids were imaged, or collected for further analysis. When indicated, inactivation of cell proliferation was performed by treating the cells with mitomycin C (Sigma-Aldrich) at 10 µg/ml for 2 hr in M199, 24 hr prior spheroids generation. When spheroids assay was performed in the presence of drugs, the drugs were added at the moment of collagen I embedding. The fluorescent ECs used in the tip competition assay were generated by transduction with lentiviral particles carrying the plasmid pLVX-DsRed-Express2-N1 (Takara, Mountain View, CA, USA) followed by puromycin selection for 48 hr. For experiment of Notch pathway modulation, spheroids were incubated with either DAPT (Sigma-Aldrich) 2 µM or human recombinant DLL4 (R and D Systems) 1 mg/ml.

Imaging

Spheroids in 3D collagen matrix were fixed with 4% PFA for 30 min at room temperature and imaged under bright field using an AF6000LX-TIRF workstation (Leica, Wetzlar, Germany). Measurement of the total sprout area of individual spheroids was performed using the Image J software package. For each experimental condition, the sprout area of at least 20 spheroids was measured and averaged to achieve 5% significance and 80% power.

RNA isolation

To isolate ECs after the sprouting assay, the collagen matrix was digested by incubation with 0.25% Collagenase A (Sigma-Aldrich) in M199 medium at 37˚C for 10 min. Total RNA was isolated from HUVECs by using TRIzol (ThermoFisher Scientific, Waltham, MA, USA) reagent and an miRNeasy Mini Kit (Qiagen, Hilden, Germany). Residual DNA was removed by treatment with Rnase-Free Dnase Set (Qiagen). The quality and concentration of RNAs were assessed with a NanoDrop ND-1000 spectrophotometer (ThermoFisher Scientific). The quality of the RNA samples that were subsequently processed for RNA-sequencing and microarray analysis was further assessed using a Qubit RNA HS Assay Kit and an Agilent RNA 6000 Nano Kit in an Agilent Bioanalyzer (Agilent, Santa Clara, CA, USA).

RNA-sequencing analysis

Total RNA from spheroids exposed to VEGF-A for 18 hr (SPHV) and control spheroids (SPHC) that were not exposed to VEGF-A were subjected to high throughput sequencing for poly-A + RNAs by an external next generation sequencing (NGS) facility (Fasteris, Geneva, Switzerland). Three biological replicates from each biological condition were analyzed. RNA sequencing was performed on a HiSeq 2000 sequencer (Illumina, San Diego, CA, USA), obtaining a mean of 100 million paired-end reads of 100 bps per sample. Reads to counts conversion and differential expression analysis were performed using the software implementation described by ***Beccuti et al. (2018)***. In brief, fastq files were mapped with STAR-2.5 to the reference genome (hg19 assembly) and gene counts were generated using RSEM-1.3.0 and ENSEMBL annotation. Differential expression analysis was performed using DESeq2 version 1.14.1 (***Love et al., 2014***) to detect modulated genes ($|\log_2 FC| > 0.5$ and FDR < 0.05). Data were deposited in the GEO database, with accession number GSE115817.

For miRNAs, the same external NGS facility (Fasteris, Geneva, Switzerland) was used to perform small-RNA sequencing profiling on the same matched samples as those used for mRNA sequencing. Sequencing was performed on a HiSeq 2000 sequencer (Illumina), obtaining a mean of 8 million 50-bps single-end reads per sample. From the raw data, adaptors were first trimmed by the FASTX-Toolkit. Then, inserts were mapped by the BWA tool (***Li and Durbin, 2010***) on mature miRNA sequences from miRBase v22 (***Kozomara and Griffiths-Jones, 2014***), thus producing an expression level for all annotated miRNAs. Data were deposited in the GEO database, with accession number GSE115954.

Microarray analysis

450 ng total RNA was employed to synthetize biotinylated cRNA probes using an Illumina TotalPrep RNA Amplification Kit (ThermoFisher Scientific), according to the manufacturer's instructions. After quantification in an Agilent Bioanalyzer, 750 ng cRNAs were hybridized to an Illumina HumanHT-12

v4.0 Expression Bead Chip for 18 hr at 58˚C. Biotinylated probes were then labeled with streptavidin-Cy3. Fluorescent signal was acquired by an Illumina BeadArray Reader, and data were extracted using the GenomeStudio software V2011.01. Probe intensities across the chip were normalized by applying the cubic spline normalization algorithm. For subsequent analysis, only probes with a detection p-value <0.05 were selected. For each gene, we retained the associated probe with the largest mean expression value across all samples. For each probe, the $\log_2$ signal was converted to the $\log_2$ ratio against the global average expression of that probe in all samples. Each experimental point was assessed with two biological replicates. Data were deposited in the GEO database, with accession numbersGSE116039 and GSE129275.

Gene set enrichment analysis (GSEA)

GSEA was run on the dataset of protein-coding genes in SPHV versus SPHC against the canonical pathway genesets collection (c2.cp.v5.2, Broad Institute) by using 1000 genesets permutations. Only genesets with FDR < 0.05 were considered. Meta-analysis on colorectal cancer was performed on RNAseq data provided by The Cancer Genome Atlas (TCGA) (***Cancer Genome Atlas Network, 2012***), and on microarray data from the GEO Series GSE53127. GSEA was performed by evaluating the enrichment of upregulated modules and miRNA targets for genes that had high correlation with endothelial scores. Only genesets with FDR < 0.05 were considered.

Generation of the post-transcriptional network

Pair-wise correlation analysis was performed on the gene expression profiles of protein-coding genes and miRNAs from the RNA-sequencing data of SPHC and SPHV samples by using Pearson correlation as co-expression measure. Association between functional biological pathways and miRNAs was performed using the GSEA algorithm. Briefly, miRNA expression data were used as the phenotype to calculate the Pearson correlation coefficient between each pair of miRNA and protein-coding genes and to find association with biological processes. Genesets with FDR < 0.05 that positively or negatively correlated with miRNAs expression were extracted and used to generate a matrix that was subsequently clusterized using GenePattern (Broad Institute). Genes constituting the core enrichment were extracted from significant genesets and subjected to functional annotation using the online David functional annotation platform. To find associations between miRNA and their protein-coding target genes, we extracted data from TargetScan database V7.1, selecting evolutionarily conserved interactions with a weighted context++ score percentile >50. For non-conserved interactions, we considered a weighted context++ score percentile >90. Graphical representation of networks was performed using Cytoscape software, version 3.3.0 (***Shannon et al., 2003***). Power-law fitting and the corresponding statistical analysis were performed in MATLAB, according to ***Clauset et al. (2009)***.

Real-time PCR

To analyze mRNAs expression, 1 µg of DNAse-treated RNA was reverse-transcribed using a High Capacity cDNA Reverse Transcription kit and random primers (ThermoFisher Scientific). cDNA amplification was performed using gene-specific TaqMan assays and TaqMan PCR Universal MasterMix (ThermoFisher Scientific) in a CFX96 thermocycler (Bio-Rad, Hercules, CA, USA). Each assay was run in triplicate. To analyze miRNA expression, 350 ng of DNAse-treated RNA was reverse-transcribed using a High Capacity cDNA Reverse Transcription kit in the presence of a miRNA-specific primer (ThermoFisher Scientific). Real-time PCR was performed using miRNA-specific TaqMan MicroRNA Assays and TaqMan Universal PCR Master Mix (ThermoFisher Scientific) in a CFX96 (Bio-Rad) Real-Time PCR. Each assay was run in triplicate. Expression of *TBP* or *RNU44* was used as the endogenous control for mRNA or miRNA relative quantifications, respectively. Relative quantification of gene expression levels between samples (Rq) was performed using the comparative Ct (threshold cycle number) method (***Livak and Schmittgen, 2001***). A complete list of the Real-time PCR assays used is provided in ***Supplementary file 2***.

miRNA expression profiling under miRNA hubs modulation was performed using TaqMan Advanced miRNA Human A Card (ThermoFisher Scientific). 10 ng of total RNA from each sample were retrotranscribed using a TaqMan Advanced miRNA cDNA Synthesis Kit (ThermoFisher Scientific). Each sample was run in biological duplicate. Expression data were first normalized following

manufacturer's instructions; subsequently, the ΔΔCt method was used to evaluate the relative expression level (fold change) in each condition versus the corresponding control. ΔΔCt values were loaded in the R environment software for statistical analysis and the heatmap function was used to perform hierarchical clustering analysis and to represent data in a heatmap.

Transient transfections

Sub-confluent ECs were transfected with the mirVana miRNA mimic, to overexpress miRNAs, or with mirVana miRNA inhibitor (ThermoFisher Scientific), to inhibit miRNAs activity, at a final concentration of 90 nmol/L by using RNAiMAX lipofectamine in Optimem medium (ThermoFisher Scientific), according to the manufacturer protocol. Effective overexpression or inhibition was verified by real-time PCR, as described. Subsequent assays were performed 24 hr post-transfection.

shRNA-mediated gene knock-down

DICER1 knock-down was performed by transducing ECs with shRNAs carried by lentiviral particles. Self-inactivating, replication-incompetent lentiviral particles were generated by cotransfection of expression plasmid (TRC1 pLKO.1-puro Non-Target shRNA as negative control or TRC1 pLKO.1-puro carrying *DICER1*-targeting shRNAs, Sigma-Aldrich), envelope plasmid (pVSV-G) and packaging plasmid (pCMV-Dr8.91) into HEK-293t cells using the calcium phosphate method, as previously described (***Follenzi et al., 2000***). ECs were transduced with lentiviral particles at a multiplicity of infection (MOI) = 1 in the presence of 8 μg/ml polybrene. Medium was replaced after 24 hr, and cells stably expressing the shRNA were selected by growth in puromycin (1 μg/ml) for 24 hr. Effective *DICER* knock-down of two different shRNAs was evaluated by real-time PCR. The shRNA with the highest silencing efficacy was chosen (sh#3) and used for subsequent experiments. Spheroid assays were performed 48 hr post-transduction.

Western blot analysis

Total proteins were obtained by cell lysis in an extraction buffer containing 0.125 M Tris-HCl (pH 6.8), 4% SDS, 20% glycerol, and quantified by BCA assay (ThermoFisher Scientific). Equal amounts of protein extract per sample were separated on an SDS-PAGE and subsequently blotted onto a PVDF membrane. Membranes were incubated with specific primary antibodies and appropriate HRP-conjugated secondary antibodies. Immunoreactive proteins were visualized using an enhanced chemiluminescence (ECL) system and acquired using a ChemiDoc Touch Gel Imaging System (Biorad). Images were analyzed with Image Lab software 5.2.1 (Biorad). Antibodies used were anti-VEGFR2, anti-P38, anti-phospho-P38, anti-ERK1/2, anti-phospho-ERK1/2 (Cell Signaling Technology, Danvers, MA, USA), and anti-GAPDH (Abcam, Cambridge, UK).

ERK activity assessment

Total ERK and phospho-ERK proteins were measured using the Meso Scale Discovery (MSD) technology. MAP Kinase (Total Protein) Whole Cell Lysate Kit and MAP Kinase Whole Cell Lysate Kit MULTI-SPOT plates were used (Meso Scale Diagnostics, Rockville, MA, USA) according to the MSD manufacturer's information. 7 μg of each sample were used for the detection. The amount of phosphoprotein was calculated according to the MSD directions using the following formula: % phosphoprotein = ((2 x phospho-signal) / (phospho-signal + total signal)) x 100.

Whole-mount immunofluorescent staining

Collagen gels containing spheroids were fixed with 4% paraformaldehyde for 30' min, followed by 3 hr incubation in blocking buffer (PBS 0.5% Triton + 0.1% tween 20% and 10% donkey serum). Anti-DLL4 antibody (Abcam) or anti-CXCR4 antibody (Abcam) were diluted 1:1000 in blocking buffer and incubated overnight at 4˚C. After extensive washing in blocking buffer, collagen gels were incubated with AF555-conjugated secondary antibody (ThermoFisher Scientific) in the same buffer for 1 hr. Cell nuclei were counterstained with DAPI.

Notch signaling activity

The plasmid pWPT-12XCSL-DsRedExpressDR was generated by subcloning the Notch fluorescent reporter 12xCSL-DsRedExpressDR (***Hansson et al., 2006***) into the lentiviral vector pWPT.

Generation of lentiviral particles and transduction of ECs were performed as described above. Spheroid assays were performed 48 hr post-transduction.

Proliferation assay

A proliferation assay was performed using Click-It EdU Flow Cytometry Cell Proliferation Assay (ThermoFisher Scientific). For 2D proliferation assays, 2.5×10^3 ECs were plated in six well plates and starved in serum-free M199 supplemented with 0.1% BSA for 10 hr. Cell proliferation was induced by the addition of 20 ng/ml VEGF-A to the culture medium, and maintained for additional 18 hr. 10 µM of 5-ethynyl-2′-deoxyuridine (EdU) was added 2 hr prior to cell harvesting. For cell proliferation measurement in spheroids, 10 µM EdU was added 2 hr prior to spheroids collection. EdU detection was performed according to the manufacturer's protocol and samples were analyzed in a CyAn ADP flow cytometer with Summit five software (Beckman Coulter, Brea, CA, USA).

Migration assay

Real-time directional cell migration was measured with an xCELLigence RTCA DP instrument in a CIM plate (ACEA Biosciences, San Diego, CA, USA). The bottom of the upper chamber was coated with 1% gelatin for 5 min at room temperature. The lower chamber was filled with M199 medium, 10% FBS, and VEGF 20 ng/ml as chemoattractant. 3×10^5 HUVECs were seeded in the upper chamber in 100 µl M199 medium. ECs migration was continuously monitored by measuring the Cell Index every 30 min for 24 hr in a CO_2 incubator at 37˚C. Data were analyzed with the xCELLigence RTCA software (ACEA Biosciences). The slope of the curve obtained by Cell Index measurements, which represents the speed of cell migration, was calculated the slope.

Enzymatic activity measurements

Purine synthesis

The activity of glutamine amidophosphoribosyltransferase (PPAT) was measured as described previously (***Capello et al., 2016***). The [^{14}C]-L-glutamate generated from the reaction was separated from [^{14}C]-L-glutamine by ion exchange chromatography in a 2 ml column. The radioactivity of the eluate containing [^{14}C]-L-glutamate was counted by liquid scintillation and expressed as nmol glutamate (Glu)/h/mg cell proteins. The activity of aminoimidazole-4-carboxamide ribonucleotide formyltransferase/inosine monophosphate cyclohydrolase (ATIC) was measured as reported previously (***Boccalatte et al., 2009***). Results were expressed as nmol NADP+/min/mg cell proteins.

Pyrimidine synthesis

The activity of carbamoyl phosphate synthetase II (CAD) was measured as described previously (***Capello et al., 2016***). Results were expressed as pmol carbamoyl aspartate (CA)/min/mg cell proteins.

ERK and p38 pharmacological inhibition

6×10^5 cells were plated in six well plates and pretreated with the ERK inhibitor SHC772984 (Cayman Chemical, Ann Arbor, MI, USA) or the p38 inhibitor SB 202190 (Sigma-Aldrich) for 18 hr, using the following concentrations: 30, 100 or 300 nM for ERK inhibitor, and 10, 100 or 300 µM for p38 inhibitor. Cells were starved for 3 hr in serum-free M199 and then stimulated with 20 ng/ml VEGF-A for 10 min. Starving and stimulation were performed in the presence of the drugs. Cells were then processed for protein extraction and western blot analysis.

Statistical analyses

All statistical analyses were performed using the GraphPad Prism six software, the R statistical package, or MATLAB. For all the datasets included in t-tests, Shapiro-Wilk normality test was applied to assess normal distribution. Pooled data are expressed as the mean ± SEM. n represents the number of biological replicates, each performed with different HUVEC batches. Significance was determined by using unpaired Student's t-test (two tailed); $p<0.05$ was considered significant. Specific details for each experiment can be found in the corresponding figure legend. Elsewhere, for hypergeometric tests, $p<0.05$ was considered significant; for the Kolmogorov-Smirnov test, $P > 0.1$ was considered significant.

Data access

All raw and processed sequencing data generated in this study have been submitted to the NCBI Gene Expression Omnibus (GEO; http://www.ncbi.nlm.nih.gov/geo/) and are available under the accession numbers GSE116039, GSE115954, GSE115817 and GSE129276.

Acknowledgements

This work was supported by AIRC – Associazione Italiana Per la Ricerca sul Cancro (grants 22910, 12182 and 18652), Regione Piemonte (grant A1907A, Deflect), Fondazione CRT, Ministero dell'Università e della Ricerca (PRIN 2017, grant 2017237P5X), FPRC 5xmille 2016 MIUR (Biofilm) and ERA-Net Transcan-2 (grant TRS-2018–00000689) to FB. We thank Prof. Urban Lendahl for the gift of the Notch reporter plasmid and Dr. Jeffrey F Thompson for revising the manuscript.

Additional information

Funding

Funder	Grant reference number	Author
Associazione Italiana per la Ricerca sul Cancro	12182	Federico Bussolino
Associazione Italiana per la Ricerca sul Cancro	18652	Federico Bussolino
Regione Piemonte	A1907A Deflect	Federico Bussolino
Ministero dell'Istruzione, dell'Università e della Ricerca	PRIN 2017, 2017237P5X	Federico Bussolino
Ministero della Salute	Era-net TRS-2018-00000689	Federico Bussolino
Fondazione CRT		Federico Bussolino
Associazione Italiana per la Ricerca sul Cancro	22910	Federico Bussolino
Ministero dell'Istruzione, dell'Università e della Ricerca	FPRC 5xmille 2016 Biofilm	Federico Bussolino

The funders had no role in study design, data collection and interpretation, or the decision to submit the work for publication.

Author contributions

Stefania Rosano, Conceptualization, Validation, Investigation, Methodology; Davide Corà, Data curation, Formal analysis; Sushant Parab, Formal analysis, Bioinformatics analyses on publicly available databases; Serena Zaffuto, Chiara Riganti, Validation, Investigation; Claudio Isella, Formal analysis, Methodology; Roberta Porporato, Roxana Maria Hoza, Investigation, Methodology; Raffaele A Calogero, Software, Formal analysis; Federico Bussolino, Conceptualization, Supervision, Funding acquisition; Alessio Noghero, Conceptualization, Formal analysis, Supervision, Validation, Investigation, Visualization, Methodology

Author ORCIDs

Alessio Noghero https://orcid.org/0000-0002-8266-9247

Ethics

Human subjects: Informed consent was obtained from all subjects involved. Collection of umbilical cords is governed by an agreement between Università degli Studi di Torino and the Azienda Ospedaliera Ordine Mauriziano di Torino, protocol number 1431 02/09/2014.

Decision letter and Author response

Decision letter https://doi.org/10.7554/eLife.48095.sa1

Author response https://doi.org/10.7554/eLife.48095.sa2

Additional files

Supplementary files

- Supplementary file 1. Key resources table.
- Supplementary file 2. Real-time PCR assays list.
- Transparent reporting form

Data availability

Sequencing data have been deposited in GEO under accession codes GSE116039, GSE115954, GSE115817, GSE129276.

The following datasets were generated:

Author(s)	Year	Dataset title	Dataset URL	Database and Identifier
Noghero A, Bussolino F, Corà D, Rosano S	2019	A Regulatory microRNA Network Controls Endothelial Cell Phenotypic Switch During Sprouting Angiogenesis	https://www.ncbi.nlm.nih.gov/geo/query/acc.cgi?acc=GSE116039	NCBI Gene Expression Omnibus, GSE116039
Noghero A, Bussolino F, Corà D, Rosano S	2019	A Regulatory microRNA Network Controls Endothelial Cell Phenotypic Switch During Sprouting Angiogenesis	https://www.ncbi.nlm.nih.gov/geo/query/acc.cgi?acc=GSE115954	NCBI Gene Expression Omnibus, GSE115954
Noghero A, Bussolino F, Corà D, Rosano S	2019	A Regulatory microRNA Network Controls Endothelial Cell Phenotypic Switch During Sprouting Angiogenesis	https://www.ncbi.nlm.nih.gov/geo/query/acc.cgi?acc=GSE115817	NCBI Gene Expression Omnibus, GSE115817
Noghero A, Bussolino F, Corà D, Rosano S	2019	A Regulatory microRNA Network Controls Endothelial Cell Phenotypic Switch During Sprouting Angiogenesis	https://www.ncbi.nlm.nih.gov/geo/query/acc.cgi?acc=GSE129276	NCBI Gene Expression Omnibus, GSE129276

The following previously published dataset was used:

Author(s)	Year	Dataset title	Dataset URL	Database and Identifier
Pentheroudakis G, Kotoula V, Fountzilas E, Kouvatseas G, Basdanis G, Xanthakis I, Makatsoris T, Charalambous E, Papamichael D, Samantas E, Papakostas P, Dimitrios B, Razis E, Christodoulou C, Varthalitis I, Fountzilas G	2013	Study of gene expression markers for predictive significance for bevacizumab benefit in patients with metastatic colon cancer: A translational research study of the Hellenic Cooperative Oncology Group (HeCOG)	https://www.ncbi.nlm.nih.gov/geo/query/acc.cgi?acc=GSE53127	NCBI Gene Expression Omnibus, GSE53127

References

Agarwal V, Bell GW, Nam J-W, Bartel DP. 2015. Predicting effective microRNA target sites in mammalian mRNAs. *eLife* **4**:e05005. DOI: https://doi.org/10.7554/eLife.05005

Ausprunk DH, Folkman J. 1977. Migration and proliferation of endothelial cells in preformed and newly formed blood vessels during tumor angiogenesis. *Microvascular Research* **14**:53–65. DOI: https://doi.org/10.1016/0026-2862(77)90141-8, PMID: 895546

Barabási A-L, Pósfai M. 2016. *Network Science*. Cambridge, United Kingdom: Cambridge University Press.

Battaglin F, Puccini A, Intini R, Schirripa M, Ferro A, Bergamo F, Lonardi S, Zagonel V, Lenz H-J, Loupakis F. 2018. The role of tumor angiogenesis as a therapeutic target in colorectal cancer. *Expert Review of Anticancer Therapy* **18**:251–266. DOI: https://doi.org/10.1080/14737140.2018.1428092

Beccuti M, Cordero F, Arigoni M, Panero R, Amparore EG, Donatelli S, Calogero RA. 2018. SeqBox: rnaseq/ChIPseq reproducible analysis on a consumer game computer. *Bioinformatics* **34**:871–872. DOI: https://doi.org/10.1093/bioinformatics/btx674

Biyashev D, Veliceasa D, Topczewski J, Topczewska JM, Mizgirev I, Vinokour E, Reddi AL, Licht JD, Revskoy SY, Volpert OV. 2012. miR-27b controls venous specification and tip cell fate. *Blood* **119**:2679–2687. DOI: https://doi.org/10.1182/blood-2011-07-370635

Boccalatte FE, Voena C, Riganti C, Bosia A, D'Amico L, Riera L, Cheng M, Ruggeri B, Jensen ON, Goss VL, Lee K, Nardone J, Rush J, Polakiewicz RD, Comb MJ, Chiarle R, Inghirami G. 2009. The enzymatic activity of 5-aminoimidazole-4-carboxamide ribonucleotide formyltransferase/IMP cyclohydrolase is enhanced by NPM-ALK: new insights in ALK-mediated pathogenesis and the treatment of ALCL. *Blood* **113**:2776–2790. DOI: https://doi.org/10.1182/blood-2008-06-161018, PMID: 18845790

Cancer Genome Atlas Network. 2012. Comprehensive molecular characterization of human Colon and rectal Cancer. *Nature* **487**:330–337. DOI: https://doi.org/10.1038/nature11252, PMID: 22810696

Capello M, Ferri-Borgogno S, Riganti C, Chattaragada MS, Principe M, Roux C, Zhou W, Petricoin EF, Cappello P, Novelli F. 2016. Targeting the warburg effect in Cancer cells through ENO1 knockdown rescues oxidative phosphorylation and induces growth arrest. *Oncotarget* **7**:5598–5612. DOI: https://doi.org/10.18632/oncotarget.6798, PMID: 26734996

Carmeliet P, Jain RK. 2011. Molecular mechanisms and clinical applications of angiogenesis. *Nature* **473**:298–307. DOI: https://doi.org/10.1038/nature10144, PMID: 21593862

Chamorro-Jorganes A, Araldi E, Penalva LO, Sandhu D, Fernández-Hernando C, Suárez Y. 2011. MicroRNA-16 and microRNA-424 regulate cell-autonomous angiogenic functions in endothelial cells via targeting vascular endothelial growth factor receptor-2 and fibroblast growth factor receptor-1. *Arteriosclerosis, Thrombosis, and Vascular Biology* **31**:2595–2606. DOI: https://doi.org/10.1161/ATVBAHA.111.236521, PMID: 21885851

Chou CH, Shrestha S, Yang CD, Chang NW, Lin YL, Liao KW, Huang WC, Sun TH, Tu SJ, Lee WH, Chiew MY, Tai CS, Wei TY, Tsai TR, Huang HT, Wang CY, Wu HY, Ho SY, Chen PR, Chuang CH, et al. 2018. miRTarBase update 2018: a resource for experimentally validated microRNA-target interactions. *Nucleic Acids Research* **46**:D296–D302. DOI: https://doi.org/10.1093/nar/gkx1067, PMID: 29126174

Clauset A, Shalizi CR, Newman MEJ. 2009. Power-Law distributions in empirical data. *SIAM Review* **51**:661–703. DOI: https://doi.org/10.1137/070710111

Cora' D, Re A, Caselle M, Bussolino F. 2017. MicroRNA-mediated regulatory circuits: outlook and perspectives. *Physical Biology* **14**:045001. DOI: https://doi.org/10.1088/1478-3975/aa6f21, PMID: 28586314

Craig EA, Stevens MV, Vaillancourt RR, Camenisch TD. 2008. MAP3Ks as central regulators of cell fate during development. *Developmental Dynamics* **237**:3102–3114. DOI: https://doi.org/10.1002/dvdy.21750, PMID: 18855897

Dang LT, Lawson ND, Fish JE. 2013. MicroRNA control of vascular endothelial growth factor signaling output during vascular development. *Arteriosclerosis, Thrombosis, and Vascular Biology* **33**:193–200. DOI: https://doi.org/10.1161/ATVBAHA.112.300142, PMID: 23325476

De Bock K, Georgiadou M, Schoors S, Kuchnio A, Wong BW, Cantelmo AR, Quaegebeur A, Ghesquière B, Cauwenberghs S, Eelen G, Phng LK, Betz I, Tembuyser B, Brepoels K, Welti J, Geudens I, Segura I, Cruys B, Bifari F, Decimo I, et al. 2013. Role of PFKFB3-driven glycolysis in vessel sprouting. *Cell* **154**:651–663. DOI: https://doi.org/10.1016/j.cell.2013.06.037, PMID: 23911327

del Toro R, Prahst C, Mathivet T, Siegfried G, Kaminker JS, Larrivee B, Breant C, Duarte A, Takakura N, Fukamizu A, Penninger J, Eichmann A. 2010. Identification and functional analysis of endothelial tip cell-enriched genes. *Blood* **116**:4025–4033. DOI: https://doi.org/10.1182/blood-2010-02-270819, PMID: 20705756

Ebert MS, Sharp PA. 2012. Roles for MicroRNAs in conferring robustness to biological processes. *Cell* **149**:515–524. DOI: https://doi.org/10.1016/j.cell.2012.04.005

Eilken HM, Adams RH. 2010. Dynamics of endothelial cell behavior in sprouting angiogenesis. *Current Opinion in Cell Biology* **22**:617–625. DOI: https://doi.org/10.1016/j.ceb.2010.08.010

Erhard F, Haas J, Lieber D, Malterer G, Jaskiewicz L, Zavolan M, Dölken L, Zimmer R. 2014. Widespread context dependency of microRNA-mediated regulation. *Genome Research* **24**:906–919. DOI: https://doi.org/10.1101/gr.166702.113, PMID: 24668909

Fish JE, Santoro MM, Morton SU, Yu S, Yeh RF, Wythe JD, Ivey KN, Bruneau BG, Stainier DY, Srivastava D. 2008. miR-126 regulates angiogenic signaling and vascular integrity. *Developmental Cell* **15**:272–284. DOI: https://doi.org/10.1016/j.devcel.2008.07.008, PMID: 18694566

Follenzi A, Ailles LE, Bakovic S, Geuna M, Naldini L. 2000. Gene transfer by lentiviral vectors is limited by nuclear translocation and rescued by HIV-1 pol sequences. *Nature Genetics* **25**:217–222. DOI: https://doi.org/10.1038/76095, PMID: 10835641

Friedman RC, Farh KK, Burge CB, Bartel DP. 2009. Most mammalian mRNAs are conserved targets of microRNAs. *Genome Research* **19**:92–105. DOI: https://doi.org/10.1101/gr.082701.108, PMID: 18955434

Gerhardt H, Golding M, Fruttiger M, Ruhrberg C, Lundkvist A, Abramsson A, Jeltsch M, Mitchell C, Alitalo K, Shima D, Betsholtz C. 2003. VEGF guides angiogenic sprouting utilizing endothelial tip cell filopodia. *The Journal of Cell Biology* **161**:1163–1177. DOI: https://doi.org/10.1083/jcb.200302047, PMID: 12810700

Ghosh G, Subramanian IV, Adhikari N, Zhang X, Joshi HP, Basi D, Chandrashekhar YS, Hall JL, Roy S, Zeng Y, Ramakrishnan S. 2010. Hypoxia-induced microRNA-424 expression in human endothelial cells regulates HIF-α

isoforms and promotes angiogenesis. *Journal of Clinical Investigation* **120**:4141–4154. DOI: https://doi.org/10.1172/JCI42980, PMID: 20972335

Guo H, Ingolia NT, Weissman JS, Bartel DP. 2010. Mammalian microRNAs predominantly act to decrease target mRNA levels. *Nature* **466**:835–840. DOI: https://doi.org/10.1038/nature09267

Ha M, Kim VN. 2014. Regulation of microRNA biogenesis. *Nature Reviews Molecular Cell Biology* **15**:509–524. DOI: https://doi.org/10.1038/nrm3838, PMID: 25027649

Hansson EM, Teixeira AI, Gustafsson MV, Dohda T, Chapman G, Meletis K, Muhr J, Lendahl U. 2006. Recording notch signaling in real time. *Developmental Neuroscience* **28**:118–127. DOI: https://doi.org/10.1159/000090758, PMID: 16508309

Heiss M, Hellström M, Kalén M, May T, Weber H, Hecker M, Augustin HG, Korff T. 2015. Endothelial cell spheroids as a versatile tool to study angiogenesis *in vitro*. *The FASEB Journal* **29**:3076–3084. DOI: https://doi.org/10.1096/fj.14-267633, PMID: 25857554

Hornstein E, Shomron N. 2006. Canalization of development by microRNAs. *Nature Genetics* **38**:S20–S24. DOI: https://doi.org/10.1038/ng1803, PMID: 16736020

Inui M, Montagner M, Piccolo S. 2012. miRNAs and morphogen gradients. *Current Opinion in Cell Biology* **24**:194–201. DOI: https://doi.org/10.1016/j.ceb.2011.11.013

Isella C, Terrasi A, Bellomo SE, Petti C, Galatola G, Muratore A, Mellano A, Senetta R, Cassenti A, Sonetto C, Inghirami G, Trusolino L, Fekete Z, De Ridder M, Cassoni P, Storme G, Bertotti A, Medico E. 2015. Stromal contribution to the colorectal Cancer transcriptome. *Nature Genetics* **47**:312–319. DOI: https://doi.org/10.1038/ng.3224, PMID: 25706627

Ivey KN, Srivastava D. 2015. microRNAs as Developmental Regulators. *Cold Spring Harbor Perspectives in Biology* **7**a008144. DOI: https://doi.org/10.1101/cshperspect.a008144

Jakobsson L, Franco CA, Bentley K, Collins RT, Ponsioen B, Aspalter IM, Rosewell I, Busse M, Thurston G, Medvinsky A, Schulte-Merker S, Gerhardt H. 2010. Endothelial cells dynamically compete for the tip cell position during angiogenic sprouting. *Nature Cell Biology* **12**:943–953. DOI: https://doi.org/10.1038/ncb2103

Kanehisa M, Sato Y, Kawashima M, Furumichi M, Tanabe M. 2016. KEGG as a reference resource for gene and protein annotation. *Nucleic Acids Research* **44**:D457–D462. DOI: https://doi.org/10.1093/nar/gkv1070

Karagkouni D, Paraskevopoulou MD, Chatzopoulos S, Vlachos IS, Tastsoglou S, Kanellos I, Papadimitriou D, Kavakiotis I, Maniou S, Skoufos G, Vergoulis T, Dalamagas T, Hatzigeorgiou AG. 2018. DIANA-TarBase v8: a decade-long collection of experimentally supported miRNA-gene interactions. *Nucleic Acids Research* **46**:D239–D245. DOI: https://doi.org/10.1093/nar/gkx1141, PMID: 29156006

Korff T, Augustin HG. 1998. Integration of endothelial cells in multicellular spheroids prevents apoptosis and induces differentiation. *The Journal of Cell Biology* **143**:1341–1352. DOI: https://doi.org/10.1083/jcb.143.5.1341, PMID: 9832561

Kozomara A, Griffiths-Jones S. 2014. miRBase: annotating high confidence microRNAs using deep sequencing data. *Nucleic Acids Research* **42**:D68–D73. DOI: https://doi.org/10.1093/nar/gkt1181, PMID: 24275495

Kuehbacher A, Urbich C, Zeiher AM, Dimmeler S. 2007. Role of dicer and drosha for endothelial microRNA expression and angiogenesis. *Circulation Research* **101**:59–68. DOI: https://doi.org/10.1161/CIRCRESAHA.107.153916, PMID: 17540974

Kuosmanen SM, Kansanen E, Sihvola V, Levonen A-L. 2017. MicroRNA profiling reveals distinct profiles for Tissue-Derived and cultured endothelial cells. *Scientific Reports* **7**:e10943. DOI: https://doi.org/10.1038/s41598-017-11487-4

Li D, Zhao Y, Liu C, Chen X, Qi Y, Jiang Y, Zou C, Zhang X, Liu S, Wang X, Zhao D, Sun Q, Zeng Z, Dress A, Lin MC, Kung HF, Rui H, Liu LZ, Mao F, Jiang BH, et al. 2011. Analysis of MiR-195 and MiR-497 expression, regulation and role in breast Cancer. *Clinical Cancer Research* **17**:1722–1730. DOI: https://doi.org/10.1158/1078-0432.CCR-10-1800, PMID: 21350001

Li JH, Liu S, Zhou H, Qu LH, Yang JH. 2014. starBase v2.0: decoding miRNA-ceRNA, miRNA-ncRNA and protein–RNA interaction networks from large-scale CLIP-Seq data. *Nucleic Acids Research* **42**:D92–D97. DOI: https://doi.org/10.1093/nar/gkt1248, PMID: 24297251

Li H, Durbin R. 2010. Fast and accurate long-read alignment with Burrows-Wheeler transform. *Bioinformatics* **26**:589–595. DOI: https://doi.org/10.1093/bioinformatics/btp698, PMID: 20080505

Livak KJ, Schmittgen TD. 2001. Analysis of relative gene expression data using Real-Time quantitative PCR and the $2^{-\delta\delta ct}$ method. *Methods* **25**:402–408. DOI: https://doi.org/10.1006/meth.2001.1262

Love MI, Huber W, Anders S. 2014. Moderated estimation of fold change and dispersion for RNA-seq data with DESeq2. *Genome Biology* **15**:550. DOI: https://doi.org/10.1186/s13059-014-0550-8, PMID: 25516281

Nakashima T, Jinnin M, Etoh T, Fukushima S, Masuguchi S, Maruo K, Inoue Y, Ishihara T, Ihn H. 2010. Down-regulation of mir-424 contributes to the abnormal angiogenesis via MEK1 and cyclin E1 in senile hemangioma: its implications to therapy. *PLOS ONE* **5**:e14334. DOI: https://doi.org/10.1371/journal.pone.0014334, PMID: 21179471

Nicoli S, Knyphausen CP, Zhu LJ, Lakshmanan A, Lawson ND. 2012. miR-221 is required for endothelial tip cell behaviors during vascular development. *Developmental Cell* **22**:418–429. DOI: https://doi.org/10.1016/j.devcel.2012.01.008, PMID: 22340502

Nowak-Sliwinska P, Alitalo K, Allen E, Anisimov A, Aplin AC, Auerbach R, Augustin HG, Bates DO, van Beijnum JR, Bender RHF, Bergers G, Bikfalvi A, Bischoff J, Böck BC, Brooks PC, Bussolino F, Cakir B, Carmeliet P, Castranova D, Cimpean AM, et al. 2018. Consensus guidelines for the use and interpretation of angiogenesis assays. *Angiogenesis* **21**:425–532. DOI: https://doi.org/10.1007/s10456-018-9613-x, PMID: 29766399

Okabe K, Kobayashi S, Yamada T, Kurihara T, Tai-Nagara I, Miyamoto T, Mukouyama YS, Sato TN, Suda T, Ema M, Kubota Y. 2014. Neurons limit angiogenesis by titrating VEGF in retina. *Cell* **159**:584–596. DOI: https://doi.org/10.1016/j.cell.2014.09.025, PMID: 25417109

Pentheroudakis G, Kotoula V, Fountzilas E, Kouvatseas G, Basdanis G, Xanthakis I, Makatsoris T, Charalambous E, Papamichael D, Samantas E, Papakostas P, Bafaloukos D, Razis E, Christodoulou C, Varthalitis I, Pavlidis N, Fountzilas G. 2014. A study of gene expression markers for predictive significance for Bevacizumab benefit in patients with metastatic Colon cancer: a translational research study of the hellenic cooperative oncology group (HeCOG). *BMC Cancer* **14**:111. DOI: https://doi.org/10.1186/1471-2407-14-111, PMID: 24555920

Raman M, Earnest S, Zhang K, Zhao Y, Cobb MH. 2007. TAO kinases mediate activation of p38 in response to DNA damage. *The EMBO Journal* **26**:2005–2014. DOI: https://doi.org/10.1038/sj.emboj.7601668, PMID: 17396146

Rousseau S, Houle F, Kotanides H, Witte L, Waltenberger J, Landry J, Huot J. 2000. Vascular endothelial growth factor (VEGF)-driven actin-based motility is mediated by VEGFR2 and requires concerted activation of stress-activated protein kinase 2 (SAPK2/p38) and geldanamycin-sensitive phosphorylation of focal adhesion kinase. *Journal of Biological Chemistry* **275**:10661–10672. DOI: https://doi.org/10.1074/jbc.275.14.10661, PMID: 10744763

Shannon P, Markiel A, Ozier O, Baliga NS, Wang JT, Ramage D, Amin N, Schwikowski B, Ideker T. 2003. Cytoscape: a software environment for integrated models of biomolecular interaction networks. *Genome Research* **13**:2498–2504. DOI: https://doi.org/10.1101/gr.1239303, PMID: 14597658

Sholley MM, Ferguson GP, Seibel HR, Montour JL, Wilson JD. 1984. Mechanisms of neovascularization vascular sprouting can occur without proliferation of endothelial cells. *Laboratory Investigation; a Journal of Technical Methods and Pathology* **51**:624–634. PMID: 6209468

Simons M, Gordon E, Claesson-Welsh L. 2016. Mechanisms and regulation of endothelial VEGF receptor signalling. *Nature Reviews Molecular Cell Biology* **17**:611–625. DOI: https://doi.org/10.1038/nrm.2016.87, PMID: 27461391

Strasser GA, Kaminker JS, Tessier-Lavigne M. 2010. Microarray analysis of retinal endothelial tip cells identifies CXCR4 as a mediator of tip cell morphology and branching. *Blood* **115**:5102–5110. DOI: https://doi.org/10.1182/blood-2009-07-230284, PMID: 20154215

Suárez Y, Fernández-Hernando C, Pober JS, Sessa WC. 2007. Dicer dependent microRNAs regulate gene expression and functions in human endothelial cells. *Circulation Research* **100**:1164–1173. DOI: https://doi.org/10.1161/01.RES.0000265065.26744.17, PMID: 17379831

Suárez Y, Fernández-Hernando C, Yu J, Gerber SA, Harrison KD, Pober JS, Iruela-Arispe ML, Merkenschlager M, Sessa WC. 2008. Dicer-dependent endothelial microRNAs are necessary for postnatal angiogenesis. *PNAS* **105**:14082–14087. DOI: https://doi.org/10.1073/pnas.0804597105, PMID: 18779589

Subramanian A, Tamayo P, Mootha VK, Mukherjee S, Ebert BL, Gillette MA, Paulovich A, Pomeroy SL, Golub TR, Lander ES, Mesirov JP. 2005. Gene set enrichment analysis: a knowledge-based approach for interpreting genome-wide expression profiles. *PNAS* **102**:15545–15550. DOI: https://doi.org/10.1073/pnas.0506580102

Tsang J, Zhu J, van Oudenaarden A. 2007. MicroRNA-mediated feedback and feedforward loops are recurrent network motifs in mammals. *Molecular Cell* **26**:753–767. DOI: https://doi.org/10.1016/j.molcel.2007.05.018, PMID: 17560377

Tsang JS, Ebert MS, van Oudenaarden A. 2010. Genome-wide dissection of microRNA functions and cotargeting networks using gene set signatures. *Molecular Cell* **38**:140–153. DOI: https://doi.org/10.1016/j.molcel.2010.03.007, PMID: 20385095

Voellenkle C, Rooij J, Guffanti A, Brini E, Fasanaro P, Isaia E, Croft L, David M, Capogrossi MC, Moles A, Felsani A, Martelli F. 2012. Deep-sequencing of endothelial cells exposed to hypoxia reveals the complexity of known and novel microRNAs. *RNA* **18**:472–484. DOI: https://doi.org/10.1261/rna.027615.111, PMID: 22282338

Weidemann A, Breyer J, Rehm M, Eckardt K-U, Daniel C, Cicha I, Giehl K, Goppelt-Struebe M. 2013. HIF-1α activation results in actin cytoskeleton reorganization and modulation of Rac-1 signaling in endothelial cells. *Cell Communication and Signaling* **11**:80. DOI: https://doi.org/10.1186/1478-811X-11-80

Wong C, Jin Z-G. 2005. Protein Kinase C-dependent Protein Kinase D Activation Modulates ERK Signal Pathway and Endothelial Cell Proliferation by Vascular Endothelial Growth Factor. *Journal of Biological Chemistry* **280**:33262–33269. DOI: https://doi.org/10.1074/jbc.M503198200

Yang Z, Wu L, Zhu X, Xu J, Jin R, Li G, Wu F. 2013. MiR-29a modulates the angiogenic properties of human endothelial cells. *Biochemical and Biophysical Research Communications* **434**:143–149. DOI: https://doi.org/10.1016/j.bbrc.2013.03.054

Yin KJ, Olsen K, Hamblin M, Zhang J, Schwendeman SP, Chen YE. 2012. Vascular endothelial cell-specific *microRNA-15a* inhibits angiogenesis in hindlimb ischemia. *Journal of Biological Chemistry* **287**:27055–27064. DOI: https://doi.org/10.1074/jbc.M112.364414, PMID: 22692216